UNIVERSITY OF CALIFORNIA, SAN DIEGO

Anti-inflammatory capabilities of compounds from marine bacteria in a mouse model of allergic inflammation and asthma

A dissertation submitted in partial satisfaction of the requirements for the degree

Doctor of Philosophy

in

Oceanography

by

Wendy K. Strangman

Committee in charge:

Professor William Fenical, Chair
Professor Lihini Aluwihare
Professor David Broide
Professor William Gerwick
Professor Victor Vacquier

2007

The dissertation of Wendy K. Strangman is approved, and is acceptable in quality and form for publication on microfilm:

_____

_____

_____

_____

_____

_____

Chair

University of California, San Diego

2007

TABLE OF CONTENTS

LIST OF FIGURES

Chapter I.1

Chapter I.2

Chapter I.3

Chapter II.2

Chapter II.3

Chapter II.4

Chapter III.1

Chapter III.2

Chapter III.3

LIST OF TABLES

Chapter II.1

Chapter II.3

Chapter III.2

Chapter III.3

Chapter IV.2

LIST OF ABBREVIATIONS

CD	circular dichroism
ELISA	enzyme linked immunosorbent assay
ESI	electrospray ionization
gCOSY	gradient correlation spectroscopy
gHMBC	gradient heteronuclear multiple bond correlation
gHSQC	gradient heteronuclear single quantum coherence
HPLC	high performance liquid chromatography
HR	high resolution
IL	interleukin
IR	infra red
LC/MS	liquid chromatography / mass spectroscopy
MS	mass spectroscopy
NOESY	nuclear overhauser effect spectroscopy
NMR	nuclear magnetic resonance
TOCSY	total correlation spcetroscopy
TOF	time of flight
UV	ultraviolet

ACKNOWLEDGEMENTS

There are so many people that I need to thank for their invaluable help and support. First and foremost I need to thank my parents. They have always been my rock and my foundation and I would not be the person I am today without their constant love and support. They are fantastic and I love them very much. I also need to thank my brother Robert, he has always been great at not letting me take myself seriously and I love him for that. My grandparents, aunts and uncles also deserve my thanks for keeping me grounded and inspired.

One of the great mentors in my life, Rev. Gene Lefebvre deserves a large thank you as well. He always pushed me to be good to people and to try and make a difference in the world and hopefully the results of this thesis and my time in graduate school are a small step in that direction. His voice in my heard reminds me nearly every day that no matter what, helping people, and putting my faith in God are the most important things I can do. This has proved to be true on many occasions throughout graduate school and I thank him for his teachings.

I also need to thank all of the amazing friends I have made during my time at UCSD, both in undergrad and grad school. Without their support and friendship, grad school would have been a much less enjoyable place. Especially, I would like to thank my roommate Roberta for putting up with me for five years and for the hours of wonderful television she watched with me. I also need to thank my friends outside of Scripps; Suzie, Erin, Jyothi, and Matt for always being there when I needed them and for their constant friendship no matter where in the country they are.

I have had the privilege of working with so many great people during my time at Scripps. There have been many wonderful postdocs that have been instrumental in shaping my research and my life. Those that I consider "my postdocs" include Dr. Markus Huebes, who mentored me as an undergrad in the Faulkner lab. I knew basically nothing about natural products chemistry before joining the lab and he, with a great amount of patience, set about teaching me how to be a chemist. In addition, he was a great friend as well as mentor. I also need to thank Dr. Lyndon West for taking over as "my postdoc" after Markus left. Lyndon's energy and excitement for natural products research was really infectious and I learned a lot from him. His continued friendship is invaluable to me and I can't say enough good things about him. Lyndon also makes an excellent cappuccino. After I joined the Fenical lab, Dr. Phillip Williams became a wonderful friend and mentor to me and I wish his great success in his career in Hawaii. Dr. Chambers Hughes has been my lab and office mate for 3 years and has had to endure sitting next to me for all of that time. Dr. Ratnakar Asolkar has also shared the joy of Kaplan East with Chambers and I for about 2 years. Both of them make coming to lab every day much more fun and both of them have taught me a lot of chemistry. Drs. San-Jip Nam, Takashi Fukuda, Mickea Rose and Susana Gaudencio have come recently to the lab have made my last year a lot more fun and rewarding. In the UCSD Medical School, Dr. Marina Miller and Dr. Jae-Youn Cho took me under their wings and taught me pretty much everything I know about immunology, including how to run an ELISA experiment, how to immunize a mouse, how to culture cells, how to count splenocytes, and how to run in vivo mouse experiments.

I am deeply indebted to Dr. Hak-Cheol Kwon for the time and care he took and continues to take in molding me into a (hopefully) great scientist. Kwon taught me much of what I know about structural elucidation. Most importantly, he demonstrated the time and effort, and work ethic it takes to be successful in our field and I am truly grateful. Kwon is a true friend and a brilliant natural products chemist and I am confident that he will be a powerhouse of Korean science very soon.

I am also grateful for Dr. Katherine Maloney for her inspirational friendship during the last year of my PhD and also for her amazing editing of my thesis. She is about to embark on a fantastic career as a professor and I wish her great success.

In the Faulkner lab, Christian Ridley, Joel Sandler, and Roman De Jesus and Chollarat Boolarpradab taught me a lot and really helped make things fun as well as being my support net once John passed away. In the Fenical lab, the 3 other women that were my year, Erin Gontang, Alejandra Preito-Davo, and Anna Paula Espindola really made me feel welcome and I really appreciate their friendship. Dr. Dong-Chan Oh was and is a role model for me. He is a great friend, and our collaborations on several projects mentioned in Chapter two were very rewarding for me. I have no doubt that Dong-Chan will definitely be a great scientist. Lauge Farnaes, the latest addition to the Fenical lab has made my last two years a wonderful adventure and is always up for a coffee.

Several staff deserve my thanks because without them, nothing would get done and none of this would have been possible. From the Faulkner lab, Catherine Sincich was responsible for keeping the lab together after John's passing. I would also like to thank her for the invaluable conversations that we had over the years about assay

development, which were a great help in the early stages of my thesis research. In the Fenical lab, Chris Kauffman preformed the lion's share of the microbial culturing and I have learned a great deal from him. Matt Woolery keeps everything running and the Fenical lab would be a disaster with out him. I've had many illuminating conversations with Dr. Paul Jensen which will be quite helpful in my carrer. Beth Gardella has been a wonderful friend and a constant source of warmth and strength to me during my graduate career. She is a woman who knows how to get things done and I am very thankful for her.

Finally, I need to thank my advisors. It has been my privilege to be mentors by the true leader of my field. First was Professor D. John Faulkner who accepted me into his lab as an undergraduate, despite my lack of knowledge and experience. John was a genius at natural products chemistry. Both his sincerity as a scientist and his true love for his work have stuck with me and I will carry those values with me throughout my life. John took a chance on me in accepting me into his lab as a graduate student and I hope that I can live up to his expectations and standards of excellence. His passing affected me deeply and I will always carry his memories in my mind and my heart.

Professor David Broide, at the UCSD School of Medicine has been an amazingly kind and patient mentor throughout my last seven years of graduate and undergraduate research. Having little knowledge of the field of natural products chemistry, he willingly opened up is lab to me, taught me everything I know about asthma and allergic inflammation, and helped me to design my assay. He has also

exposed me to a number of rewarding opportunities that have greatly enhanced my research career and my life and I thank him very much.

Professor Bill Fenical is an amazing advisor. I have learned many invaluable lessons from him about not only how do to great science, but how to inspire people and motivate them to think big and go after their dreams. He has given me many, many amazing opportunities and has truly changed my life, for which I am deeply thankful. Bill is the epitome of the work hard play hard attitude and a great role model.

The rest of my PhD committee, professors Lihini Aluwihare, William Gerwick, and Victor Vacquier are great role models who I will try to emulate during my career. They have given me amazing insight into both my thesis research, and my life and I could not have asked for a better committee.

VITA

2002 B.S. Biochemistry and Cell Biology, University of California, San Diego

2007 Ph. D. Oceanography (marine natural products chemistry), Scripps Institution of Oceanography, University of California, San Diego.

PUBLICATIONS

"Potent Inhibitors of Pro-Inflammatory Cytokine Production Isolated From a Marine Bacterium" W. Strangman, H.C. Kwon, D. Broide, W. Fenical. (In Preparation)

"Thalassospiramides A and B, Immunosuppressive Peptides from the Marine Bacterium *Thalassospira* sp." Oh, D.C., Strangman W., Kauffman, C., Jensen, PR, Fenical, W., *Org. Lett.*; **2007**; 9(8) pp 1525 - 1528

"Anti-Siglec-F antibody inhibits oral allergen induced intestinal eosinophilic inflammation in a mouse model of food allergy.," JY. Cho, DJ Song, W. Strangman, D. Broide. J. Immunol. **2007** (Submitted)

"New Anticancer Drugs from Cultured and Collected Marine Organisms" William Fenical, Paul R. Jensen, Christopher Kauffman, Stephanie L. Mayhead, John D. Faulkner, Catherine Sincich , Rama M. Rao , Eric J. Kantorowski , Lyndon M. West , Wendy K. Strangman , Yuzuru Shimizu , Bo Li , Sudhakararao Thammana , Katherine Drainville , Michael T. Davies-Coleman , Robert A. Kramer , Craig R. Fairchild, William C. Rose, Robert C. Wild, Gregory D. Vite, Russell W. Peterson. *Pharmaceutical Biology* **2003**, 41S1, 6-14

ABSTRACT OF THE DISSERTATION

Anti-inflammatory capabilities of compounds from marine bacteria in a mouse model of allergic inflammation and asthma.

by

Wendy K. Strangman

Doctor of Philosophy in Oceanography

University of California, San Diego, 2007

Professor William Fenical, Chair

Plants, animals, and microorganisms produce an incredible variety of biologically active natural products, which are the result of secondary metabolism. Many of these molecules are highly toxic to a variety of cell types and organisms. Scientists have exploited these properties for decades to create effective anti-cancer, anti-fungal, anti-bacterial and anti-viral agents that have saved millions of lives. However, until the 1990s, comparatively little effort had been invested in tapping into this resource of bioactive small molecules for the discovery of compounds that act by other, non-toxic means. Asthma research and the underlying issue of allergic inflammation are two of these areas that have received relatively scant attention from

natural products scientists. Recent advances in immunology, cellular, and molecular biology have begun teasing apart the pathways and mechanisms involved in allergic inflammation, making assay development for drug discovery feasible. This thesis aims to describe a new approach to screen natural products for their ability to inhibit allergic inflammation.

Chapter one provides an overview of asthma and allergic inflammation as well as describing past natural products remedies and current drug therapies. Chapter two details the rationales and methodologies implemented in the development of a biological assay used to screen for compounds in extracts of marine microbial cultures that inhibit the production of pro-inflammatory molecules. It includes the results from a screen of 2,500 microbial extracts as well as discussions regarding previously reported molecules shown to be active in the assay, nuisance compounds, and collaborative efforts with others in the Fenical Laboratory that resulted in novel activity for exciting new marine bacterial natural products. Chapter three centers on a new group of molecules called the splenocins that were isolated from extracts of the marine actinomycete bacterial strain CNQ431. Included are the isolation, structure elucidation, and *in vitro* results for these molecules which were the most potent to be isolated thus far. Chapter four discusses the isolation, structure elucidation and cytokine inhibition activity of two novel nor-diterpenes isolated from a different marine actinomycete bacterium.

I

Introduction to the Thesis Research

I.1

Overview of Asthma

I.1. Overview of asthma

Asthma is a disease that has been afflicting humans for many thousands of years. First formally described in modern Western medical terms by Hippocrates sometime around 300BC, the word asthma comes from the Greek word for gasping[1]. Symptoms of asthma include a reversible restriction of airflow, which can manifest itself outwardly in the form of wheezing, coughing and shortness of breath[2]. In serious cases of asthma, sufferers may experience chronic problems such as tissue remodeling and irreversible airway obstruction[2].

While asthma has always been present in human populations, over the last several decades, especially in developed countries such as the US, Canada, England and Australia, the numbers of reported asthmatics has been rising steadily[3]. The last 40 years have seen a disturbing increase in the number of diagnosed asthmatics, a trend some experts have labeled an epidemic[2]. Fortunately, since about 2000, this trend appears to be leveling out[3]. However, the overall number of reported asthmatics in developed countries is still staggering with over 17 million cases in the US alone[4]. In a recent report released in 2003, the National Center for Health Statistics stated that the number of children diagnosed with asthma was near 6%, and was the third leading cause of hospitalizations, behind pneumonia and injury, of children under 18 years old. Current estimates show that between 8-10% of the US population now suffers from asthma to some degree. It is estimated that roughly 300 million people globally currently suffer from asthma and some estimates suggest that this number increases by 50% every decade[5]. Much of this increase can be attributed to the rise in asthma cases reported from developing countries as they become more westernized[5].

Economically, the costs of asthma treatment are staggering as well. In the United States, between 1990 and 1998, the costs of treating asthma including medication, hospital visits, and time missed from work/school rose from 6.2 billion dollars to 12.7 billion in just 8 years[6]. While there are several highly effective asthma drugs on the market, there is a significant subset of asthmatics whose disease remains uncontrolled. This portion of severe, uncontrolled asthmatics, while relatively small (about 10-20% of asthma sufferers) accounts for roughly half of all the direct and indirect costs related to asthma while those with mild asthma (about 70% of the asthmatic population) account for only about 20% of the costs[5].

Until about a century ago, asthma was primarily viewed as an affliction of the airway smooth muscles because this is where the majority of the symptoms occur. Consequently, treatments centered on treating these symptoms and returning air flow to the lungs. However, recent advances in our understanding of immunology, biochemistry, and physiology have made increasingly clear the fact that asthma is actually an inflammatory disease and that bronchial constriction and airway obstruction are merely the end result[7]. The Global Initiative for Asthma (GINA) defines asthma as "a chronic inflammatory disorder in which cells and cellular elements play a role. Chronic inflammation causes an associated increase in airway hyper-responsiveness that leads to recurrent episodes of wheezing, breathlessness, chest tightness and coughing, particularly at night or in the early morning. These episodes are usually associated with widespread but variable airflow obstruction that is often reversible spontaneously or with treatment."[5]

Allergic asthma is a complex and only partially understood disease that has both genetic and environmental contributions. To date, a large number of mediators, cytokines, chemokines, cell signaling molecules, and have been implicated in disease pathogenesis. Taken together, these studies suggest that no single mediator is likely to be the casue of asthma, which is primarily due to the interaction of multiple mediators with multiple cell types.

Genetics:

Asthma and related diseases have a strong genetic component. Studies with families and twins have shown that this is likely due to > 100 genes that are exerting a modest effect in creating the asthmatic phenotype[7]. No single gene is likely to contribute more than 5% to the asthma phenotype. Molecular genetics studies have uncovered several polymorphic gene clusters that are found on different chromosomes that influence the development of asthma[7]. Once such gene cluster codes for the major histocompatibility complex (MHC), which is comprised of proteins that display characteristic antigen peptides on the surface of dendritic cellls[7,8]. Similar studies also identified asthma-related genes that code for cytokine production and expression which could serve to regulate the intensity of the allergic response.[7]

Hygiene Hypothesis:

There is growing body of evidence that environmental factors play a significant role in asthma by affecting the development of the immune system and subsequent immune responses. Over the last 40 years, the numbers of reported asthma cases has risen sharply in Westernized countries.[6] This time frame is much to short to allow for genetic evolution. One alternative explanation is that environmental factors must

play a large part in these increasing numbers. Components of a Western lifestyle that are linked to increases in asthma include changes in early childhood exposures to a wide range of microorganisms such as the increase in exposure to dust mites resulting from modern housing conditions and an increased amount of time spent indoors.[9] Statistical epidemiological studies have shown several environmental factors that have an impact on the probability of asthma development in children including vaccination rates (increase), antibiotic use (increase), infections with parasitic helminthic worms (decrease), rural (decrease) vs. urban living (increase), numbers of older siblings (decreases with number), and the presence of pets such as dogs in the house (mixed).[10]

This environmental component, often termed "the hygiene hypothesis" incorporates these elements of a Western lifestyle into a theory to explain the prevalence of asthma in developed countries.[10] The explanation begins *in utero* through the transplacental transport of allergens from fetus to mother.[11] These allergens cause the mother's immune system to mount an immune response against the fetus. The fetus's immune system then responds by polarizing its progenitor T-cells weakly towards a T-helper type 2 (Th2) or pro-allergic phenotypic subset.[9,11] After birth, the infant is exposed to a much higher and more varied allergen load which further drives its immune system development and regulation.[11] Depending on the genetic makeup of the newborn, as well as the types of allergens to which the infant is exposed, the immune system either redirects towards a more normal non-allergic Th1 cellular phenotype, or is further biased towards the pro-allergic Th2 phenotype.[11] Without appropriate Th1 inducing environmental stimulants such as viral infection, and exposure to bacterial endotoxin to enhance Th1 cell proliferation, the infant

immune system can remain biased towards a pro-allergic Th2 immune system and related diseases such as asthma become more prevalent[9]. Additionally, chronic helminth worm infection, which is much less prevalent in developed countries, plays an active role in immune system development by suppressing the development of allergies.[12] The evolving paradigm of the hygiene hypothesis now encompasses both fetal development and genetic elements, for laying the groundwork for dysregulated immunity, and environmental factors for the instigation and propagation of dysregulation in the immune response.[11]

Cellular Mechanisms and Cytokines:

At the cellular level, allergic asthma begins with the introduction of an allergen into the airway where it comes in contact with an allergen -presenting cell (APC) such as a dendritic cell or a macrophage.[8] The APC digests the allergen and displays a characteristic peptide portion of the allergen on its cell surface.[8] This peptide is then recognized by receptors of the major histocompatibility complex class II (MHC Class II) on the surface of progenitor T cells.[8] At the same time, the APC expresses co-stimulatory molecules which bind to counter-receptors on the T cell.[8] Upon receiving both signals from the APC, the T cells proliferate and differentiate to become a Th2 cellular phenotype.[8] Repeated exposure to the APC-presented peptides leads to clonal expansion of these Th2 cells, which are all specific for the allergen.[8]

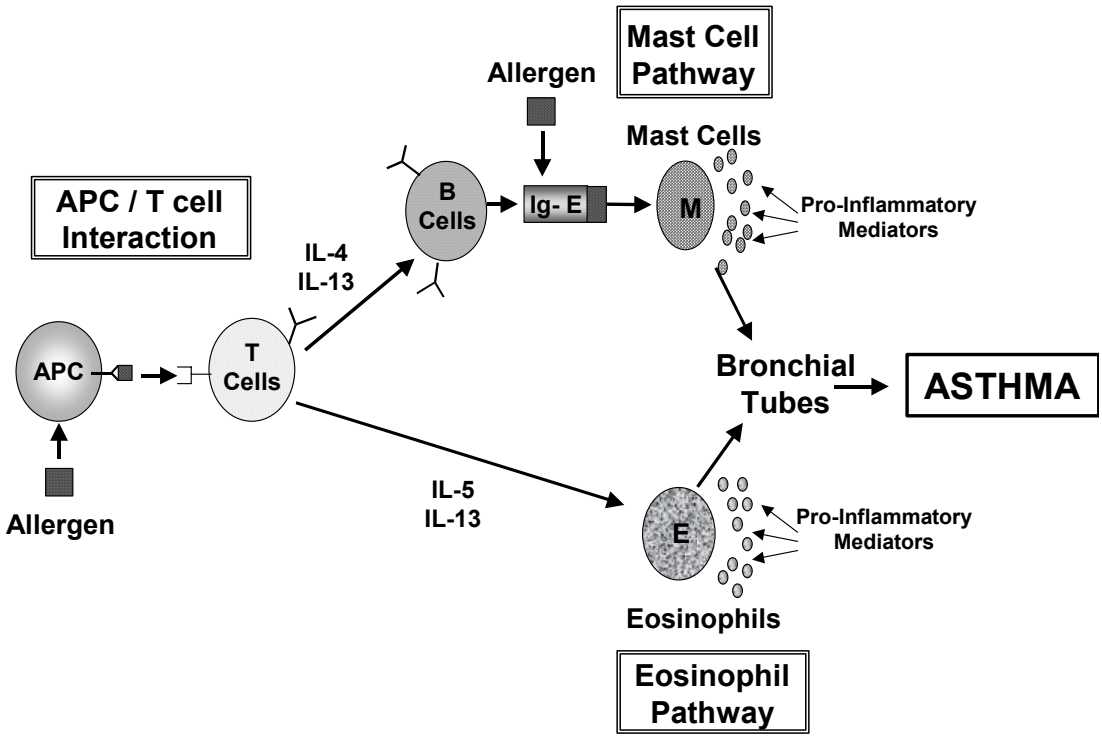

Figure I.1A: Generalized schematic of pathways involved in the asthmatic cellular cascade.

When the allergen-specific MHC Class II receptors on Th2 cells again encounter the APC- allergen complex, the Th2 cells are activated and secrete a number of their own cytokines initiating several pro-inflammatory pathways.[8] One pathway is mediated by mast cells which release histamine. Mast cell activation requires cross-linking of allergen specific immunoglobulin E (IgE) on mast cells leading to inflammation (Figure I.1A). The synthesis of IgE is mediated by activated Th2 cells which secrete the cytokines IL-4 and IL-13, which then bind to specific receptors on B-cells, inducing them to begin synthesizing and releasing IgE antibodies into the

blood.[8] The IgE antibodies then bind to high affinity IgE receptors (FcεRI) on the surface of mast cells in the tissue.[8] Binding of allergen induces the IgE receptors to dimerize, causing the mast cells to become activated and undergo degranulation to release a load of preformed cytosolic mediators (such as histamine), and newly generated mediators (such as leukotrienes and cytokines) which cause acute and chronic inflammation in the lungs leading to constriction of the bronchial tubes and the resulting loss of airflow.[8]

Another pathway activated by allergen stimulated Th2 cells is the eosinophil pathway, which is implicated in chronic asthma. This pathway begins with the activated Th2 cell's secretion of the cytokine IL-5.[13] IL-5 activates bone marrow derived leukocytes called eosinophils. It is thought that eosinophils evolved as one of the primary immune responses to infections by parasitic worms.[14] IL-5 plays many roles in the maturation and activation of eosinophils. Eosinophils originate in the bone marrow as CD34-positive hematopoetic progenitor cells which differentiate upon contact with IL-5 and generate several pro-inflammatory mediators including major basic protein (MBP), leukotrienes, prostaglandins and platelet activating factor, to name only a few.[15] After maturation, eosinophils leave the bone marrow and circulate through the bloodstream until they come in contact with adhesion molecules expressed on the surface of inflamed endothelial cells in the blood vessels of the airways. Once attached to the endothelium, the eosinophils flatten out and then migrate between the endothelium into the connective tissues.[15] As they migrate through the lattice of matrix proteins such as fibronectin and laminin in the connective tissues, eosinophils are partially activated by further stimulus with IL-5, as well as

other factors such as eotaxin, chemokines and lipid mediators.[15] Further stimulation by these mediators cause the eosinophils to become fully activated, and they release their inflammatory mediators into the bronchial epithelium.[15] Eosinophils are key players in the long lasting tissue damage and airway remodeling seen in patients with chronic asthma. The granular proteins they release are toxic to airway epithelium cells.[15] MBP also increases vascular permeability, and stimulates other inflammatory cells such as basophils.[15]

Activated Th2 release not only IL-5, but also the cytokine IL-13. In addition to its role in activating B-cells to synthesize IgE, IL-13 has a much broader impact in developing the pathogenesis of asthma. Recent studies have shown that IL-13 plays a central role in allergic asthma through its actions on epithelial cells.[16] IL-13, through its stimulation of epithelial cells, is implicated as a central molecule responsible for increases in subepithelial fibrosis in the airway wall.[16] Additionally, although the mechanisms are still being investigated, the influence of IL-13 on epithelial cells also leads to hyper secretion of mucus in the airways which blocks the flow of air into the bronchial tubes.[16] IL-13 also plays a significant role in airway hyper-responsiveness by affecting the proliferation, contractile and relaxant responses, and chemokine generating abilities of smooth muscle cells.[17]

There are a large number of other cytokines with roles implicated in the pathogenesis of asthma. These include interleukins 1-18, basic fibroblast growth factor, granulocyte colony stimulating factor, interferons α, β, and γ, macrophage colony stimulating factor, platelet-derived growth factor, and stem cell factor (*c-kit* ligand).[18] Recent efforts to find inhibitors of specific cytokines have met with

varying levels of success.[19-21] Because of the overlap of activities and the wide array of cytokines and other protein mediators of asthma that have been implicated in the disease, the suppression of a single cytokine is unlikely to have much downfield effect on the disease in patients with severe asthma.[20] Inhibiting the inflammatory cascade at positions further upstream in the cellular cascade has much greater potential for an effective response. One way to more completely downregulate the response would be to inhibit a Th2 cell's ability to secrete pro-inflammatory mediators. This could be achieved either through direct inhibition of the activated Th2 cells or by preventing their activation by the APCs. For example, a new class of drugs currently in development called immunostimulatory- oligodeoxynucleotides (ISS-ODNs), causes dendritic cells to secrete cytokines which activate the Th1 cellular response and dampen the Th2 response leading to the prevention and reversal of Th2 mediated inflammation.[22, 23]

In summary, asthma is an extremely complex disease that incorporates elements from both genes and the environment and encompasses a wide variety of cellular types, bound and secreted proteins, and small molecules. An improved understanding of the pathways and mechanisms involved in the pathogenesis of asthma is important for developing new treatments. Because of the multidimensional nature of the disease, treatment options can be complex. Drugs which can target multiple pathways, or that act at positions upstream in the allergic cascade will exert a stronger immunosuppressive effect and have greater potential for effective therapy.

I.2

Historical Summary of Asthma Drugs from Natural Products

I.2. Historical overview of asthma drugs from natural products

Asthma has been noted in medical literature for millennia and natural products have a long and successful history in treating its sufferers. In pre-industrial times, the only remedies for this condition came from herbal sources. Through trial and error over millennia medicine men and women discovered plants that had efficacy in the treatment of asthma. Recent scientific advances in chemistry and biology have shown that often the potent activity seen from these plants results from small molecule secondary metabolites acting on specific protein targets.

One of the first records of natural products use in treating asthma comes from ancient China. Nearly five thousand years ago, healers prescribed the ephedra or "Ma Huang" plant as treatment for asthma.[21] Chemical investigations have revealed the active component of ephdea to be the small molecule ephedrine, which works in the human body as a bronchodilator by releasing endogenous catecholamines (Figure 1.2a).[21]

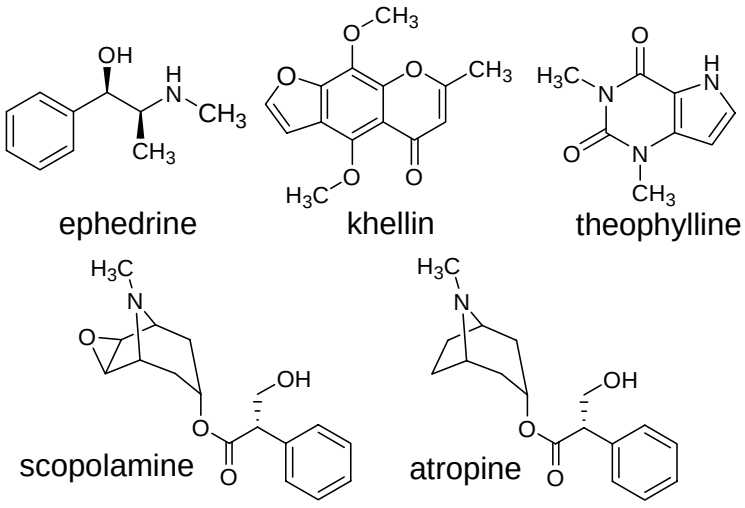

Figure I.2a. The active components of historically used natural products in the treatment of asthma.

Around the same time period in ancient human history, the Egyptians, one of the other medically advanced cultures of the time, prescribed other natural remedies for asthma. For example, they prescribed inhaling the vapor of the heated henbane plant.[21] This plant produces the small molecule scopolamine, a potent anti-muscarinic agent (Figure I.2a)[21]. Ancient Egyptians also combated asthma by ingesting an extract of the medicinal plant *Amni visnaga*, which contains khellin, a member of the chromone class of molecules with potent vasodilating properties (Figure I.2a).[21]

More recently, several centuries ago in India, asthma sufferers smoked the leaves of the *Datura* sp. or Jimson weed plant.[21] Similar to the henbane plant, the *Datura* sp. also has antimuscarinic properties in this case due to the presence of another small molecule, atropine (Figure I.2a).[21] Unfortunately, atropine also causes hallucinations.[21] However, recent synthetic modifications at the quaternary

ammonium center have eliminated the molecule's ability to cross the blood-brain barrier thereby eliminating these side effects.[21]

Drinking teas and coffees has long been prescribed for the treatment of asthma. In the beginning of the last century, chemists discovered that tea leaf extract contained the methyl xanthine, theophylline, which works as a bronchodilator (Figure I.2a).[21] However, unlike ephedrine, which activates catecholamines, theophylline inhibits phosphodiesterases, thereby relaxing airway smooth muscles and ultimately dilating bronchial tubes.[21] Recent biological studies show that theophylline also works at much lower concentrations as an anti-inflammatory agent by activating histone deacetylase (HDAC) proteins, which leads to a decrease in the expression of inflammatory genes.[24] These natural products and others have laid most of the groundwork for asthma drug discovery and development and have spawned many of the chemical scaffolds used in asthma drug development today.

I.3

Summary of Current Asthma Drug Therapy

I.3. Summary of current asthma drug therapy

While historical asthma treatments worked primarily by treating the symptoms such as mucus production and wheezing, recent advances in our understanding of the underlying inflammatory processes involved in asthma have greatly increased our ability to develop drugs effective in treating the disease. Today, treatments for asthma can be grouped loosely into three categories (bronchodilators, anti-inflammatories, and biologics). The vast majority of advances in asthma therapy of the last several decades have been in the pharmacological improvement of the selectivity and duration of action of pre-existing drug classes.[20] With the exceptions of a monoclonal antibody to IgE and synthetic bacterial DNA sequences which will be described later in this chapter, only one of the drug classes for asthma currently on the market, the anti-leukotrienes, can be classified as a new class of small molecule asthma inhibitor.[20]

Bronchodilators:

The first category of asthma drugs are the bronchodilators, which either maintain airway viability or reopen airways after an asthma attack.[20] These drugs are used to treat the symptoms of asthma, but generally have no effect on inflammation, the underlying cause of the disease.[20] The most efficacious of these bronchodilators are agonists of the β_2 adrenoreceptor, which relax airway smooth muscle by opening potassium channels and by increasing the concentrations of cAMP.[20] β_2 agonists, such as albutrerol, were originally developed as short-term drugs for the immediate treatment of an asthma attack (Figure I.3.A).[20] Recent derivatives of these drugs

exhibit a more prolonged effect and compounds such as serevant (Figure I.3.A) need only be taken once a day.[20] Unfortunately, β_2 agonists can cause side effects such as tremors and cardiac arrythmias.[20]

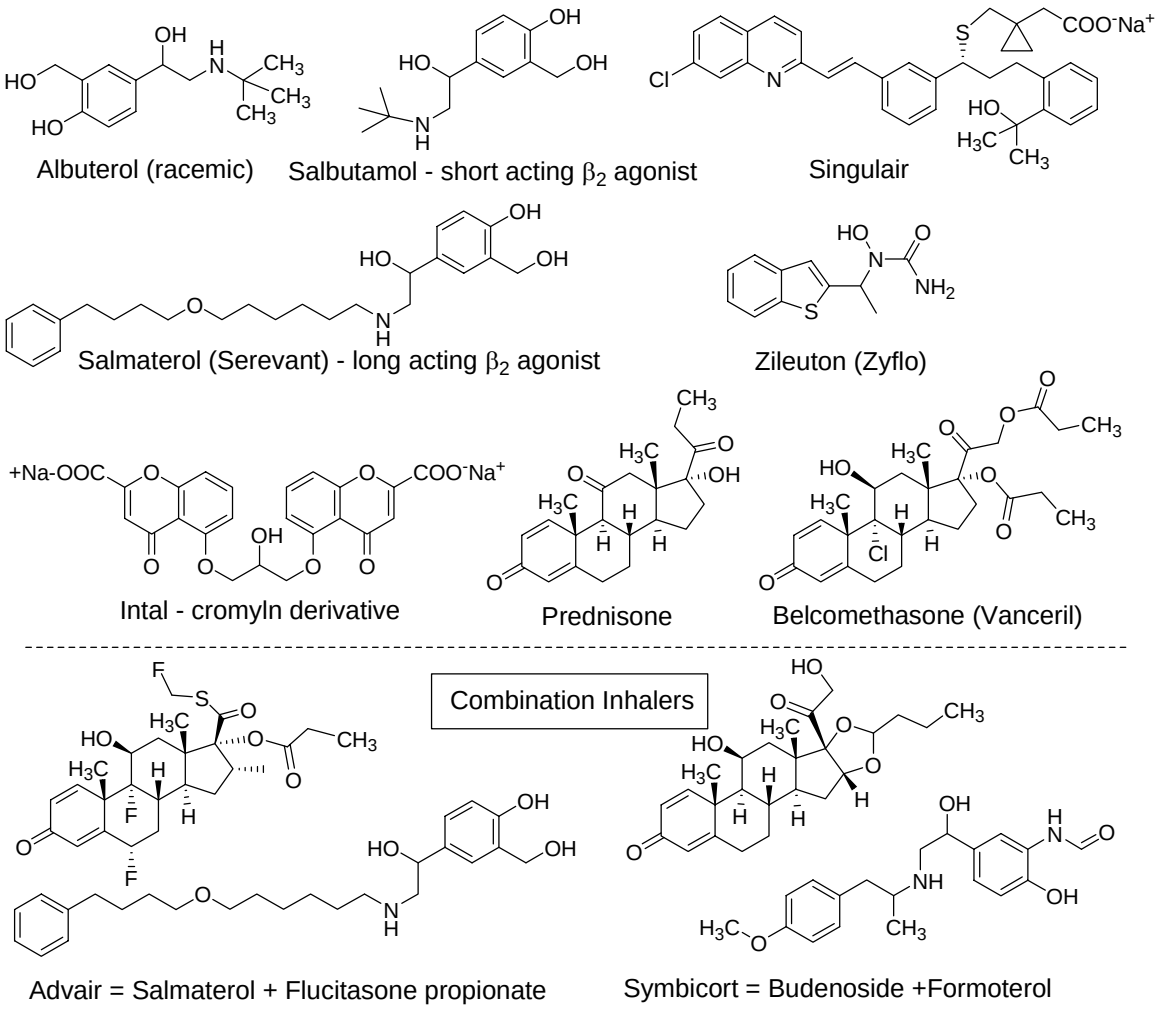

Figure I.3a. Structures of some drugs currently prescribed for the treatment of asthma.

Other bronchodialators such as Slo-bid are derivatives of theophylline, one of the active components from tealeaf extract (Figure I.2a). Theophylline derivatives act principally by inhibiting phosphodiesterases 3 and 4 in airway smooth muscle. They may also act as anti-inflammatory agents by activating histone deacetylase (HDAC) and subsequent inactivation of pro-inflammation genes.[20] However, like the β_2 agonists, theophylline does not have significant anti-inflammatory efficacy *in vivo*.

Anti-inflammatories:

The second category of current asthma drugs targets the inflammatory processes underlying the asthmatic response. By far the most effective drugs for the treatment of asthma are the corticosteroids. Corticosteroids are a class of steroid hormones that are naturally produced in the adrenal cortex and then travel to target cells where they bind to the glucocorticoid receptors. Synthetic corticosteroids enter the body and bind to the same receptors. After binding, they are transported to the nucleus where the zinc fingers of the steroid-bound receptors bind to glucocorticoid response elements (GREs) of DNA. This binding serves to activate transcription of some genes while suppressing transcription of others such as those coding for the pro-inflammatory transcription factor NF-κB.[26]

Corticosteroid asthma drugs fall into two subclasses based on bioavailability. Oral corticosteroids were the first class to be developed. The most widely prescribed of these is Prednisone (Figure I.3a). The natural corticosteroids such as hydrocortisone, cortisone, and corticosterone all posses key structural features that are linked to their potent antiinflammatory activity including a 3-keto group, a double bond between carbons 4 and 5, and hydroxyl groups at carbons-11,-17, and-21.[27]

Structure-activity relationship studies have shown additional chemical modifications that increase the anti-inflammatory effect, including a double bond between carbons 1 and 2 in the A ring. Selective additions of methyl, hydroxyl, flouro, and chloro groups also lead to increases in anti-inflammatory potency (Figure 1.3b).[27] However, since corticosteroids are potent, but somewhat non-specific inhibitors of inflammation, they can often have severe side effects. This is especially true when taken orally, because they must circulate throughout the body before reaching the lungs. The side effects of prolonged corticosteroid usage can be quite severe and include adrenocortical suppression, osteoporosis, muscle wasting, skin thinning, cataracts, stunted growth in children, facial rounding, decreased glucose tolerance, increased blood pressure, weight gain, and acne.[27] The use of oral corticosteroids is now generally restricted to patients with severe asthma, or in brief courses for 5-10 days for patients with milder levels of disease that are having acute exacerbations.[27]

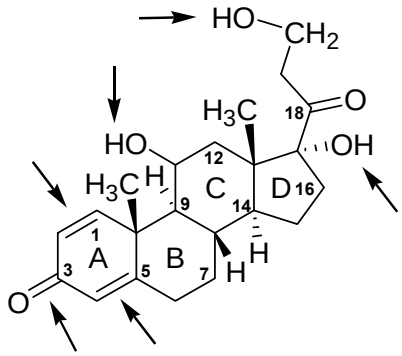

Figure 1.3b. Corticosteroid carbon skeleton. Arrows indicate structural features with important biological implications.

Corticosteroids (eg. Belcomethasone, Budenoside, Fluticasone - Figure I.3a) that can be taken in an inhaler form have the advantage of being applied directly to the

areas of desired impact, the lungs. Despite being a dramatic improvement over oral corticosteroids in terms of a reduction in side effects, inhaled corticosteroids still lead to some systemic side effects resulting from systemic absorption through oral ingestion or lung diffusion. Specific local side effects of inhaled corticosteroids include hoarseness, oral fungal infections, sore throats and coughs.[27]

An emerging paradigm in asthma drug therapy involves combining long acting β_2 agonists with inhaled corticosteroids. Drugs such as Advair, a mixture of the long acting β_2 agonist Salmeterol and the corticosteroid Fluticasone; and Symbicort, which is a combination of the long acting β_2 agonist Formoterol and the corticosteroid Budesonide, have shown increased efficacy in patients (Figure I.3a).[28] These combination inhalers facilitate asthma management in two ways: the two drugs work through complementary mechanisms of inhibition and patient compliance is increased as they only need to use a single inhaler instead of using multiple inhalers.[28]

The most recent class of anti-inflammatory asthma drugs to come to market, and the only new class of small molecule inhibitors in the last 30 years, are the antileukotrienes[25] including drugs such as Singulair, a potent and selective antagonist of the leukotriene receptor $CysLt_1$ (Figure I.3a).[20] Activation of this receptor mediates bronchoconstriction, as well as plasma and mucus secretion.[20] In a different approach to modifying the leukotriene pathway of inflammation, Zileuton inhibits of the 5-LO enzyme, blocking the production of CysLts as well as the LBT_4 leukotriene receptor which has a potential role in severe asthma (Figure I.3a).[20]

Biologics:

The third class of asthma drugs are biological drugs, such as Omalizumab, a monoclonal antibody therapy against the pro-inflammatory protein Immunoglobulin E (IgE).[29] While success has been seen in asthma management with Omalizumab, it must be taken subcutaneously and is expensive.

Another investigational biological asthma drug, Tolamba, is a synthetic analog of specific sequences of synthetic DNA that prompt the immune system to suppress Th2 cells, leading to reduced inflammation.[23,30] The synthetic drugs are based on natural sequences of bacterial DNA called CpG sequences, a shortened name for cytosine-guanine dinucleotide DNA.[31] These sequences, which are unmethylated in bacteria, are either suppressed or methylated in vertebrates.[23] This difference allows the innate immune system to recognize these bacterial DNA sequences as foreign and mount an immune response against them.[32] Synthetic modifications of these sequences, such as modification of sequence length and composition, as well as substitution of the phosphodiesterase backbone with a phosphorothioate backbone, make the compounds more stable and increases their bioavailability.[23] In humans, CpG sequences are recognized by Toll-Like Receptor 9 (TLR-9).[33] TLRs are pattern recognition receptors that are expressed on certain cells of the innate immune system such as macrophages and dendritic cells.[33] Some TLRs are activated upon the recognition of certain bacterial products such as lipopolysaccharides, peptidoglycan, zymosan, and CpG dinucleotides; while others are specific for viral products and still others for characteristic products of helminthic worms.[33] In humans, TLR-9 is activated by CpG sequences and then stimulates both T-regulatory cells and Th1

cells.[23] Both of these subsets of T-cells, through secretion of cytokines and other mediators, serve to suppress Th2 cells and their mediators, and thus weaken the asthmatic response and other related forms of inflammation.[23]

While there are several potent and effective drugs on the market for asthma, all of these have a variety of harmful side effects. Alarmingly, there are small but important subpopulations of asthmatics who are resistant to every current form of asthma medication including corticosteroid therapy.[34] Especially concerning is the rising level of severe asthma attacks and even deaths that may in some cases be related to the use of β2 agonists.[28] As was previously mentioned, in the last 30 years the FDA has approved only the anti-IgE monoclonal antibody and the antileukotriene class of small molecules as novel asthma drug therapies. These data indicate that new sources of molecules and news mechanisms of action need to be explored for the treatment of asthma if new drugs are to be developed.

References:

1. Marketos, S. G., Bronchial Ashtma in the Medical Literature of Greek Antiquity. *Journal of Asthma* **1982,** 19, (4), 263-269.

2. Elias, J. A.; Lee, C. G.; Zheng, C. G.; Ma, B.; Homer, R. J.; Zhu, Z., New Insights Into the Pathogenesis of Asthma. *The Journal of Clinical Investigation* **2003,** 111, (3), 219-297.

3. Eder, W.; Ege, M. J.; Von Mutius, E., The Asthma Epidemic. *New England Journal of Medicine* **2006,** 355, (21), 2226-2235.

4. Holt, P. G.; Sly, P. D.; Martinez, F. D.; Weiss, S. T.; Bjorksten, B.; von Mutius, E.; Wahn, U., Drug Development Strategies for Asthma: In Search of a New Paradigm. *Nature Immunology* **2004,** 5, (7), 695-698.

5. Braman, S. S., The Global Burden of Asthma. *CHest* **2006,** 130, 4S-12S.

6. Devereux, G., The Increase in the Prevalence of Asthma and Allergy: Food for Thought. *Nature Reviews: Immunology* **2006,** 6, 869-874.

7. Cookson, W., The Alliance of Genes and Environment in Asthma and Allergy. *Nature* **1999,** 402, (SUPP 25), B5-B11.

8. Abbas, A. K.; Lichtman, A. H., *Cellular and Molecular Immunology*. 5th ed.; Elsevier Saunders: Philadelphia, 2005.

9. Umetsu, D. T.; McIntire, J. J.; Akbari, O.; Macaubas, C.; DeKruyff, R. H., Asthma: an Epidemic of Dysregulated Immunity. *Nature Immunology* **2002,** 3, (8), 715-720.

10. Wills-Karp, M.; Santeliz, J.; Karp, C. L., The Germless Theory of Disease: Revisiting the Hygiene Hypothesis. *Nature Reviews: Immunology* **2001,** 1, 69-75.

11. Holt, P. G.; Macaubas, C.; Stumbles, P. A.; Sly, P. D., The Role of Allergy in the Development of Asthma. *Nature* **1999,** 402 supp., B12-B-16.

12. Fallon, P. G.; Mangan, N. E., Suppression of Th2-Type Allergic Reactions by Helminth Infections. *Nature Reviews: Immunology* **2007,** 7, 220-230.

13. Broide, D.; Sriramarao, P., Eosinophil Trafficking to Sites of Allergic Inflammation. *Immunological Reviews* **2001,** 179, 163-172.

14. Mangan, N. E.; Fallon, P. G., Suppression of Th2-Type Allergic Reactions By Helminth Infection. *Nature Reviews: Immunology* **2007,** 7, 220-230.

15. Gleich, G., Mechanisms of Eosinophil-Associated Inflammation. *Journal of Allergy and Clinical Immunology* **2000,** 105, 651-663.

16. Wills-Karp, M.; Chiaramonte, M., Interleukin-13 in Asthma. *Current Opinion in Pulmonary Medicine* **2003,** 9, 21-27.

17. Shore, S., Dirent Effects of Th2 Cytokines on Airway Smooth Muscle. *Current Opinion in Pharmacology* **2004,** 4, 235-240.

18. Busse, W. W.; Lemanske, R. F. J., Asthma. *The New England Journal of Medicine* **2001,** 344, (5), 350-362.

19. Barnes, P. J., Therapeutic Strategies for Allergic Diseases. *Nature* **1999,** 402, (SUPP), B31-B38.

20. Barnes, P. J., New Drugs for Asthma. *Nature Reviews: Drug Discovery* **2004,** 3, 831-844.

21. Barnes, P. J., Drugs For Asthma. *British Journal of Pharmacology* **2006,** 147, S297-S303.

22. Horner, A.; Van Uden, J. H.; Zubeldia, J. M.; Broide, D.; Raz, E., DNA-Based Immunotherapuetics of the Treatment of Allergic Disease. *Immunological Reviews* **2001,** 179, 102-118.

23. Krieg, A. M., Therapeutic Potential of Toll-Like Receptor 9 Activation. *Nature Reviews: Drug Discovery* **2006,** 5, 471-484.

24. Ito, K.; Lim, S.; Caramori, G.; Cosio, B.; Chung, K. F.; Adcock, I. M.; Barnes, P. J., A Molecular Mechanism of Action of Theophylline: Induction of Histone Deacetylase Activity to Decrease Inflammatory Gene Expression. *PNAS* **2002,** 99, (13), 8921-8926.

25. Cockcroft, D. W., Pharmacologic Therapy for Asthma: Overview and Historical Perspective. *Journal of Clinical Pharmacology* **1999,** 39, 216-223.

26. Barnes, P. J., How Do Corticosteroids Work in Asthma. *Annals of Internal Medicine* **2003,** 139, 359-370.

27. Gupta, R.; Jindal, D. P.; Kumar, G., Corticosteroids: The Mainstay in Asthma Therapy. *Bioorganic and Medicinal Chemistry* **2004,** 12, 6331-6342.

28. Barnes, P. J., Scientific Rationale for Using a Single Inhaler for Asthma Control. *European Respiratory Journal* **2007,** 29, 587-595.

29. Busse, W.; Corren, J.; Lanier, B. Q.; McAlary, M.; Fowler-Taylor, A.; Cioppa, G. D.; van As, A.; Gupta, N., Omalizumab, Anti-IgE Recombinant Humanized Monoclonal Antibody, for the Treatment of Severe Allergic Asthma. *Journal of Allergy and Clinical Immunology* **2110,** 108, (2), 184-190.

30. http://www.dynavax.com/ragallergy.htm

31. Raclia, D. M.; Kline, J. N., Perspectives in Asthma: Molecular Use of Microbial Products in Asthma Prevention and Treatment. *Journal of Allergy and Clinical Immunology* **2005,** 116, 1202-1205.

32. Krieg, A. M., CpG Motifs: the Active Ingredient in Bacterial Extracts? *Nature Medicine* **2003,** 9, (7), 831-835.

33. Modlin, R. L.; Cheng, G., From Plankton to Pathogen Recognition. *Nature Medicine* **2004,** 10, (11), 1173-1174.

34. Barnes, P. J.; Adcock, I. M., Steroid Resistance in Asthma. *Journal of Immunology* **1995,** 88, 455-468.

II

Screening a Natural Products Extract Library for *In Vitro* Inhibition of Pro-Inflammatory Cytokine Production by Ova-Stimulated Splenocytes

II.1

Natural Products Drug Discovery: Sources and Strategies

II.1. Natural Products drug discovery: sources and strategies.

Nearly all organisms are continuously in competition for resources including light, space, and nutrients. These stressors drive evolutionary processes and lead organisms to develop mechanisms for offense, defense, and communication, which serve to increase their overall fitness. Those organisms that did not evolve physical defenses such as a hard shell, spines, sharp teeth, or motility instead developed the ability to produce rich chemical arsenals to aid them in attack, defense, and communication. These so-called "natural products" represent an incredibly rich source of biologically active compounds.[1, 2] With respect to drug discovery, natural products, arguably, have many significant advantages over molecules from combinatorial synthetic molecular libraries because they have evolved over millennia to specifically interact with biological systems and thus have a higher likelihood in displaying activity in biological assays.[3, 4] Additionally, within a single extract of an organism, tens to upwards of a hundred biologically active molecules can be found. Often, several structural analogs of a molecule can be found allowing structure- activity relationships to be explored.

Over the last several decades, natural products have been tested for efficacy in a wide range of *in vitro* and *in vivo* models of disease. Recently, Dr. David Newman and Dr. Gordon Cragg from the Natural Products Branch of the National Cancer Institute (NCI), completed a survey of all new chemical entities (NCEs) in clinical and pre-clinical development for a wide variety of diseases between the years 1981-2006.[5] The NCEs were categorized both by disease and by molecular origin and were divided into 6 major categories including biologics, natural products, natural

product derivatives, synthetic molecules, natural product inspired synthetic molecules, and vaccines (Table II.1a) . In certain drug classes such as antibacterials and anticancer agents, natural products and related molecules comprise 63% and 69% respectively of developed drugs.[6] Other therapeutic classes such as the hypnotics, are 100 percent synthetically derived.[6] In nearly every other disease therapeutic area however, natural products and related molecules comprise a substantial number of the new chemical entities presented.[6]

Table II.1a: New Chemical Entities and Medical Indications by Source of Compound (Edited from complete reference courtesy of Dr. David Newman, personal communication).[6] (B) = biologics including large peptides and proteins, (N) = Natural Products, (ND), = Natural Product Derivatives – molecules that have semi-synthetic modifications to a natural product, (S) = Synthetic molecules, (S*) = Synthetic molecules with a natural product derived pharmacaphore, and (V) = Vaccines.[2]

generic name	trade name	chemical class	disease	year intro	source
tiotropium bromide	Spiriva		COPD	2002	S*/NM
gamolenic acid	Epogam	fatty acid	antiallergic	1988	N
loteprednol etabonate	Lotemax	Steroid	antiallergic	1998	ND
nedocromil sodium	Tildade	chromoglycate analog	antiallergic	1986	ND
pimecrolimus (SDZ-ASM-981)	Elidel		antiallergic	2002	ND
betotastine besilate	Talion		antiallergic	2000	S
emedastine difumarate	Daren	H-1 antagonist	antiallergic	1993	S
epinastine hydrochloride	Alesion	H-1 antagonist	antiallergic	1994	S
fexofenadine	Allegra	seldane metabolite	antiallergic	1996	S
lodoxamide tromothamine	Almide	aniline	antiallergic	1992	S
olopatadine HCl	Patanol		antiallergic	1997	S
oxatomide	Tinset		antiallergic	1981	S
ramatroban	Baynas		antiallergic	2000	S
repirinast	Romet	quinochromone	antiallergic	1987	S

Table II.1a: New Chemical Entities and Medical Indications by Source of Compound Continued.

rupatidine fumarate	Rupafin		antiallergic	2003	S
suplast tosylate	IPD		antiallergic	1995	S
tazanolast	Tazalest	tetrazole	antiallergic	1990	S
omalizumab	Xolair	Mab	antiasthmatic	2003	B
amlexanox	Solfa	chromoglycate analog	antiasthmatic	1987	ND
budesonide	Pulmicort	steroid	antiasthmatic	1981	ND
ciclesonide	Alvesco	steroidal	antiasthmatic	2005	ND
pemirolast potassium	Pemilaston	pyridopyridine	antiasthmatic	1991	S
tranilast	Rizaben		antiasthmatic	1982	S
levalbuterol HCl	Xopenex	R-albuterol	antiasthmatic	1999	S*/NM
pranlukast	Onon	Chromone	antiasthmatic	1995	S*/NM
broxaterol	Summair		antiasthmatic	1994	S/NM
ibudilast	Ketas	quinazoline	antiasthmatic	1989	S/NM
montelukast sodium	Singulair		antiasthmatic	1998	S/NM
seratrodast	Bronica	benzoquinone	antiasthmatic	1995	S/NM
zafirlukast	Accolate		antiasthmatic	1996	S/NM
zileuton	Zyflo	Benzothiazole-urea	antiasthmatic	1997	S/NM
acrivastine	Semprex	H-1 antagonist	antihistamine	1988	S
astemizole	Hismanal	benzodiazole	antihistamine	1983	S
azelastine HCl	Azeptin	azepine	antihistamine	1986	S
cetirizine HCl	Zyrtec	H-1 antagonist	antihistamine	1987	S
desloratidine	Clarinex / Neoclarityn		antihistamine	2001	S
ebastine	Ebastel	H-1 antagonist	antihistamine	1990	S
levocabastine hydrochloride	Livostin	morpholine	antihistamine	1991	S
levocetirizine	Xyzal / Xusal		antihistamine	2001	S
loratadine	Claritan	H-1 antagonist, tricyclic	antihistamine	1988	S
mizolastine	Mizollen		antihistamine	1998	S
rupatadine fumarate	Rupafin		antihistamine	2001	S
setastine HCl	Loderix	H-1 antagonist	antihistamine	1987	S
interferon, gamma	Polyferon	protein	antiinflammatory	1989	B
alclometasone dipropionate	Vaderm	steroid	antiinflammatory	1985	ND
betamethasone butyrate propionate	Antebate	steroid	antiinflammatory	1994	ND
deflazacort	Deflan	steroid	antiinflammatory	1986	ND
deprodone propionate	Eclar	steroid	antiinflammatory	1992	ND
fluticasone propionate	Flixonase	steroid	antiinflammatory	1990	ND
halobetasol propionate	Ultravate	steroid	antiinflammatory	1991	ND
halometasone	Sicorten	steroid	antiinflammatory	1983	ND
hydrocortisone aceponate	Retef	steroid	antiinflammatory	1988	ND
hydrocortisone butyrate	Pandel	steroid	antiinflammatory	1983	ND
mometasone furoate	Elocon	steroid	antiinflammatory	1987	ND
nabumetone	Relifex	naproxen analog	antiinflammatory	1985	ND
prednicarbate	Dermatop	steroid	antiinflammatory	1986	ND
rimexolone	Vexol	Corticosteroid	antiinflammatory	1995	ND
aceclofenac	Airtal	diphenylamine	antiinflammatory	1992	S

Table II.1a: New Chemical Entities and Medical Indications by Source of Compound Continued.

amfenac sodium	Fenazox	ketoprofen	antiinflammatory	1986	S
aminoprofen	Aldospray	ibuprofen analog	antiinflammatory	1990	S
ampiroxicam	Nacyl	isosulfostyril	antiinflammatory	1994	S
amtolmetin guacil	Enfans		antiinflammatory	1998	S
bromfenac sodium	Duract		antiinflammatory	1997	S
butibufen	Butilopan	ibuprofen analog	antiinflammatory	1992	S
butyl flufenamate	Fenazole	fenfluramine analog	antiinflammatory	1983	S
dexibuprofen	Seractyl	phenylacetic acid	antiinflammatory	1994	S
dexketoprofen trometamol	Enantyum		antiinflammatory	1996	S
droxicam	Ombolan	pyroxicam analog	antiinflammatory	1990	S
etodolac	Lodine	indomethacin analog	antiinflammatory	1985	S
felbinac	Napageln	diphenylacetic acid	antiinflammatory	1986	S
fepradiinol	Flexidol		antiinflammatory	1989	S
flunoxaprofen	Priaxim	phenylacetic acid	antiinflammatory	1987	S
flurbiprofen sodium	Ocufen		antiinflammatory	1987	S
ibuprofen guaiacol ester	Benflogin	ibuprofen analog	antiinflammatory	1987	S
isofezolac	Sofenac	imidazole	antiinflammatory	1984	S
isoxicam	Pacyl	sudoxicam analog	antiinflammatory	1983	S
lobenzarit sodium	Carfenil	mefanamic acid	antiinflammatory	1986	S
lonazolac calcium	Lonax		antiinflammatory	1981	S
lornoxicam	Xeto		antiinflammatory	1997	S
loxoprofen sodium	Loxonin	phenylpropionic acid	antiinflammatory	1986	S
mesalamine	Asacol	aminosalicylate	antiinflammatory	1984	S
mofezolac	Disopain	oxazole	antiinflammatory	1994	S
nepafenac	Nevanac	ketoprofen	antiinflammatory	2005	S
nimesulide	Aulin	nitrosulfonamide	antiinflammatory	1985	S
osalazine sodium	Dipentum	salicylate	antiinflammatory	1986	S
oxaprozin	Duraprox	oxazole	antiinflammatory	1983	S
piketoprofen	Calmatel	ibuprofen analog	antiinflammatory	1984	S
pimaprofen	Besicum	ibuprofen analog	antiinflammatory	1984	S
piproxen	Piproxen	naphthalene	antiinflammatory	1986	S
piroxicam cinnamate	Sinartrol	benzothiazoline	antiinflammatory	1988	S
pranoprofen	Niflan		antiinflammatory	1982	S
tenoxicam	Tilcotil	pyroxicam	antiinflammatory	1987	S
tropesin	Repanidal		antiinflammatory	1990	S
zaltoprofen	Soleton	tricyclic antidepressant	antiinflammatory	1993	S
doxofylline	Ansimar	theophylline analog	bronchodilator	1985	ND
oxitropium bromide	Oxivent	scopolamine analog	bronchodilator	1983	ND
bambuterol	Bambec	ephedrine analog	bronchodilator	1990	S*/NM
formoterol fumarate	Atock	propranolol analog	bronchodilator	1986	S*/NM
mabuterol HCl	Broncholin	propranolol analog	bronchodilator	1986	S*/NM
pirbuterol HCL	Exirel		bronchodilator	1983	S*/NM
salmeterol xinafoate	Serevent	propranolol analog	bronchodilator	1990	S*/NM
tulobuterol HCl	Berachin		bronchodilator	1981	S*/NM

Interestingly, of the 1,184 therapeutics described, only 102 or 8.6% fall into categories relating directly to asthma, allergy and other inflammatory mediated diseases (Table II.1a).[6] The therapeutic mechanisms of these potential drugs include antiallergic, antiasthmatic, anti-COPD, anti-inflammatory, antihistamine, and bronchodilatory (Table II.1a).[6] Of the 102 inflammation related drugs, roughly 52% (53) of them have their origins in small molecule natural products with another 10.8 % (11) of them arising from large peptide or protein sources.[6]

Large potions of these natural products and natural product related molecules fall into a few distinct categories. One of the most prevalent of these molecular scaffolds is the steroidal motif, of which there are 14 mentioned in this study.[6] Although these new steroids are modifications of previously described and heavily investigated chemical scaffolds, they are still considered new chemical entities and have contributed a substantial portion of the natural product related molecules seen in the inflammatory related categories.[6] Another significant fraction of the inflammation-related natural products and derivatives arises from terrestrial plant sources discovered from treatments used by indigenous peoples including derivatives of cromolyn and ephedrine.[6]

Data from the study by Newman and Cragg illustrate two important points. One of these is that relative to other disease states such as cancer, drugs for treating allergy, asthma, and inflammation are in short supply. The second is that roughly half of the drugs developed for allergy, asthma, and inflammation are derived from or inspired by natural products. Thus, naturally occurring molecules represent a relatively under-investigated source of small molecule drugs and drug-like molecules.

Although natural product extracts represent a veritable gold mine of potent biologically active molecules, they also come with their own sets of challenges. When creating a natural products screening program, two critical components that need careful consideration are the types or organisms used and the methods used to screen them. In deciding which sources of material to investigate, biological novelty is one of the most important factors in discovering novel chemistry. Marine bacteria are a vast, yet largely unexplored source of both biological and chemical diversity. For decades, natural products chemists have shown that marine sponges, corals, and ascidians contain a wide variety of chemically unique, potently bioactive natural products.[7] Similarly, cyanobacterial mats and larger scale assemblages have also proven to be chemically rich.[7] However, it is only quite recently that marine bacteria, both free-living and symbiotic, have been shown to produce a significant fraction of natural products.[8] This discovery has important implications for chemists and biologists searching for biologically active natural products, as marine bacteria provide many benefits over macro-organisms.

One of the most important advantages of working with natural products from marine bacteria is molecular supply. Because many of these organisms can be cultured in the laboratory, additional material for biological and chemical investigations can be obtained with minimal environmental damage. Advances in culturing techniques such as novel media use, cultivation using seawater, and culturing time optimization through time-course studies of metabolite production, have begun to further open the door towards accessing this chemical treasure trove. By contrast, the repeated and wide spread collecting efforts often required in order to obtain sufficient

material from macroorganisms can be devastating.[9] One of the most famous of these examples was the early isolation effort of the cancer drug Taxol from the Pacific Yew tree *Taxus brevifolia*. During the course of bringing Taxol through development and clinical trials, hundreds of thousands of these trees were harvested in order to procure the tens of thousands of pounds of tree bark needed to extract the amount of Taxol used in the trials.[10]

An additional advantage to working with microbes is the accessibility of their genetic makeup and our increasing ability to discover and modify their metabolic capabilities to increase production of and modify their biologically active metabolites.[11, 12] For example, genes are clustered in bacteria and fungi and not in plants and animals, and bacterial generation times are much shorter making mutation experiments more efficient. Additionally, in general, microbial genomes are much smaller than in plants and animals, making sequencing, gene identification and knockout experiments more feasible.

Biological screening efforts using natural product extracts can be frustrated by factors including nuisance compounds. In the search for novel drugs, these molecules are called nuisance compounds either because they act in a non-specific manner, such as allosterically binding to proteins, or because their chemical motifs are already known to drug discovery.[13] Additionally, other compounds can interfere with assay detection capabilities. For example, molecules with conjugated double bond systems often interfere with fluorescence based detection systems, leading to false hits. Fortunately, sample preparation technology has advanced to begin to address the problems of these common nuisance compounds. Steps such as pre-treatment of

extracts and chromatography fractionation prior to assay screening aids greatly in removing these compounds before the samples enter the biological assay.[13]

Microbes produce their own sets of nuisance compounds that might interfere with assay results. In addition to a range of compounds similar to those of macro-organisms, such as polysaccharides, peptides and saturated and unsaturated fatty acids, the extracts of microbial cultures also contain components derived from the culture media, which may exert a biological influence. Many of these compounds can be removed through extraction and pre-fractionation procedures such as solvent partitioning and chromatography.

The choice of organism to be screened can also influence the false positives and nuisance compounds. For example, when screening for compounds with anti-inflammatory properties, gram-positive bacterial extracts hold a particular value for assay screening in relation to other types of organisms in that they do not produce many of the compounds that may be seen as nuisance or false positives. Specifically, compounds such as hopanoids, prostaglandins, polyunsaturated fatty acids, and lipopolysaccharides; (seen in plant, animal and gram-negative bacterial extracts) are not produced by gram-positive bacteria and so will not show up in screening results.

II.2

Development and application of an *in vitro* assay for detecting compounds that inhibit the production of pro-inflammatory cytokines

II.2. Development and application of an *in vitro* assay for detecting compounds that inhibit the production of pro-inflammatory cytokines

Before this thesis work began, marine microbial natural products had never been screened for their ability to inhibit cellular pathways related to allergic asthma. With the assistance of Professor David Broide at the UCSD School of Medicine, I developed an assay amenable to the screening of marine microbial extracts in a mouse model of allergic inflammation. To reflect the complex, multi-cellular pathogenesis of asthma, we utilized primary cell cultures of mouse spleen cells (a mixture of several cell types, including dendritic cells, T-cells, and B-cells, all of which are found in the lung in asthma and play key roles in the development of allergic inflammation) as the cellular basis of our assay. Since the allergic asthma cascade is created and propagated through specific interactions between these cell populations, it can be more accurately and effectively modeled through a mixed cell population (T cells, B-cells, dendritic cells) as opposed to a single homogeneous cell line.

In the initial phase of the assay, juvenile BALB C mice (approximately 6 weeks old) are sensitized to the allergen, chicken ovalbumin (OVA). The mice are given weekly injections over a four-week period of OVA allergen combined with an aluminum adjuvant in order to create a Th2 biased immune response specific for the OVA allergen. In the initial period, mouse allergen presenting cells such as dendritic cells ingest the OVA allergen + adjuvant, digest the allergen, and present a characteristic peptide fragment to the Th-2 cells. Those Th-2 cells that recognize the allergen then undergo clonal expansion, creating a larger Th-2 cell population that is

specific for the OVA allergen. With each subsequent weekly injection, the number of OVA-specific Th2 cells grows exponentially.

At the conclusion of the 4-week sensitization period, the mice are sacrificed and their spleens are surgically removed to provide material for the primary splenocyte cell culture. The spleens of 4 age-matched BalbC mice are combined and passed through a 0.5-micron filter into RPMI-1640 media to remove the majority of the organ tissue. The cell suspension is then centrifuged to create a splenocyte cell pellet. The supernatant is removed and the cells are then re-suspended in media. Cell concentrations are calculated by dilution in Trypan Blue cell-staining solution and counted using a hemocytometer. Media is added until the cells reach a concentration of 1.3×10^7 cells per milliliter. One hundred μL of this cell suspension is added to each well of a 96 well plate, except for the outer rows and columns of the plate that are left as blanks with 200 μL of PBS added to prevent sample well evaporation during the incubation period.

The sample cell culture plates are all internally standardized with positive and negative controls, as well as with a drug standard. The positive control consists of cultured splenocytes with added OVA antigen and dimethyl sulfoxide (DMSO) and the negative control consists of cultured splenocytes with added DMSO but no stimulating antigen. The drug standard added is the anti-inflammatory corticosteroid Dexamethasone. By comparing the activities of our microbial samples to corticosteroids in our assay, we are measuring the potency of our active samples against that of the most potent anti-inflammatory drugs available, thereby ensuring that only potent molecules are pursued further. In the remaining wells, the samples to

be tested are added. In the initial phase of the screen, crude microbial extracts were screened and later, extract fractions and pure molecules.

The Fenical laboratory at the Scripps Institution of Oceanography houses a library of over 10,000 crude extracts of marine derived microbes collected from around the world. Samples of these extracts are preserved in DMSO at concentrations of 25 mg/ml and are stored in 96-well plates at -20º C. From these mother plates, I prepared daughter plates at the diluted concentration of 5 mg/ml, a concentration determined through trial experiments to yield a 2% hit rate per plate. This hit rate allowed me to focus on the most potent of the extracts as well as to provide a sample size that could reasonably be examined by a single person.

Aliquots from the these daughter plates were diluted 10-fold in cell culture media to give a 0.5 mg/ml extract concentration and 10 µL of these diluted extracts was then added to the cell suspensions in the 96-well culture plates. After addition of the extracts, 10 µL of OVA allergen suspended in PBS was added to the spleen cells in each well, bringing the final volume to 120 µL/well and the final microbial extract concentration to 42 µg/well.

Once the marine microbial extracts and the OVA allergen were added to the cell suspensions in the culture plates, the plates were incubated at 36 ºC for 48 hours. During this time, stimulated splenocytes that were not otherwise inhibited produced a suite of pro-inflammatory cytokines, which were secreted into the media. At the same time, the splenocytes settled to the bottom of the cell culture plate and adhered to the surface. At the end of the 48-hour culture period, the supernatants of the cell culture wells were removed for cytokine quantification by enzyme linked

immunosorbent assays (ELISAs) as described below. I then stained the splenocytes, which adhered to the bottom of the cell culture wells, with Trypan blue and visualized them under a microscope to qualitatively determine cell viability. Trypan blue is a dye that is readily adsorbed by dead cells but is excluded from live cells, giving a robust and inexpensive indication of cell viability.

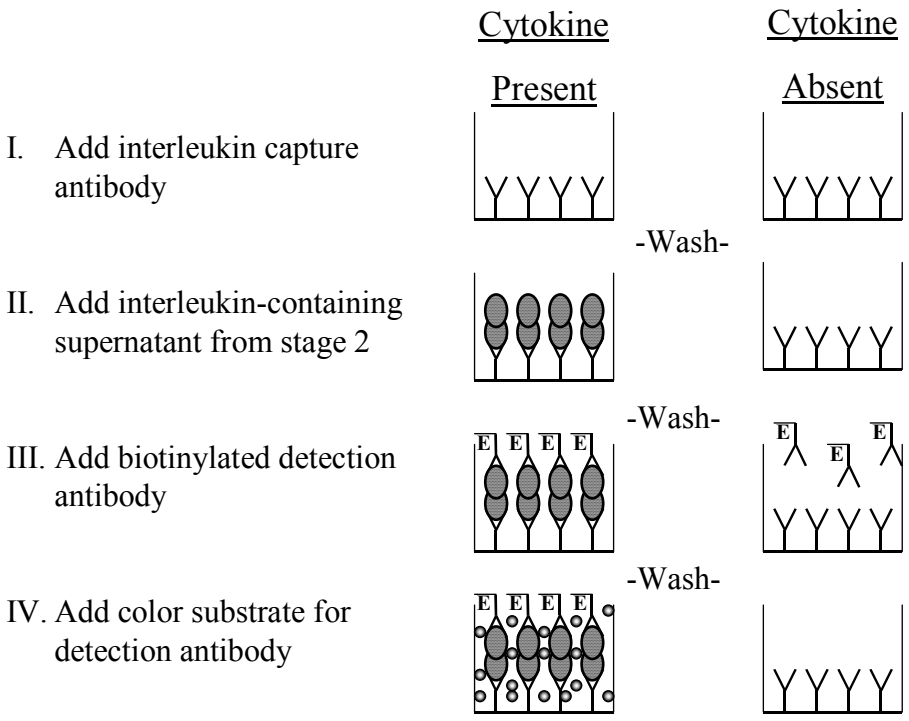

Figure II.2a: ELISA assay schematic

In the initial screening of crude extracts and active fractions, ELISAs specific for the eosinophil activating cytokine IL-5 were utilized.[14-16] ELISAs work by capturing a specific protein (in this case IL-5) from a heterogeneous mixture. The first step was to incubate a 96-well ELISA plate with an IL-5a capture antibody with high affinity for a specific epitope (the part of a protein recognized by antibodies and other parts of

the immune system such as T-cells and B-cells) of IL-5. The remaining capture antibody that did not bind IL-5 was washed off the plate. Next, the blocking protein, bovine serum albumin (BSA) was added to occupy the remaining surface area of the well. After blocking, the remaining BSA was washed off and the cell culture supernatants were added. In separate wells of the same plate, serial dilutions of known concentrations of IL-5 were incubated to create standard curves for IL-5 assay calibration. After a one-hour incubation period, the adhered IL-5 capture antibodies bind the IL-5 present in the cell culture supernatants. The supernatants are then removed by aspiration and the plates are washed again.

To detect the bound IL-5, a second IL-5 'detection' antibody is added to each well. The antibody, which is a biotin-coated monoclonal antibody specific for a second epitope of IL-5 is incubated for one hour, and then the remaining unbound antibody is washed away. A streptavidin horseradish peroxidase (SHRP) is then added and binds to the biotin on the detection antibody. The remaining unbound SHRP is then washed away and a substrate reagent comprised of hydrogen peroxide and chromogen (tetramethylbenzidine) that is oxidized by SHRP to give a blue reaction product is added. The reaction is stabilized through the addition of a dilute concentration of sulfuric acid, which changes the blue color to yellow. The absorbance of each well is measured at 450 nm and then sample wells are calibrated to the absorbance values of the IL-5 standard curve wells. The result is quantitatively related to the amount of the IL-5 bound in each ELISA plate well and hence the amount of IL-5 present in the cell culture supernatants of each splenocyte culture well.

One of the strengths of this assay is its ability to produce both cytotoxicity and cytokine inhibition data from the same culture well, thereby ensuring a more direct correlation. We investigated extracts that displayed strong inhibition of IL-5 production with little to no cytotoxicity. We defined a positive hit in this primary screen as an extract that inhibited IL-5 production by greater than 75% in allergen stimulated cell cultures relative to the allergen stimulated control cultures. A high level of inhibition was chosen in order to initially focus on only those extracts with the strongest activity.

Another strength of the assay is that it permits facile screening for inhibition of a whole suite of cytokines within a single supernatant. Due to the exquisite selectivity of the ELISA assays, after our cell culture supernatants have been examined for one cytokine, (for example IL-5), the same supernatants can be transferred to another ELISA plate specific for a different cytokine (such as IL-13).

The ELISA data also has the potential to reveal cell-specificity including where in the cellular inflammatory cascade the samples may be acting. The splenocyte cell culture used in this assay consists of a heterogeneous cell population in which several types of cells communicate with each other, and certain cytokines are primarily produced by specific cell types. As was shown earlier, in our model of allergic inflammation the activated antigen presenting cells (which produce IL-1 and TNF-α) are responsible for activating Th2 cells (which then produce IL-5). Therefore, if the ELISA results showed that a compound significantly inhibited the production of IL-5 and not IL-1 and TNF-α, then it is more likely that the compound is acting primarily on the Th2 cells and not the allergen presenting cells (APCs). However, if both APC

and Th2 cytokines are inhibited, the data is consistent with either a global suppression mechanism of both APCs and Th2 cell populations, or specific inhibition of only the APCs, preventing concomitant activation of Th2 cells ultimately resulting in a lack of IL-5 production.

Although this assay is relatively labor intensive, the quality of information more than offsets this initial investment of time. The quantitative data obtained for production of a whole suite of cytokines allows us to begin teasing apart mechanisms of action at a relatively early stage of the screening process. By combining cytotoxicity data with cytokine production in the same assay well the assay eliminated the need for an additional separate assay to directly correlate the two results. With respect to therapeutic relevance, the heterogeneous cell population of splenocytes used in this assay closely models *in vivo* the system observed in animal models. Finally, this assay is readily translated to a whole animal model. Once active compounds are isolated and identified in the *in vitro* mouse assay, an *in vivo* mouse asthma model can be readily implemented using the same sensitization procedure used to produce the primary cells for the *in vitro* experiment, thereby increasing the chances of translational efficacy from a cellular to a whole animal model.

II.3

Hit Identification from the Fenical Laboratory's Marine Microbial Extract Library

II.3. Hit Identification from the Fenical Laboratory's Marine Microbial Extract Library

In an initial screening of natural products extracts, there are two approaches that can be taken. One method is to screen a large number of crude extracts and this is the method I utilized in the thesis research. The second method is to screen a potentially smaller number of extracts but enhance the data obtained from these strains through a process of pre-fractionation of the extracts into several sub-fractions of varying polarity. Recent studies show that the process of pre-fractionation has yielded great benefits in the removal of nuisance compounds as well as in unmasking potentially highly active compounds that were present in concentrations too low to be detected in the crude extract mixture. While the process of pre-fractionation has proved very beneficial to current screening programs, it is also a very time and labor intensive effort. At the time of the screening efforts for the thesis research, a pre-fractionated extract library did not exist in the Fenical Laboratory and so screening was performed with crude extracts, thereby increasing the number of microbial strains examined but perhaps missing out on some important compounds with therapeutic potential. Currently, there is a serious effort being invested by others in the Fenical Laboratory to create a pre-fractionated library of the new microbial extracts collected. It would be interesting in the future to screen this pre-fractionated library in the splenocyte assay to investigate whether other strains contained IL-5 inhibitory activity.

I performed a large-scale screen of 2,500 crude extracts from the marine microbial extract library in the splenocyte assay and identified ninety-five of the most potent of these extracts for further chemical and biological investigations (Table II.3a). I also

compared the splenocyte assay data with available screening data for the same extracts against HCT-116, a human colon cancer cell line (courtesy of Sara Kelly in the Fenical Laboratory) (Table II.3a). Interestingly, many of the extracts that showed little to no levels of cytotoxicity in the splenocyte cell cultures showed high levels of cytotoxicity against the HCT-116 cell line and vice versa. To maximize the therapeutic relevance of molecules discovered, I chose to focus primarily on extracts that displayed low cytotoxicity levels in both the cancer and splenocyte cellular assays. In addition to providing data on non-toxic compounds for the purposes of this thesis research, these data could also be used by others for selecting anti-cancer projects to investigate. Extracts which show high HCT-116 toxicity with little toxicity against spleen cells would be a desirable target to investigate for compounds with selective activity towards cancer cells.

Table II.3a: HCT-116 cell survival data for marine microbial extracts exhibiting greater than 75% IL-5 inhibition and less than 50% cytotoxicity in the splenocyte assay.

Strain #	HCT	Strain #	HCT	**Strain #**	HCT
CNQ585	80%	CNR696	21%	CNR268	91%
CNQ542	0%	CNQ275	-	CNR090	45%
CNQ544	0%	CNQ339	-	CNR329	5%
CNQ610	3%	CNR002	99%	CNR334	2%
CNQ614	2%	CNP249	9%	CNQ857	65%
CNQ544	3%	CNR046	4%	CNR291	57%
CNQ805	34%	CNR054	1%	CNR687	80%
CNQ804	2%	CNR037	0%	CNR431	79%
CNQ805	43%	CNP242	-	CNQ418	35%
CNQ956	99%	CNP372	1%	CNQ552	1%
CNQ980	29%	CNB903	67%	CNQ565	-
CNQ956	18%	CNP351	2%	CNR717	54%
CNQ914	19%	CNB908	10%	CNR717	59%
CNQ9414	30%	CNP446	4%	CNQ688	2%
CNQ956	2%	CNP448	3%	CNQ359	51%
CNR014	66%	CNP965	100%	CNQ573	5%
CNR091	35%	CNQ097	100%	CNQ443	99%
CNR125	1%	CNP969	100%	CNQ524	20%
CNR106	84%	CNB927	100%	CNQ501	84%
CNR132	44%	CNQ084	100%	CNQ624	113%
CNR266	37%	CNB924	100%	CNQ651	21%
CNR525	79%	CNJ739	2%	CNJ834	77%
CNR685	83%	CNJ728	2%	CNJ865	88%
CNR685	94%	CNJ734	-	CNJ742	82%
CNR687	84%	CNN936	100%	CNJ863	16%
CNR380	91%	CNT002	100%	CNJ826	74%
CNR371	116%	CNN933	94%	CNJ820	100%
CNQ435	100%	CNJ751	68%	CNJ850	100%
CNR291	100%	CNJ742	91%	CNJ836	98%
CNP982	100%	CNJ754	68%	CNJ772	84%
CNH004	100%	CNJ805	77%	CNJ781	86%
CNJ738	2%	CNJ803	89%		

Microbial strains that displayed non-cytotoxic, IL-5 inhibition were then re-grown in 1-5 L liquid cultures. The resulting culture broths were extracted, and the extracts

were concentrated, and then fractionated to yield samples with sufficient mass for assay screening and chemical investigation. The microbial culture extraction was performed using Amberlite XAD resin added to the culture broth. XAD is a polymeric highly porous adsorbent that can adsorb and desorb a wide variety of substances depending on the solvent it is suspended in.[17] XAD resin preferentially captures the more hydrophobic organic material and excludes polar media components, often increasing the yields of desired compounds and minimizing the effort needed to concentrate extracts. After shaking for several hours, the cultures were strained through cheesecloth and the cellular material and XADresin were extracted with acetone and concentrated by rotary evaporation.

Once the marine microbial cultures were extracted, I performed an initial fractionation step using Diaion HP-20 (polystyrene-divinylbenzene) resin before re-tesing them in the splenocyte assay.[18] I fractionated the microbial extracts by passing them through a glass column filled with HP-20 that was pre-equilibrated with methanol. The eluents were then diluted with water and passed through the column a second time to ensure binding of the non-polar molecules to the resin. Fractions of decreasing polarity were then eluted from the column using a water and acetone step gradient to give 5 fractions for bioassay. These fractions were then diluted with water and passed back through the columns, and then eluted with 100% acetone to facilitate ease of sample drying. Results from several of the extracts fractionated in this manner revealed that this method concentrated certain nuisance compounds (including fatty acids and diketopiperazines) resulting in cytotoxic fractions that may have

masked the activity of other molecules. For this reason, we altered the fractionation procedure for the remaining active extracts.

The remaining active marine microbial extracts were fractionated as follows. After concentrating the acetone extract, I partitioned it between H_2O and EtOAc. I then subjected the EtOAc fraction to preparative C18 reversed phase HPLC with an acetonitrile (MeCN) : water step gradient starting with an isocratic step of 20% MeCN for 10 minutes to separate the most polar compounds and then increasing the MeCN concentration from 20 to 100% over a total of 60 minutes followed by a final MeOH washing step. The fractions obtained were concentrated to dryness and then suspended in DMSO for bioassay. Fractions obtained using this method generally contain only 1-3 compounds, resulting in facile compound isolation. Additionally, the 96-well format of the splenocyte assay was readily expanded to accommodate the increased number of fractions. The fractionation process can be further streamlined through automation for industrial application.

During the course of identifying the molecules responsible for cytokine inhibition in the spleocyte assay, several compounds were isolated whose structures and biological activities had been previously described in the literature. One of these groups is the staurosporines (Figure II.3a). Staurosporines are characterized by an indolo [2,3-α] carbazole core and contain various modifications and functionalities.[19] They have been shown to display activity in a host of biological assays such as anti cancer, anti fungal, and anti bacterial.[19-21] Staurosporine analogs are potent inhibitors of multiple cellular processes, such as inhibition of protein kinase C at nanomolar levels through competition with ATP at the PKC catalytic site.[20] Interestingly, at sub-

lethal levels (i.e. picomolar), staurosporines exhibit potent anti-proliferative activities in several cancer cell models through complex interactions with cyclin dependent kinases (CDK).[19-21] These interactions lead to the reversible arrest of non-proliferating cells in the G_1 phase of the cell cycle[21]. This sub-lethal cell cycle arrest could explain the reduction in cytokine production seen in the splenocyte assay in the presence of trace amounts of staurosporines. Becasue staurosporines have a very characteristic UV absorption spectrum, their presence is readily detected even in trace amounts by LCMS or photo-diode-arrayed-HPLC.

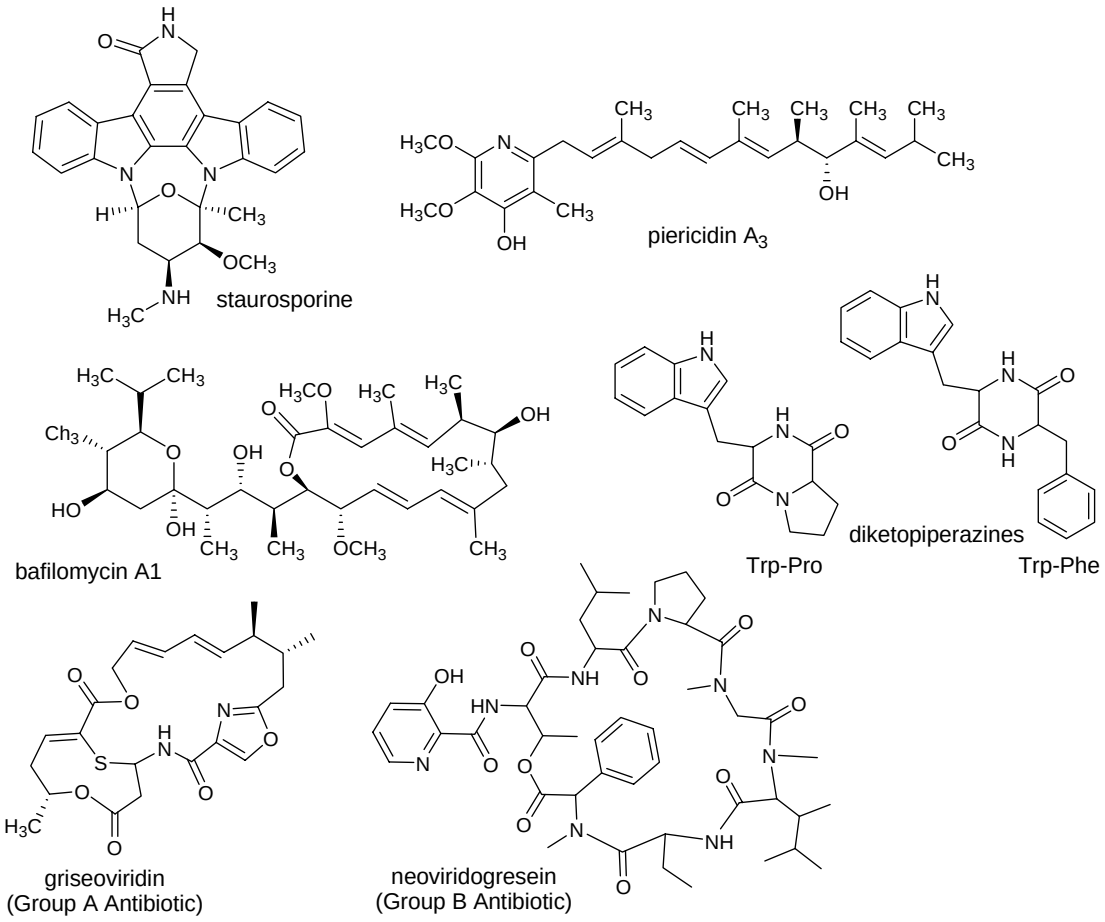

Figure II.3a: Known compounds that display activity in the splenocyte assay

The piericidins also appeared frequently as the active components of the IL-5 inhibitory microbial extracts (Figure II.3a).[22-25] Piericidins consist of a terminal pyridine moiety coupled to an olefinic carbon chain of variable length and functionality.[22-25] Much like the staurosporines, the piericidins are active at nanomolar levels in the splenocyte assay in addition to exhibiting activity in a number of other bioassays.[26-28] Biological studies have shown that these compounds act in cellular systems through inhibition of complex I in mitochondria.[27] In the

splenocyte assay this type of activity could decrease cellular respiration, leading to a decrease in cytokine production levels.

Additional IL-5 inhibitory molecules, whose structures have previously been described in the literature, include a variety of cyclic dipeptides called diketopiperazines (Figure II.3a). These molecules originate from the fusion of two amino acids to form a central bis-lactam ring. They can be produced biosynthetically or via abiotic processes such as the heating of the extract media, which may occur during isolation procedures. Diketopiperazines have been shown to display a wide variety of biological activites, including anti-inflammatory and immunosuppressive activities. [29-31]

The streptogramin antibiotics, including griseoviridin, and neoviridogrisein also displayed activity in the splenocyte assay (Figure II.3a). These antibiotics have been known for several decades to be produced by terrestrial microbes of the genus *Streptomyces*. However, this is the first time this class of compounds is being reported from a marine bacterial strain. Streptogramin antibiotics consist of two different groups, type A and type B antibiotics, both of which were isolated from microbial strains active in this assay. Members of type A (such as griseoviridin, Figure II.3a) are cyclized polyketide-amino acid hybrids consisting of a C-terminal D-proline, alanine, or cysteine, an oxazole ring derived from serine, and a polyketide portion.[32] The type B streptogramin antibiotics (such as neoviridogrisein, Figure II.3a) are comprised of hexa- or heptadepsipeptides and consist of both D and L amino acids cyclized through an ester bond between a C-terminal phenylglycine and the hydroxyl group of an N-terminal threonine.[32] Both type A and type B streptogramin

antibiotics independently exert a bacteriostatic effect on staphylococci and streptococci by temporarily inhibiting protein synthesis.[32] When present together, they exert a bacteriocidal effect on these same types of bacteria, however their possible mechanism of action in the splenocyte assay is not known.[32] Other previously described molecules that I identified in active fractions include members of the kirromycin, mytomycin, and bafilomycin families of antibiotics.

Table II.3b: Microbial strains and compounds observed and/or isolated from them:

Strain #	Phylogenetic Information	Compound Classes Isolated
*CNJ738	Actinomycete	aromatic/polyene
*CNJ772	*Bacillus*	aromatic/polyene
CNJ781	*Bacillus*	diketopiperazines
CNJ803	*Bacillus*	diketopiperazines
*CNJ820	*Dietzia*	terpenoid/sterol
CNN936	fungus	diketopiperazines: trp-trp, phen-trp, pro-trp
CNP965	Actinomycete	diketopiperazine
*CNQ275	Actinomycete	fatty acids, polyenes
*CNQ359	Actinomycete	polyene
*CNQ435	*Nocardiopsis* (Mar-11)	polypeptide
*CNR525	Actinomycete	downfield-shifted methyls
CNQ565	*Streptomyces*	Kirromycin
CNQ585	Actinomycete	mitomycins
CNQ624	Actinomycete	griseoviridin, viridogriseins
CNQ687	Mar-3A	diketopiperazines
*CNQ688	Actinomycete	polyene
CNQ857	Mar-3A	diketopiperazines
*CNR002	Mar-1-like	peptides
CNR014	Actinomycete	diketopiperazines, lipid glycerols
CNR032	Actinomycete	diketopiperazines
CNR097	Mar-1-like	diketopiperazines
*CNR106	Actinomycete	peptides
CNR251	Mar-1	Staurosporine, arenicolide
CNR268	Mar-1	Staurosporine
CNR291	*Micromonospora*	nor-diterpenes
*CNR344	Mar-1-like	polyene
*CNR371	Mar-2	polyenes
CNR536	Actinomycete	antimycin-like
*CNR685	Mar-2	polyenes
CNR717	*Nocardiopsis*	piericidins
CNR927	Mar-4	bafilomycin
CNS153	Actinomycete	diketopiperazines
CNT002	fugus	diketopiperazines

* Indicates microbial strains now under investigation by postdoctoral scholars in the Fenical Laboratory.

Through the course of fraction analysis, I identified several extract fractions, based on ^{1}H NMR data, that appear to contain interesting molecules such as polyenes (as observed by coupled signals between 5 and 7 ppm), terpenes or sterols (as observed by coupled signals between 2.4 and 4 ppm), and compounds containing several N or O methyl goups (observed as sharp three-proton equivalent singlets between 2.5 and 4 ppm). Although these fractions did not display significant activity in the splenocyte assay, twelve of these projects have now been given to postdoctoral scholars in the Fenical Laboratory for further chemical investigation and biological testing in other assays (Table II.3b).

Finally, several "nuisance compounds" were identified in many of the microbial strains. These nuisance compounds include solvent impurities, such as phthalate esters, components of primary metabolism such as indole-3-glycerol which is a precursor to tryptophan catabolism, and non-specific inhibitors such as lipophylic fatty acids. These compounds would likely have little therapeutic relevance in an *in vivo* model.

II.4

Collaborative Efforts to Discover New Inhibitors of Cytokine Production

II.4. Collaborative Efforts to Discover New Inhibitors of Cytokine Production

With the assay established, I began collaborating with other members of the Fenical Laboratory to investigate the potential biological activity of a variety of chemically interesting molecules from genetically distinct marine-derived bacteria which had failed to show cytotoxic activity in anti-cancer, anti-bacterial and anti-fungal assays. In this way, I identified two groups of molecules that exhibited non-toxic inhibition of IL-5 in the mouse splenocyte assay (Figure II.4a).

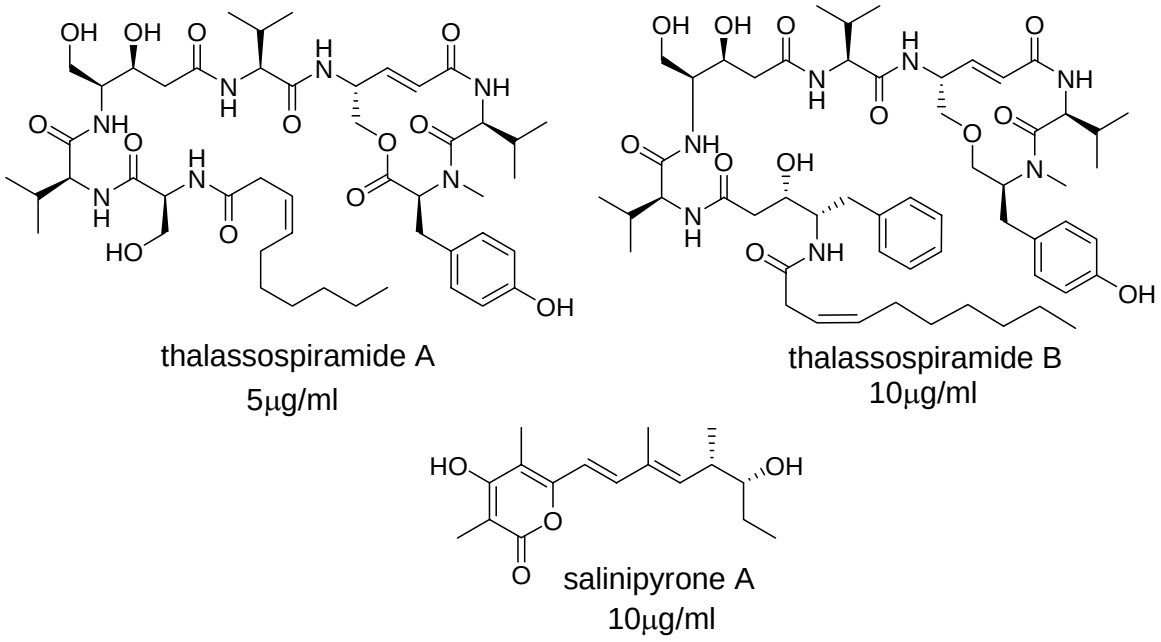

Figure II.4a: IC_{50} values of compounds isolated by collaborators that inhibited IL-5 produciton of OVA stimulated splenocytes.

The thalassospiramides are two lipopeptides isolated by Dong-Chan Oh that failed to show any cytotoxic activity in the HCT or antimicrobial assays (Figure II.4a).[33]

When tested in the splenocyte assay, thalassospiramide A had an IC_{50} of 5 μg/ml and thalassospiramide B had an IC_{50} value of 10 μg/ml. These compounds were isolated from a new marine eubacterium that is genetically related to the α-preoteobacterium *Thalassospira luceniencis* and represent the first natural products from this genus.[33] Compounds of this structural motif have never been described in allergic inflammation therapy before, making this an exciting area of future research. Additionally, although these compounds are not as potent as corticosteroids, their peptide nature presents avenues for future synthetic structural modifications in an effort to increase the potency.

Another molecule whose cytokine-suppressive activity was uncovered as a result of collaborative efforts in the Fenical Laboratory is salinipyrone A, also isolated by Dong-Chan Oh (Figure II.4a). This molecule was produced by the marine actinomycete *Salinispora pacifica* which is the third species to be described from this new genus. Like the thalassospiramides, salinipyrone A displayed no significant activity in in-house cytotoxicity assays against HCT, MSRA, and *Candida albicans* yet displayed non-cytotoxic inhibition of IL-5 production with an IC_{50} of 10 μg/ml.

Some compounds tested during this collaboration did not suppress cytokine production yet exhibited cell-specific cytotoxicity toward splenocytes, which could prove beneficial in other realms of disease therapies. Azamerone, and actinofuranones A and B are both produced by different strains of proposed new genus of marine bacteria, MAR 4.[34, 35] These compounds displayed no cytotoxic activity against HCT, *Candida albicans* fungal cell lines, or against MSRA but were cytotoxic towards splenocytes at 20 to 40 μg/ml (Figure II.4b).[34, 35] This selective cytotoxicity

suggests that these compounds target cell specific receptors or proteins in splenocyte cells. However, further experimentation is needed to elucidate the exact mechanism of splenocyte toxicity.

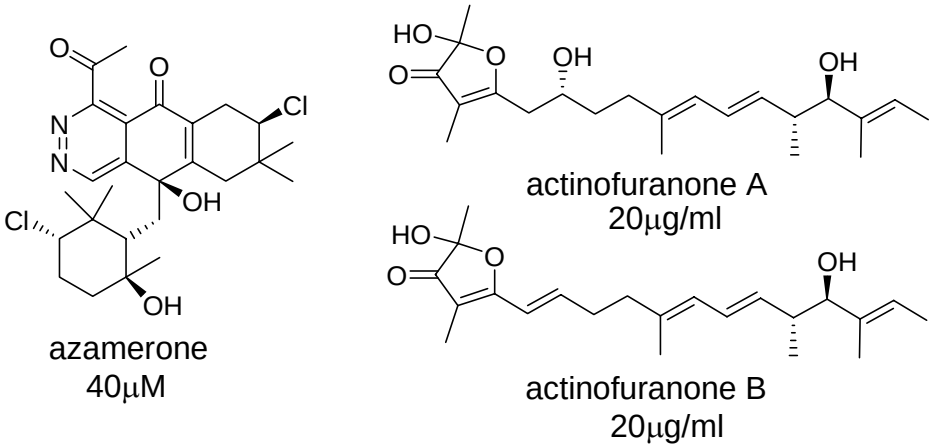

Figure II.4b: New compounds with selective cytotoxicity against splenocytes.

References:

1. Newman, D. J.; Cragg, G. M.; Snader, K. M., The Influence of Natural Products Upon Drug Discovery. *Natural Products Reports* **2000,** 17, 215-234.

2. Butler, M. S., The Role of Natural Product Chemistry in Drug Discovery. *Journal of Natural Products* **2004,** 67, 2141-2153.

3. Koehn, F.; Carter, G. T., The Evolving Role of Natural Products in Drug Discovery. *Nature Reviews: Drug Discovery* **2005,** 4, 206-220.

4. Feher, M.; Schmidt, J. M., Property Distributions: Differences Between Drugs, Natural Products, and Molecules from Combinatorial Chemistry. *J. Chem. Inf. Comput. Sci.* **2003,** 43, 218-227.

5. Newman, D. J.; Cragg, G., Natural Products as Sources of New Drugs Over the Last 25 Years. *Journal of Natural Products* **2007,** 70, (3), 461-477.

6. Newman, D. J., NCE's Excell Spreadsheet. In Strangman, W., Ed. 2007.

7. Haefner, B., Drugs from the Deep: Marine Natural Products as Drug Cantidates. *Drug Discovery Today* **2003,** 8, (12), 536-544.

8. Fenical, W.; Jensen, P. R., Developing a New Resource for Drug Discovery: Marine Actinomycete Bacteria. *Nature Chemical Biology* **2006,** 2, (12), 666-673.

9. Tucker, J. B., Drugs From the Sea Spark Renewed Interest. *BioScience* **1985,** 35, (9), 541-545.

10. Goodman, J.; Walsh, V., *The Story of Taxol - Nature and Politics in the Pursuit of an Anti-Cancer Drug*. Cambridge University Press: 2001; p 296.

11. Clardy, J.; Walsh, C., Lessons From Natural Molecules. *Nature* **2004,** 432, 829-837.

12. Schreiber, A., The Small-Molecule Approach to Biology. *Chemical and Engineering News* **2003**.

13. Rishton, G. M., Reactive Compounds and In Vitro False Potsitives in HTS. *Drug Discovery Today* **1997,** 2, 382-384.

14. Greenfeder, S.; Umland, S. P.; Cuss, F. M.; Chapman, R. W.; Egan, R. W., Th2 Cytokines and Asthma: The Role of Interleukin-5 in allergic Eosinophilic Disease. *Respiratory Research* **2001,** 2, (2), 71-79.

15. Broide, D.; Schwarze, J.; Tighe, H.; Gifford, T.; Nguyen, M.-D.; Malek, S.; Van Uden, J. H.; Martin-Orozco, E.; Gelfand, E. W.; Raz, E., Immunostimulatory DNA Sequences Inhibit IL-5, Eosinophilic Inflammation, and Airway Responsiveness in Mice. *The Journal of Immunology* **1998,** 161, 7054-7062.

16. Gleich, G., Mechanisms of Eosinophil-Associated Inflammation. *Journal of Allergy and Clinical Immunology* **2000,** 105, 651-663.

17. Co., R. a. H. AMBERLITE™ XAD™ 1180.

18. West, L.; Northcoate, P., Peloruside A: A Potent Cytotoxic Macrolide Isolated from the New Zealand Marine Sponge Mycale sp. *Journal of Organic Chemistry* **2000,** 65, (2), 445-449.

19. Omura, S.; Sasaki, Y., ;; Iwai, Y.; Takeshima, H., Staurosporine, a Potentially Important Gift from a Microorganism. *The Journal of Antibiotics* **1995,** 48, (7), 535-548.

20. Gescher, A., Staurosporine Analogues - Pharmacological Toys or Useful Antitumour Agents? *Critical Reviews in Oncology/Hematology* **2000,** 34, 127-135.

21. Chen, X.; Lowe, M.; Herliczek, T.; Hall, M. J.; Danes, C.; Lawrence, D. A.; Keyomarsi, K., Protection of Normal Proliferating Cells Against Chemotherapy by Staurosporine-Mediated, Selective, and Reversible G_1 Arrest. *Journal of the National Cancer Institute* **1999,** 92, (4).

22. Yoshida, S.; Yoneyama, K.; Shiraishi, S., *Agricultural and Biological Chemistry* **1977,** 41, 587-591.

23. Kominato, K.; Watanabe, Y.; Hirano, S.-I.; Kioka, T.; Terasawa, T.; Yoshioka, T.; Okamura, K.; Tone, H., Mer-A2026A and B, Novel Piericidins With Vasodilating Effect II. Physico-Chemical Properties and Chemcial Structures. *The Journal of Antibiotics* **1994,** 48, (2), 103-105.

24. Yoshida, S.; Yoneyama, K.; Shiraishi, S.; Watanabe, A.; Takahashi, N., Isolation and Physical Properties of New Piericidins Produced by *Streptomyces pactum*. *Agricultural and Biological Chemistry* **1977,** 41, (5), 849-853.

25. Kobuta, N. K.; Ohta, E.; Ohta, S.; Koizumi, F.; Suzuki, M.; Ichimura, M.; Ikegami, S., Piericidins C_5 andC_6: New 4-Pyridinol Compounds Produced by *Streptomyces* sp. and *Nocardiodes* sp. *Bioorganic and Medicinal Chemistry* **2003,** 11, 4569-4575.

26. Kominato, K.; Watanabe, Y.; Hirano, S.-I.; Kioka, T.; Terasawa, T.; Yoshioka, T.; Okamura, K.; Tone, H., Mer-A2026A and B, Novel Piericidins With Vasodilating Effect I. Producing Organism, Fermentation, Isolation, and Biological Properties. *The Journal of Antibiotics* **1994,** 48, (2), 99-102.

27. Mioshi, H., Structure-Activity Relationships of Some Complex I Inhibitors. *Biochimica et Biophysica Acta* **1998,** 1364, 236-244.

28. Nishioka, H.; Imoto, M.; Imaoka, T.; Sawa, T.; Takeuchi, T.; Umezawa, K., Antitumor Effect of Piericidin B_1 *N*-Oxide. *The Journal of Antibiotics* **1993,** 47, (4), 447-452.

29. Graz, C. J. M.; Grant, G. D.; Brauns, S. C.; HUnt, A.; Jamie, H.; Milne, P. J., Cyclic Depsipeptides in the Induction of Maturation for Cancer Therapy. *Jourbal of Pharmacy and Pharmacology* **2000,** 52, 75-82.

30. Borthwick, A. D.; Davies, D. E.; Exall, A. M.; Hatley, R. J. D.; Hughes, J. A.; Irving, W. R.; Livermore, D. G.; Sollis, S. L.; Nerozzi, F.; Valko, K. L.; Allen, M. J.; Perren, M.; Shabbir, S. S.; Woollard, P. M.; Price, M. A., 2,5-Diketopiperazines as Potent, Selective, and Orally Bioavailable Oxytocin Antagonists. 3. Synthesis, Pharmacokinetics, and in Vivo Potency. *Journal of Medicinal Chemistry* **2006,** 49, (14), 4159-4170.

31. Fischer, P. M., Diketopiperazines in Peptide and Combinatorial Chemistry. *Journal of Peptide Science* **2003,** 9, 9-35.

32. Johnston, N. J.; Mukhtar, T. A.; Wright, G. D., Streptogramin Antibiotics: Mode of Action and Resistance. *Current Drug Targets* **2002,** 3, 335-344.

33. Oh, D. C.; Strangman, W. K.; Kauffman, C. A.; Jensen, P. R.; Fenical, W., Thalassospiramides A and B, Immunosuppressive Peptides from the Marine Bacterium Thalassospira sp. *Organic Letters* **2007,** 9, (8), 1525-1528.

34. Cho, J. Y.; Kwon, H. C.; Williams, P. G.; Kauffman, C. A.; Jensen, P. R.; Fenical, W., Actinofuranones A and B, Polyketides from a Marine-Derived Bacterium Related to the Genus Streptomyces (Actinomycetales). *Journal of Natural Products* **2006,** 69, (3), 425-428.

35. Cho, J. Y.; Kwon, H. C.; Williams, P. G.; Jensen, P. R.; Fenical, W., Azamerone, a Terpenoid Phthalazinone from a Marine-Derived Bacterium Related to the Genus Streptomyces (Actinomycetales). *Organic Letters* **2006,** 8, (12), 2471-2474.

III

Splenocins: Potent Inhibitors of Allergic Inflammation

III.1

Splenocins A-J: Project Overview

III.1. Splenocins A-J: Project Overview

The whole culture extract of marine strain CNQ431, a *Streptomyces* sp., displayed potent biological activity in the mouse splenocyte assay (IC_{80} = 21 μg/ml for the crude extract) and was therefore highlighted for further investigation. This bacterial strain was isolated from ocean sediments at 30 m depth roughly one mile off the coast of the Scripps Institution of Oceanography in La Jolla, California. Bioactivity guided isolation of the cytokine inhibitors from this strain led us to the discovery of a new set of bioactive molecules, which we have named splenocins A-J (**1**-**10**) (Figure III.1a). These molecules displayed potent suppression of cytokine production at concentrations ranging from low nanomolar to low micromolar and exhibited minimal cytotoxicity in the low molar to high micromolar range, thereby giving therapeutic ratios in this assay from 200 in some cases to over 500 in the case of splenocin B (**2**). Further biological investigation revealed that all of these, in addition to inhibiting the production of the Th2 cytokines IL-5 and IL-13, also inhibit the production of the allergen presenting cell (APC) -associated cytokines IL-1and TNF-α, indicating immunosuppressive effects on both the APCs (*i.e.* dendritic cells) and the Th2 cells.

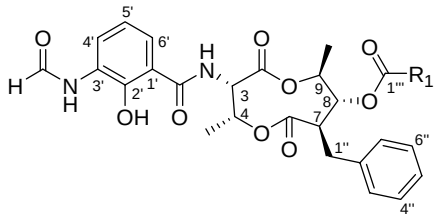

1 $R_1 = CH_3$
2 $R_1 = CH(CH_3)_2$

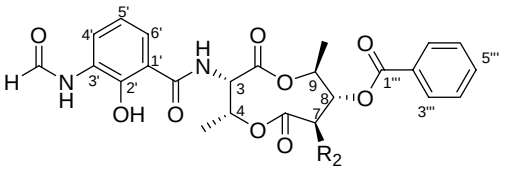

3 $R_1 = CH(CH_3)CH_2CH_3$
4 $R_1 = CH_2CH_3$
5 $R_2 = CH_2(CH_2)_2CH_3$
6 $R_2 = CH_2(CH_2)_3CH_3$
7 $R_2 = CH_2(CH_2)_4CH_3$
8 $R_2 = CH_2CH(CH_3)(CH_2)_3CH_3$
9 $R_2 = CH_2C_6H_5$

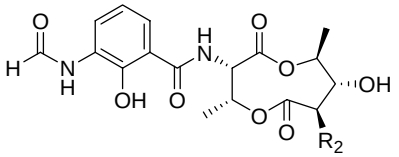

10 $R_2 = CH_2C_6H_5$
11 $R_2 = CH_2(CH_2)_2CH_3$
12 $R_2 = CH_2(CH_2)_3CH_3$
13 $R_2 = CH_2(CH_2)_4CH_3$
14 $R_2 = CH_2(CH_2)_5CH_3$

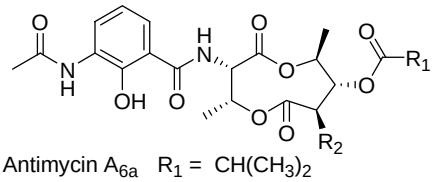

15 Antimycin A_{6a} $R_1 = CH(CH_3)_2$, $R_2 = CH_2CH_3$
16 Antimycin A_{17} $R_1 = CH_3$, $R_2 = CH_2CH_2CH(CH_3)_2$
17 Antimycin $A4_a$ $R_1 = CH(CH_3)_2$, $R_2 = CH_2(CH_2)_2CH_3$
18 Antimycin A_{7a} $R_1 = CH_2(CH_3)_2$, $R_2 = CH_2CH_2CH(CH_3)_2$

Figure III.1a: Structures of splenocins A-J (1-10), isolated 8-hydroxy antimycin analogues (11-14), and isolated antimycins (15-18).

Splenocins A-J (**1**-**10**) are characterized by a central nine-membered cyclic dilactone core. An N-formyl amino salicylic acid moiety is connected to the ring at C-3 via an amide bond in all members. This fundamental structure, together with the cyclic dilactone core, is also seen in molecules of the antimycin class, four of which were also isolated from strain CNQ431 (**15**-**18**).[1-3] The splenocins are further characterized and differentiated from antimycins by the presence of benzyl groups originating at C-7 (**1**-**3**, **10**) and benzoyl groups at C-8 (**4**-**8**) of the dilactone ring. Splenocin I (**9**) contains aromatic functionalities at both the C-7 and C-8 positions. In addition to the benzyl group at C-7, splenocin J (**10**) contains a hydroxyl group at C-8 instead of the ester functionality seen in splenocins A-I. This hydroxyl functionality

can also be seen in other previously described 8-hydroxy antimycins which contain alkyl chains at the C-7 position and differ from each other by the number of carbons in the chain.[4] Three known members of this group, deisovaleryl-blastmycin (C_4 alkyl chain)[5] (**11**), urauchimycins (C_5)[6] (**12**), and kitamycins (C_6)[7] (**13**), as well as a new linear C_7 member (**14**), were also produced by strain CNQ431.

Splenocins A-I (**1-9**) display suppression of cytokine production by OVA-stimulated splenocytes at low nanomolar concentrations similar to the corticosteroid standard dexamethasone. Splenocin J (**10**) exhibits low micromolar activity in the splenocyte assay. In this chapter, we describe the isolation, structure elucidation, and structure activity relationships of the splenocins, in the *in vitro* mouse splenocyte assay.

III.2

Splenocins A-J: Isolation and Structure Elucidation

III.2. Splenocins A-J: Isolation and Structure Elucidation

Splenocin A (**1**) was isolated as an optically active amorphous white powder which displayed strong IR bands at 3381 and 1748 cm^{-1}, indicating the presence of hydroxyl and carbonyl functional groups. A molecular formula of $C_{26}H_{28}N_2O_9$ was assigned based on interpretation of HR ESI-TOF MS data (Obsd $[M+Na]^+$ at *m/z* 535.1683). One and two-dimensional NMR experiments, together with the molecular formula and information gleaned from overall spectral data, allowed us to assemble several substructures (Table III.2a, Figure III.2a).

Table III.2a: NMR data from splenocins A-C (1-3) in $CDCl_3$.

Position	Splenocin A (**1**)		Splenocin B (**2**)		Splenocin C (**3**)	
	δ_C[a]	δ_H[b] (*J* in Hz)	δ_C[a]	δ_H[b] (*J* in Hz)	δ_C[a]	δ_H[b] (*J* in Hz)
2	170.0		170.1		170.0	
3	53.8	5.24 dd (8.0, 8.0)	53.4	5.26 dd (7.5, 7.5)	53.5	5.25 dd (7.5, 7.5)
4	70.6	5.60 dq (8.0, 6.5)	70.9	5.60 dq (7.5, 7.0)	70.9	5.59 dq (7.5, 7.0)
6	172.8		171.9		172.4	
7	51.6	2.90 ddd (10.5, 10.5, 3.5)	51.9	2.87 ddd (11.5, 10.5, 3.0)	52.0	2.87 ddd (10.5, 10.5, 3.5)
8	75.6	5.19 t (10.5)	75.0	5.20 t (10.5)	75.1	5.21 t (10.5)
9	75.0	5.01 m	74.7	5.01 m	74.8	5.00 m
4-Me	15.0	1.16 d (6.5)	14.7	1.15 d (7.0)	14.7	1.14 br d (7.0)
9-Me	18.0	1.32 d (6.5)	17.8	1.31 d (6.5)	17.9	1.31 d (6.5)
1′	112.5		112.6		112.5	
2′	150.6		150.7		150.6	
3′	127.7		127.4		127.4	
4′	124.9	8.52 d (7.5)	124.8	8.52 d (7.5)	124.8	8.51 d (8.0)
5′	119.0	6.89 t (7.5)	118.8	6.89 t (7.5)	119.0	6.88 t (7.5)
6′	120.2	7.20 d (7.5)	120.3	7.18 d (7.5)	120.0	7.18 d (8.0)
1′-CONH	169.5		169.3		169.3	
1′-CONH		6.98 d (8.0)		7.03 d (7.5)		6.98 d (8.0)
2′-OH		12.59 br s		12.62 br s		12.60 br s
3′-NHCHO		7.87 br s		7.94 s		7.89 br s
3′-NHCHO	159.5	8.48 s	159.1	8.47 s	158.9	8.49 s
1″	34.7	2.97 dd (13.5, 10.5)	34.5	2.97 dd (13.5, 11.5)	34.5	2.97 dd (13.0, 10.5)
		2.71 dd (13.5, 3.5)		2.68 dd (13.5, 3.5)		2.70 dd (13.5, 3.5)
2″	138.5		137.9		137.9	
3″	128.8	7.12 d (8.0)	128.7	7.11 d (8.0)	128.7	7.11 d (8.0)
4″	128.6	7.24 t (8.0)	128.5	7.24 t (8.0)	128.6	7.24 t (8.0)
5″	126.6	7.18 t (8.0)	126.6	7.17 t (8.0)	126.6	7.18 t (8.0)
6″	128.6	7.24 t (8.0)	128.5	7.24 t (8.0)	128.6	7.24 t (8.0)
7″	128.8	7.12 d (8.0)	128.7	7.11 d (8.0)	128.7	7.11 d (8.0)
1‴	170.2		175.7		175.3	
2‴	20.9	2.04 s	34.1	2.59 m	41.3	2.43 m
3‴			18.9	1.22 d (7.0)	26.5	1.75 m
						1.53 m
4‴					11.8	0.95 t (7.5)
5‴					16.7	1.20 d (7.5)

[a] Assignment by 1-D ^{13}C methods at 125 MHz.
[b] Assignment by ^{1}H, gHSQC, and gHMBC NMR methods at 500MHz.

The first substructure (Figure III.2a) was assembled largely with data obtained from the ^{1}H-^{1}H correlation spectroscopy (COSY) NMR experiment. The COSY

experiment detects signals from protons that are spin-spin coupled in a molecule.[8, 9] In COSY spectra, the diagonal represents the signals seen from a 1-dimensional proton experiment while spin-spin coupled protons are visualized by cross peaks on either side of the diagonal (Figure III.2b).[8, 9] For example, Figure III.2b is an expansion of a portion of the COSY spectrum for splenocin A (1) and includes the COSY signals of substructure (i) (Figure III.2a). By connecting spin-coupled protons, spin systems can be defined within the molecule. For splenocin A (1) the first spin system was assembled starting with the methine proton H-3 (δ_H 5.24), which showed ^{1}H-^{1}H COSY correlations to both H-4 (δ_H 5.60) and a secondary amide proton (δ_H 6.98). Proton H-4 showed an additional correlation to a methyl doublet (δ_H 1.16). Similarly, a second spin system was assembled starting with oxygenated methine proton H-9 (δ_H 5.01), which showed ^{1}H-^{1}H COSY correlations to a methyl doublet (δ_H 1.32) and H-8 (δ_H 5.19). Proton H-8 showed a further correlation to H-7 (δ_H 2.90), which showed correlations to two methylene protons H1-1″a and H1″b (δ_H 2.97 and 2.71) in the ^{1}H-^{1}H COSY spectrum.

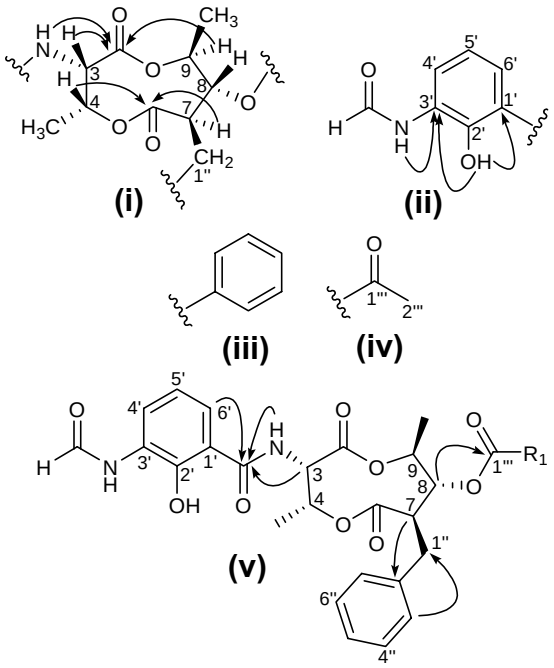

Figure III.2a: Substructures and key HMBC correlations used to define the structure of splenocin A (1).

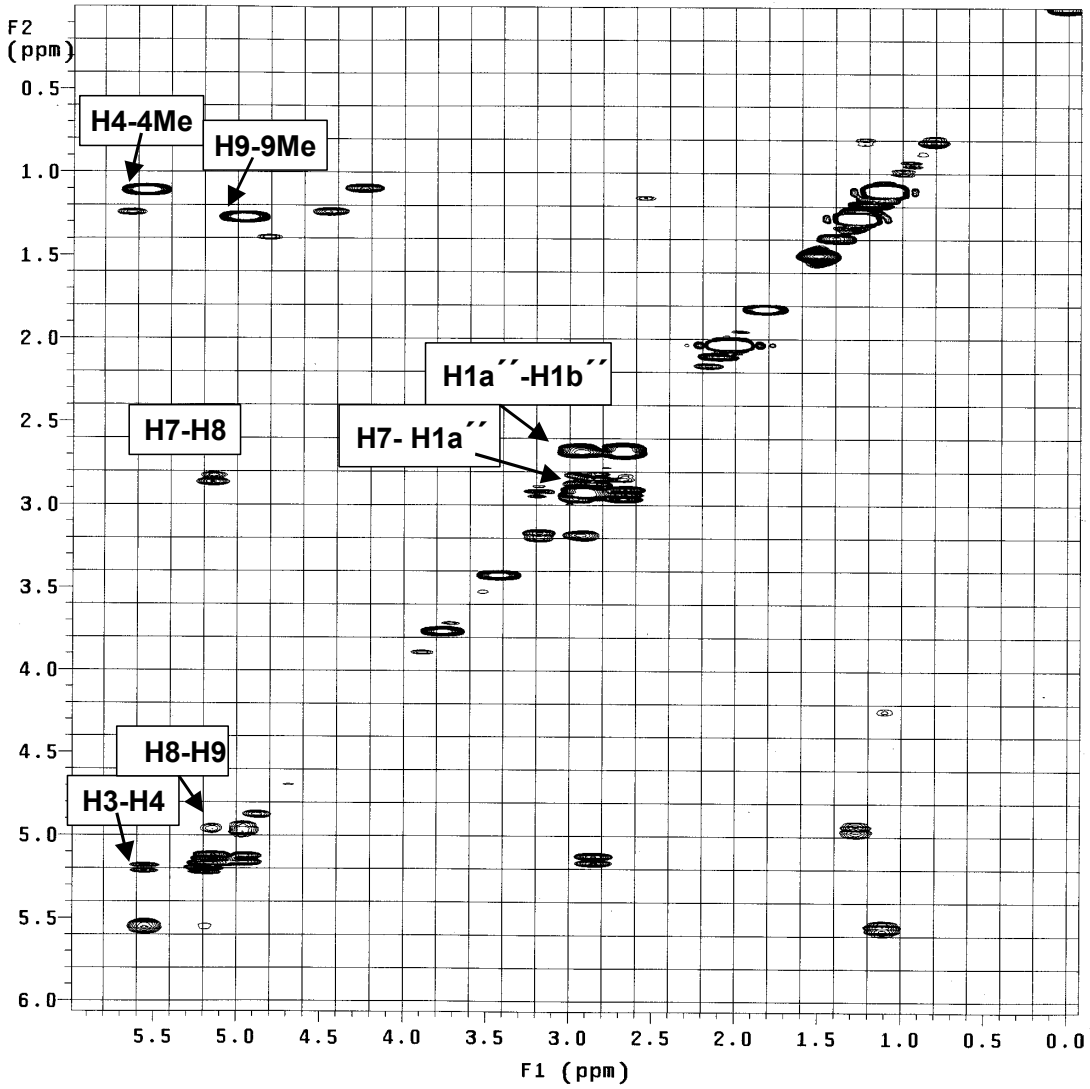

Figure III.2b. Expansion of part of the gCOSY NMR spectrum for splenocin A(1) in $CDCl_3$ (500MHz). Key COSY correlations for the assemblage of substructure (i) are noted.

The spin systems were then connected with additional information obtained from the ^{1}H-^{13}C Heteronuclear Multiple Bond Correlation (HMBC) NMR experiment, which allows correlations of protons to carbons that are two or three bonds away

(Figure III.2c).[9] Key HMBC correlations from H-4 and H-7 to carbonyl carbon C-6 (δ_c 172.8) and protons H-3 and H-9 to carbon C-2 (δ_c 170.0) allowed the assembly of the nine-membered dilactone (Figure III.2a.i). The orientations of the ester bonds within the dilactone ring were determined by ^{1}H and ^{13}C chemical shift analysis. The downfield chemical shifts of H-4 (δ_H 5.60), C-4 (δ_c 70.6), H-9 (δ_H 5.01), and C-9 (δ_c 75.0) are consistent with a position next to the oxygen portion of the lactone while the more upfield shifted resonances of H-3 (δ_H 5.24), C-3 (δ_c 53.8), H-7 (δ_H 2.90), and C-7 (δ_c 51.6) are consistent with being adjacent to the carbonyl portion of the lactone.

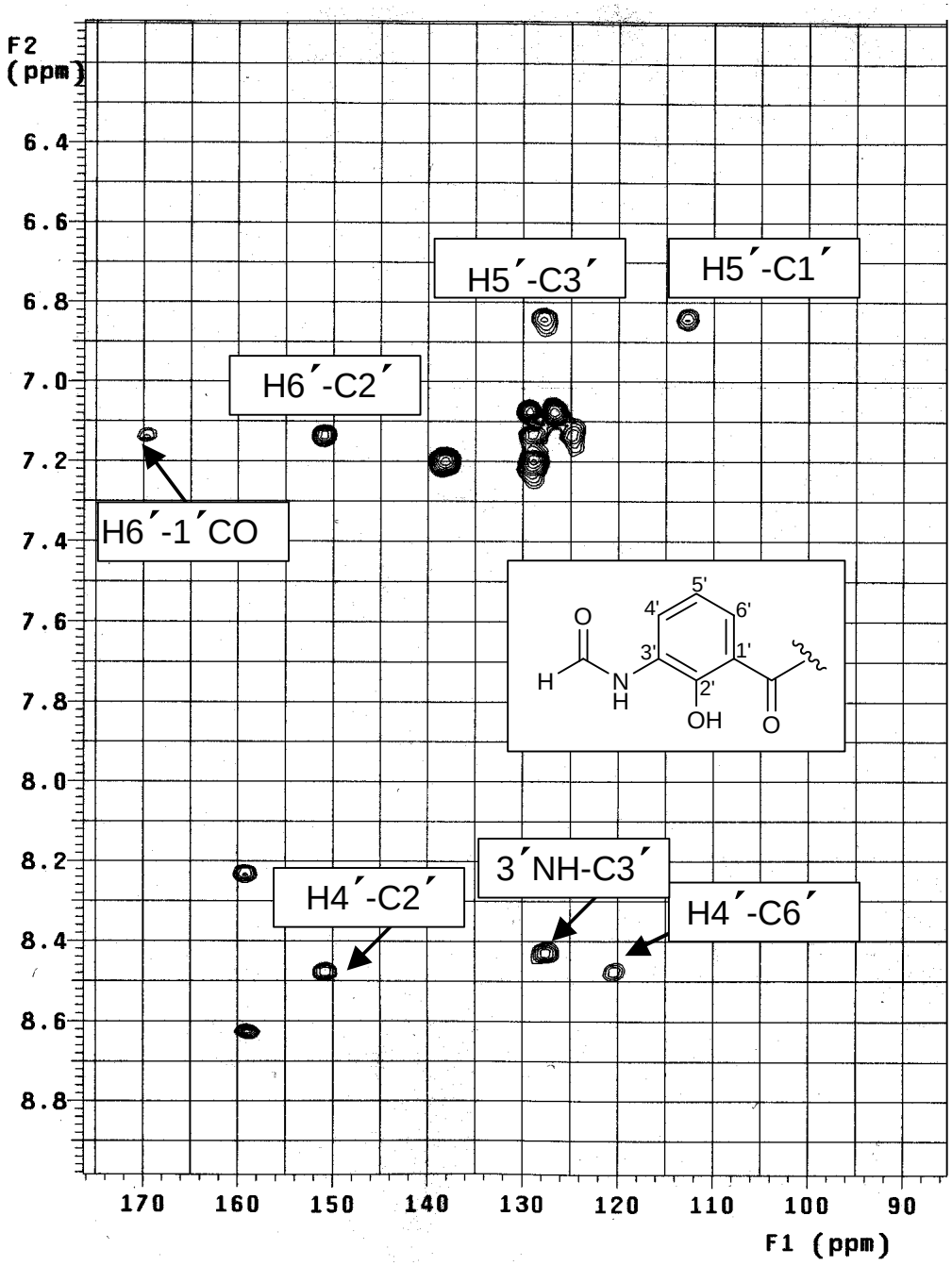

Figure III.2c: Expansion of part of the gHMBC NMR spectrum for splenocin A (1) in $CDCl_3$ (500MHz). Key HMBC correlations for the assembly of substructure (ii) are noted.

A second substructure (Figure III.2a.ii) was assembled starting with distinct aldehyde proton and carbon signals (δ_H 8.48/ δ_c 159.1). This highly deshielded proton chemical shift, combined with a ^{1}H-^{1}H COSY correlation from the aldehyde proton to an amide proton (δ_H 7.87), suggested an N-formyl group. Next, ^{1}H-^{1}H COSY correlations between aromatic protons H-4′ (δ_H 8.52), H-5′ (δ_H 6.89), and H-6′ (δ_H 7.20) and HMBC correlations from these aromatic protons to quaternary carbons C-1′ (δ_C 112.5) and C-3′ (δ_C 127.7) and hydroxyl-substituted C-2′ (δ_C 150.6) permitted assembly of a tri-substituted aromatic ring (Figure III.2a.ii). An HMBC correlation from the amide proton of the N-formyl group to the aromatic quaternary carbon C-3' allowed us to connect the two pieces, giving the unusual N-formyl salicylic acid moiety as our second substructure. Finally, ^{1}H-^{1}H COSY correlations between aromatic protons H-3″ (and *H-7″*) (δ_H 7.12), H-4″ (and H6″) (δ_H 7.24), and H-5″ (δ_H 7.18), allowed us to assemble a mono-substituted benzene ring (Figure III.2a.iii), while the methyl singlet 2‴ Me (δ_H 2.04, δ_C 20.9) showed an HMBC correlation to carbonyl carbon C-1‴ (δ_C 170.2) defining an acetate unit (Figure III.2a.iv).

The substructures were connected by HMBC NMR as follows (Figure III.2a.v). The aromatic proton H-6′ showed a C-H long-range correlation to a carbonyl carbon at δ_C 169.5. Both H-3 and the secondary amino proton adjacent to H-3 in the cyclic dilactone also showed C-H long range correlations to this carbonyl thereby allowing us to connect the N-formyl salicylic acid substructure to the dilactone ring via a carbonyl amide bridge between C-1′ and C-3 (Figure III.2a.v). This dilactone core substructure, is also seen in the antimycins[1-3] and in the 8-hydroxy antimycin derivatives, deisovaleryl blastomycin,[5] urauchimycins,[6] and kitamycins[7]. Additional

C-H long range correlations allowed us to attach the mono-substituted benzene (Figure III.2a substructure iii) to the C-1″ methylene which connects to the dilactone at C-7 while an HMBC correlation from H-8 to the C-1‴ carbonyl carbon allowed us to attach the acetate unit (Figure III.2a substructure iv) to the dilactone at the C-8 position, thereby completing the planar structure for splenocin A (Figure III.2a.v).

Splenocins B and C (**2** and **3**) are very similar to splenocin A (**1**) in that they contain a benzyl functionality originating at C-7. However, they differ from splenocin A (**1**) in the length of the acyl chain at C-8. The length and branching of their side chains were determined through a combination of HRMS and proton NMR analysis (Table III.2a).

Similar to splenocins A-C (**1**-**3**), splenocins D-H (**4**-**8**) also possess ester functionalities attached to C-8. HMBC analysis of splenocins D-H (**4**-**8**) showed correlations from the C-8 ester carbonyl to protons on a second aromatic ring H-3‴ (δ_H 8.04) and H-7‴ (δ_H 8.04) suggesting that these molecules contain a benzoyl group at C-8 rather than an acyl chain (Figure III.1a, Table III.2b). In further contrast to splenocins A-C (**1**-**3**), splenocins D-H (**4**-**8**) possess alkyl chains originating at C-7 rather than the corresponding benzyl moieties of **1**-**3**. The C-7 alkyl chains of **4**-**8** were assembled based on HRMS and proton NMR analysis (Table III.2b).

Table III.2b: NMR data from splenocins D-H (4-8) in $CDCl_3$.

Position	Splenocin D (**4**)		Splenocin E (**5**)		Splenocin F (**6**)	
	δ_C[a]	δ_H[b] (*J* in Hz)	δ_C[a]	δ_H[b] (*J* in Hz)	δ_C[a]	δ_H[b] (*J* in Hz)
2	170.5		170.1		170.1	
3	53.9	5.32 dd (8.0, 7.5)	53.7	5.30 dd (8.0, 7.5)	53.9	5.30 dd (8.0, 7.0)
4	71.2	5.76 dq (7.5, 7.0)	71.0	5.76 dq (7.5, 6.5)	71.3	5.75 dq (7.5, 7.0)
6	172.6		172.9		172.9	
7	52.0	2.62 ddd (10.0, 10.0, 3.0)	50.2	2.68 ddd (10.0, 10.0, 3.0)	50.2	2.65 ddd (10.0, 10.0, 3.0)
8	76.4	5.33 t (10.0)	76.3	5.32 t (10.0)	76.5	5.32 t (10.0)
9	75.0	5.15 m	75.0	5.14 m	75.2	5.14 m
4-Me	15.2	1.32 [d] d (7.0)	15.0	1.33 d [d] (6.5)	15.0	1.33 [d] d (7.0)
9-Me	18.0	1.33 [d] d (6.5)	17.9	1.32 d [d] (6.5)	17.9	1.33 [d] d (7.0)
1′	112.7		112.5		112.5	
2′	151.0		150.6		150.6	
3′	127.0		127.4		127.4	
4′	124.8	8.54 d (8.0)	124.8	8.54 d (8.0)	124.8	8.53 d (8.0)
5′	119.2	6.91 t (8.0)	120.1	6.91 t (8.0)	119.4	6.90 t (8.0)
6′	120.3	7.23 m[c]	120.8	7.23 m[c]	120.4	7.23 m[c]
1′-CONH	169.0		169.4		169.4	
1′-CONH		7.08 d (8.0)		7.07 d (8.0)		707 d (8.0)
2′-OH		12.60 s		12.60 s		12.60 s
3′-NHCHO		7.91 br s		7.92 s		7.92 s
3′-NHCHO	159.0	8.49 s	158.9	8.49 s	158.9	8.49 s
1″a	21.8	1.75 m	28.2	1.76 m	28.2	1.76 m
1″b		1.50 m[c]		1.40 m		1.40 m
2″	11.5	0.86 t (8.0)	29.3	1.15 m 1.24 m	36.5	1.08 m
3″			22.3	1.23 m	26.5	1.45m
4″			13.8	0.80 t (7.0)	22.3	0.77[d] d (7.0)
5″					22.3	0.78[d] d (7.0)
6″						
7″						
1‴	165.5		165.2		165.2	
2‴	129.0		129.0		129.0	
3‴	130.0	8.04 d (8.0)	129.9	8.05 d (8.0)	129.9	8.04 d (7.5)
4‴	128.7	7.47 t (8.0)	128.7	7.47 t (8.0)	128.7	7.47 t (7.5)
5‴	133.8	7.61 t (8.0)	133.7	7.61 t (8.0)	133.9	7.63 t (7.5)
6‴	128.7	7.47 t (8.0)	128.7	7.47 t (8.0)	128.7	7.47 t (7.5)
7‴	130.0	8.04 d (8.0)	129.9	8.05 d (8.0)	129.9	8.0 d (7.5)

[a] Assignment by 1-D ^{13}C methods at 125 MHz.
[b] Assignment by ^{1}H, gHSQC, and gHMBC NMR methods at 500 MHz.

Table III.2b: NMR data from splenocins D-H (4-8) in $CDCl_3$ continued.

Position	Splenocin G (**7**)		Splenocin H(**8**)	
	δ_C[a]	δ_H[b] (*J* in Hz)	δ_C[a]	δ_H[b] (*J* in Hz)
2	170.1		170.1	
3	53.7	5.32 dd (8.0, 7.5)	54.0	5.30 m[c]
4	71.0	5.76 dq (7.5, 7.5)	70.17	5.76 dq (7.0, 7.0)
6	172.9		172.9	
7	50.3	2.68 ddd (10.0, 10.0, 3.0)	50.5	2.69 ddd (10.0, 10.0, 3.0)
8	76.3	5.32 t (10.0)	76.8	5.32 t (10.0)
9	75.0	5.14 m	75.2	5.15 m
4-Me	15.0	1.32[d] d (7.5)	15.1	1.33[d] d (7.0)
9-Me	17.9	1.32[d] d (7.5)	18.3	1.32[d] d (7.0)
1′	112.6		112.6	
2′	150.6		151.0	
3′	127.5		127.8	
4′	124.8	8.55 d (8.0)	125.0	8.54 d (8.0)
5′	119.0	6.91 t (8.0)	119.2	6.91 t (8.0)
6′	120.1	7.24 m[c]	120.3	7.23 m[c]
1′-CONH	169.4		169.5	
1′-CONH		7.09 d (8.0)		7.08 d (8.0)
2′-OH		12.60 s		12.60 s
3′-NHCHO		7.96 s		7.91 s
3′-NHCHO	159.0	8.50 s	159.0	8.49 s
1″a	28.5	1.75 m	29.1	1.75 m
1″b		1.39 m		1.35 m
2″	27.5	1.25 m	24.9	1.20 m[c]
		1.18 m		
3″	29.5	1.20 m	36.5	0.95 m
				1.21 m[c]
4″	31.5	1.18 m	34.3	1.21 m[c]
5″	22.5	1.20m	29.9	1.23 m[c]
6″	13.4	0.80 t (7.0)	11.8	0.75 t (7.0)
7″			19.1	0.74 d (7.0)
1‴	165.2		165.5	
2‴	129.0		130.0	
3‴	129.9	8.04 d (8.0)	130.1	8.04 d (8.0)
4‴	128.7	7.48 t (8.0)	129.1	7.47 t (8.0)
5‴	133.7	7.61 t (8.0)	134.0	7.61 t (8.0)
6‴	128.7	7.48 t (8.0)	129.1	7.47 t (8.0)
7‴	129.9	8.04 d (8.0)	130.1	8.04 d (8.0)

[a] Assignment by 1-D ^{13}C methods at 125 MHz.
[b] Assignment by ^{1}H, gHSQC, and gHMBC NMR methods at 500 MHz.
[c] The multiplicity can not be assigned due to peak overlap
[d] Signals are interchangeable.

Splenocin I (**9**) is unique in that it contains aromatic functionalities at both C-7 and C-8 (Figure III.1a, Table III.2c). Similar to splenocins A-C (**1**-**3**), the benzyl

functionality at C-7 was connected through COSY correlations from H-7 to H-1″a and H-1″b, and by HMBC correlations from H-7 to the quaternary aromatic carbon C-2″ and from H-3″ to C-1″. Splenocin I (9) also shows similar HMBC correlations as are seen in splenocins D-H (**4**-**8**) from H-8 and H-3‴ to the C-1‴ ester carbon (δ_c 165.3).

Table III.2c. NMR data from splenocins I and J (9 and 10) in $CDCl_3$.

Position	Splenocin I (**9**)		Splenocin J (**10**)	
	δ_C[a]	δ_H[b] (*J* in Hz)	δ_C[a]	δ_H[b] (*J* in Hz)
2	170.1		170.1	
3	53.6	5.29 dd (8.0, 7.5)	53.5	5.21 dd (7.5, 7.0)
4	71.0	5.64 dq (7.5, 7.0)	70.7	5.58 dq (7.5, 7.0)
6	172.0		173.0	
7	52.0	3.06 ddd (10.0, 10.0, 10.0)	54.0	2.69 ddd (10.5, 10.0, 3.5)
8	76.1	5.45 t (10.0)	77.3	3.73 dt (10.0, 10.0)
9	74.9	5.12 m	76.9	4.87 dq (10.0, 10.0)
8-OH				1.62 br s
4-Me	14.8	1.18 d (6.5)	14.7	1.15 d (7.0)
9-Me	18.0	1.37 d (6.5)	18.4	1.47 d (6.0)
1′	112.5		112.5	
2′	150.6		150.6	
3′	127.4		127.3	
4′	124.7	8.52 d (8.0)	124.8	8.51d (8.0
5′	119.0	6.89 t (8.0)	119.0	6.88 t (8.0)
6′	120.0	7.19 t (8.0)	120.1	7.18 d (8.0)
1′-CONH	169.4		169.3	
1′-CONH		7.01 br d (8.0)		7.01 d (7.5)
2′-OH		12.6 br s		12.6 s
3′-NHCHO		7.88 br s		7.87 br s
3′-NHCHO	158.9	8.48 s	159.0	8.47 s
1″a	34.7	3.06 dd (20.0, 10.0)	35.1	3.19 dd (13.5, 3.5)
1″b		2.78 dd (20.0, 10.0)		2.98 dd (13.5, 10.5)
2″	137.8		138.4	
3″	128.7	7.09 d (7.5)	126.6	7.17 d (7.5)
4″	128.5	7.19 t (7.5)	128.6	7.26 t (7.5)
5″	126.6	7.13 t (7.5)	128.8	7.16 t (7.5)
6″	128.5	7.19 t (7.5)	128.6	7.26 t (7.5)
7″	128.7	7.09 d (7.5)	126.6	7.17 d (7.5)
1‴	165.3			
2‴	129.0			
3‴	129.9	8.05 d (8.0)		
4‴	128.7	7.48 t (8.0)		
5‴	133.9	7.62 t (8.0)		
6‴	128.7	7.48 t (8.0)		
7‴	129.9	8.05 d (8.0)		

[a] Assignment by 1-D ^{13}C methods at 125 MHz.
[b] Assignment by ^{1}H, gHSQC, and gHMBC NMR methods at 500 MHz.

Splenocin J (**10**) has the same benzyl functionality at C-7 as **1-3**, and **9** (Figure III.1a, Table III.2a, and III.2c). However, unlike any of the other splenocins, C-8 (δ_H

3.73/ δ_c 77.3) in **10** showed a ^{1}H-^{1}H COSY correlation from H-8 to a hydroxyl proton, indicating the presence of a secondary alcohol at C-8 rather than an ester. This hydroxyl group at C-8 is also shared by the previously described compounds, deisovaleryl-blastmycin (**11**),[5] urauchimycins (**12**),[6] and kitamycins (**13**),[7] which contain C_4, C_5, and C_6 alkyl chains respectively at C-7 of the dilactone. These known 8-hydroxy antimycins were also isolated from this strain. Additionally, we isolated compound **14**, a new member of the 8-hydroxy subset of molecules. ^{1}H-^{1}H COSY analysis, combined with mass spectral data, shows that **14** contains a 7-membered linear alkyl chain originating from C-7 (Figure III.1a).

Also isolated from the CNQ-431 culture were three known antimycins (**15**, **17**, and **18**) and one new antimycin derivative (**16**), as well as a mixture of several additional known antimycins (Figure III.1a). As antimycin structures differ from each other by the length and branching of their alkyl and acyl chains, their structures were determined through a combination of HRMS, ^{1}H NMR analysis, and comparison to reported values.[1-3] Antimycin A_{17} (**16**) is a new analog containing the previously unreported combination of an acetyl group at C-8 and a heptyl functionality at C-7 (Figure III.1a).

The relative configurations of the splenocins were assigned by interpretation of proton NMR coupling constant data and by spectral analysis of a NOESY (Two Dimensional Nuclear Overhauser Spectroscopy) NMR experiment (Table III.2d and Figure III.2e), respectively). On the side of the dilactone containing the N-formyl-salicylic acid group, protons H-3 and H-4 coupled to each other with a coupling constant between 7.0 and 7.5 (Table III.2d). While this value is suggestive of a *syn*

configuration, the coupling constant is not small enough to be definitive[2]. In order to further support this configurational assignment, NOESY correlations were also analyzed. The NOESY NMR experiment measures the dipolar (through-space instead of through-bond) coupling between nearby protons.[9] The methyl protons at C-4 showed strong NOESY correlations with the secondary amide proton connected to C-3 and a very weak correlation to H-3, while H-3 and H-4 show strong NOESY correlations to each other. Additionally, there was no apparent NOESY correlation between H-4 and the secondary amide proton. Taken together with the coupling constant data, this indicated that H-3 and H-4 were in the *syn* configuration although likely twisted slightly off axis from each other (Figure III.2e).

Table III.2d: Coupling constant values for protons in the dilactone ring.

	$^3J_{H3\text{-}H4}$	$^3J_{H7\text{-}H8}$	$^3J_{H8\text{-}H9}$
Splenocins A-C	7.0-7.5 Hz	10.5 Hz	10.5 Hz
Splenocins D-H	7.0-7.5 Hz	9.5-10.0 Hz	10.0 Hz
Splenocin I	7.5 Hz	10.0 Hz	10.0 Hz
Splenocin J	7.5 Hz	9.0 Hz	9.0 Hz

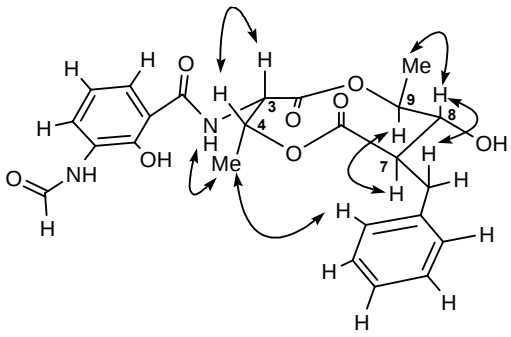

Figure III.2e: **Relative configuration of splenocin J (10). Arrows indicate key NOESY correlations.**

On the opposite side of the ring, the coupling constants between H-7 and H-8, and between H-8 and H-9, are between 9 and 10.5 Hz, which is strong evidence for *anti* configurations between the respective protons (Table III.2d). NOESY correlations were analyzed to further confirm the configuration (Figure III.2f). The methyl protons at C-9 showed strong NOESY correlations to H-8. Proton H-9 showed a strong NOESY correlation to H-7, and H-7 showed a strong NOESY correlation to a proton in the benzyl ring at C-7. All splenocins showed similar NOESY correlations between protons in the dilactone ring and displayed similar coupling constants, thereby indicating that they share similar relative configurations of the dilactone ring. Additionally, the relative configuration of the splenocins is identical to that of the anitmycins, which share the same 9-membered dilactone ring.[1-3]

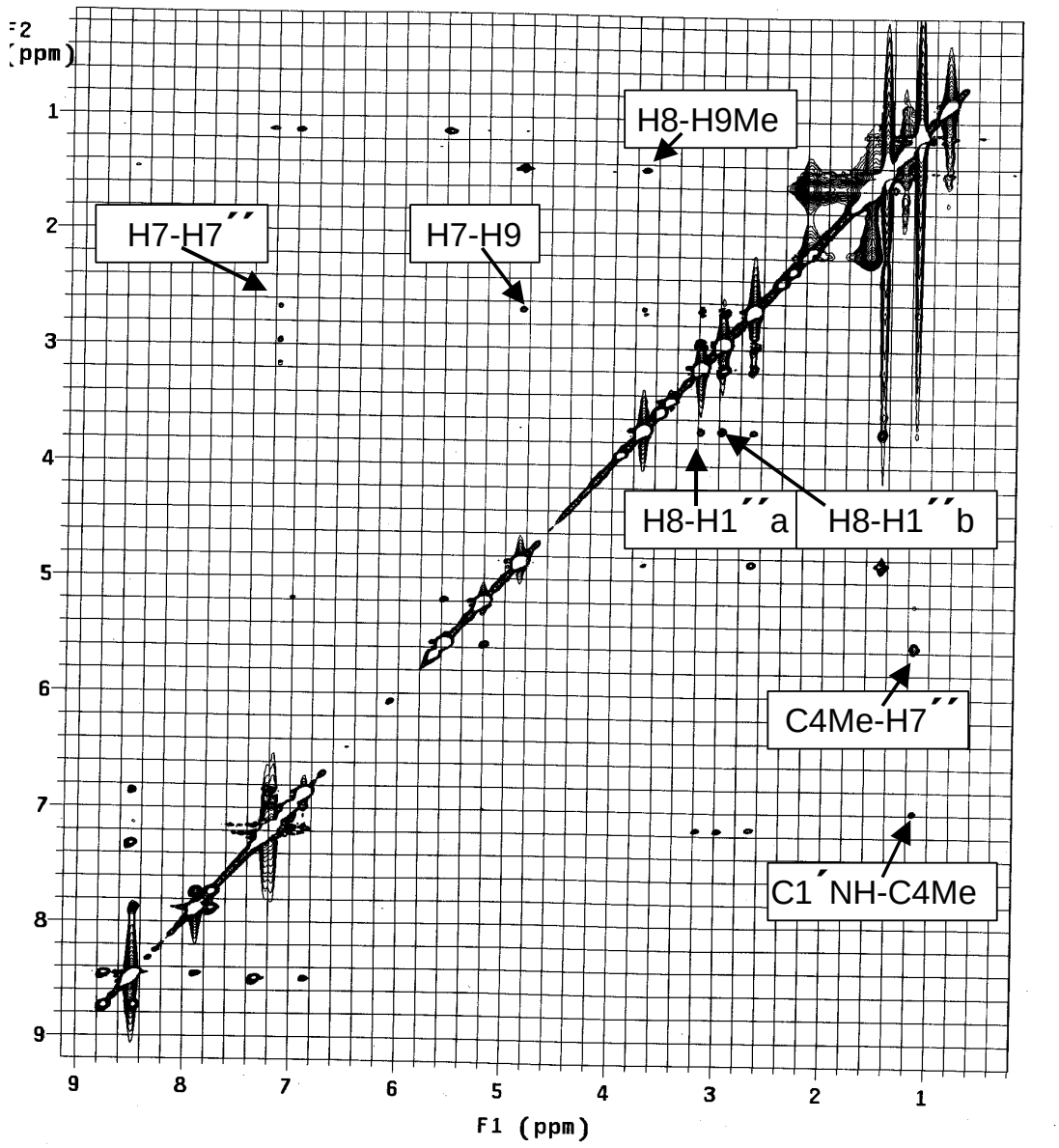

Figure III.2f: NOESY spectrum for splenocin J (10). Key correlations are noted.

For those splenocins possessing a benzyl functionality at C-7 (**1-3**, **9**, **10**), NOESY correlations are observed between H-8 and H-1′′a and between H-8 and H-1′′b, which when combined with the NOESY correlation between H-7 and the benzyl at C-7, indicated a possible spatial orientation for the benzyl functionality (Figure III.2e). In

splenocin J (**10**), a further NOESY correlation was observed between a proton on the benzyl ring at C-7 and the methyl attached to C-4 on the opposite side of the dilactone ring, thereby offering possible evidence relating the configurations of the two halves of the dilactone ring to each other (Figure III.2e). Additional NMR-based support for this connectivity for not only splenocin J (**10**), but also for the other benzyl-containing splenocins (**1**-**3**, **9**), comes from proton chemical shift analysis of the methyl at C-4. In the splenocins that contain a benzyl functionality at C-7, the methyl protons at C-4 are shifted upfield roughly 0.2 ppm (from 1.32 ppm to 1.15 ppm) relative to those of the non-benzylated splenocins (**4**-**8**) (Tables III.2a, b, and c). This upfield shift, combined with the NOESY correlation seen in splenocin J (**10**), suggests that the methyl protons at C-4 are being shielded by the pi electrons in the benzyl group at C-7 (Figure III.2e).

The availability of the secondary alcohol at C-8 made splenocin J (**10**) an appropriate candidate for absolute configuration determination. The absolute configuration of C-8 in splenocin J (**10**) was thus determined through application of the modified Mosher NMR method.[10] Compound **10** was treated with (*R*)-(-)-α-methoxy-α-(trifluormethyl) phenylacetyl chloride (MTPA-Cl) and (*S*)-(+)-MTPA-Cl in separate experiments. Somewhat surprisingly, the reactions initially yielded mono-*S*-Mosher and mono-*R*-Mosher amides at the 3' position. While this reaction is unprecedented under these conditions, similar deformylation reactions of aromatic N-formyl groups have been shown to occur upon heating, or under strongly acidic or strongly basic conditions.[11-13] The creation of the splenocin Mosher amide can be explained through an acyl transfer mechanism in which the formyl group is first

displaced by DMAP forming an aniline (Figure III.3 g). This group then attacks the Mosher-DMAP conjugate resulting in the Mosher-amide. It would be interesting to investigate this mechanism in greater detail to determine whether it is specific to the splenocins or whether it can be applied more generally to other types of N-formyl containing compounds.

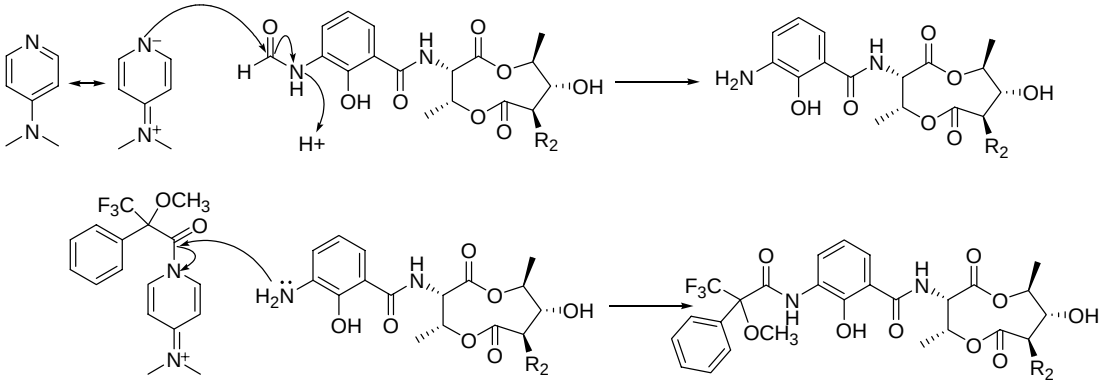

Figure III.3g: Proposed mechanism for deformylation and subsequent acylation of splenocin J (10).

Allowing the reaction to proceed longer produced the di-*S*-Mosher product **10a** and di-*R*-Mosher product **10b** respectively, with the second Mosher ester addition at the aromatic hydroxyl position of the N-formylsalicylic acid moiety (Figure III.2h.i). Continuation of the reaction finally produced the tri-*S* Mosher product **10c** and the tri-*R* Mosher product **10d** with the third ester product at the desired C-8 alcohol position (Figure III.2h.ii). After stopping the reaction and purifying the reaction products, we then obtained proton NMR spectra for each chiral product. As expected, the benzene ring of the Mosher MTPA reactant exerted a diamagnetic effect on nearby protons causing a chemical shift.[10] By subtracting the chemical shift values of the *R* product

from the *S* product, a series of positive or negative values were obtained for the protons on either side of the Mosher ester (Table III.2e).[10] Finally, a model of the molecule was constructed in which the positive values were placed on the right side of the ester and those with negative values on the left. This model should indicate the correct absolute configuration.[10]

Table III.2e. ^{1}H NMR chemical shift data for Di-Mosher and Tri-Mosher products in $CDCl_3$.

Position	*S*-Mosher Ester δ_H (*J* in Hz)	*R*-Mosher Ester δ_H (*J* in Hz)		Sign
H-1″ a	3.006	3.006	Δ (S-R) – Di-Mosher	0
H-1″ b	3.170	3.168	Δ (S-R) – Di-Mosher	+0.002
H-7	2.677	2.669	Δ (S-R) – Di-Mosher	+0.008
H-8	3.705	3.695	Δ (S-R) – Di-Mosher	+0.010
H-9	4.800	4.776	Δ (S-R) – Di-Mosher	+0.024
H-9 Me	1.461	1.449	Δ (S-R) – Di-Mosher	+0.012
H-1″ a	2.957	2.916	Δ (S-R) – Tri-Mosher	+0.041
H-1″ b	2.493	2.496	Δ (S-R) – Tri-Mosher	-0.003
H-7	2.823	2.811	Δ (S-R) – Tri-Mosher	+0.012
H-8	5.283	5.276	Δ (S-R) – Tri-Mosher	+0.007
H-9	4.942	4.931	Δ (S-R) – Tri-Mosher	+0.011
H-9 Me	1.220	1.227	Δ (S-R) – Tri-Mosher	-0.007
H-1″ a			Δ (S-R) – (Tri–Di) Mosher	+0.041
H-1″ b			Δ (S-R) – (Tri–Di) Mosher	-0.005
H-7			Δ (S-R) – (Tri–Di) Mosher	+0.004
H-8			Δ (S-R) – (Tri–Di) Mosher	+0.006
H-9			Δ (S-R) – (Tri–Di) Mosher	-0.013
H-9 Me			Δ (S-R) – (Tri–Di) Mosher	-0.019

Initial analysis of the tri-Mosher products gave inconclusive results. Specifically, subtraction of the tri-*R*-Mosher product from the tri-*S*-Mosher product

following the modified Mosher method protocol gave a negative value (-0.01) for 9-Me and a positive value (+0.01) for H-9 on the same side of the Mosher ester at C-8, as well as positive values for H-7 (+ 0.01) and H-1′′a (+0.04). Suspecting that the ambiguous data was due to anisotropic effects of the phenyl groups from the Mosher products at the 3′-aldehyde and the 2′ positions, it was reasonable to subtract the ^{1}H NMR chemical shift differences of the di-Mosher products **10a** and **10b** ($\Delta\delta_{diS\text{-}diR}$) from the differences of the tri-Mosher products **10c** and **10d** ($\Delta\delta_{triS\text{-}triR}$, Figure III.2h.iii). Analysis of these chemical shift differences ($\Delta\delta_{S(tri\text{-}di)\text{-}R(tri\text{-}di)}$) gave negative values for protons at 9-Me (-0.02) and H-9 (-0.01), and positive values for protons at H-7 (+0.01) and H-1′′a (+0.04), thus allowing the absolute configuration of C-8 to be assigned as *R* (Figure III.2h.iii).

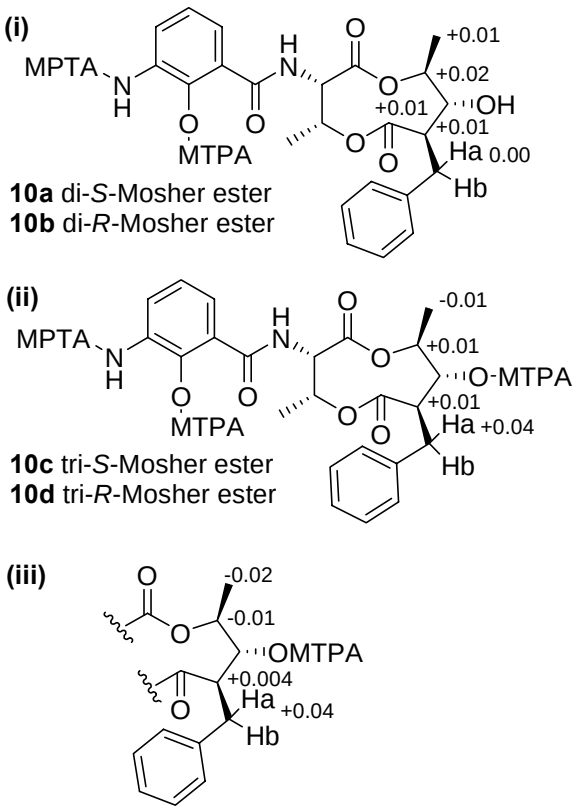

Figure III.2h: **The structures of splenocin J derivatives from Mosher acylation and the differentiation of ^{1}H NMR chemical shift values between *S* and *R* Mosher esters (Δ_{S-R}). (i) Splenocin J (10) 2', 3'-di-Mosher derivatives and Δ_{S-R} values. (ii) Splenocin J (10) 2', 3', 7-tri-Mosher derivatives and Δ_{S-R} values. (iii) Tri-Mosher Δ_{S-R} - di-Mosher Δ_{S-R}.**

Since not all splenocins displayed NOESY correlations between the left and right side of the dilactone ring as was seen for splenocin J (**10**), it was important to determine the absolute configurations of C-3 and C-4 of the embedded threonine molecule of the dilactone ring in order to assign the absolute configuration for the entire molecule. Given the *syn* relative configuration between H-3 and H-4 within

the constraints of the dilactone ring system, the D and L isomers of threonine will give opposite configurations within the molecule (Figure III.2i). To determine whether the threonine moiety was D or L, we performed an acid-catalyzed hydrolysis of splenocin J (**10**) followed by derivatization with Marfey's reagent and subsequent Marfey's analysis.[14, 15] Marfey's Method is a chromatographic technique commonly utilized in determining the absolute configuration of amino acids. In this method, amino acids are derivatized with the chiral reagent FDAA (1-fluoro-2,4-dinitrophenyl)-5-L-alaninamide.[14] Based on the relative polarities of the reaction products of one of the enantiomers of FDAA with each of the chiral amino acids, they show different retention times in a chromatography column.[14] The retention time of the derivatized threonine component of the dilactone ring compared to that of the two standards allowed us to determine that it had the L configuration, thereby confirming the complete absolute stereochemistry for splenocin J (**10**). Similar experiments were performed with splenocin F (**6**) to confirm that both benzyl and benzoyl containing splenocins contained L-threonine in the 3 and 4 positions of the dilactone ring.

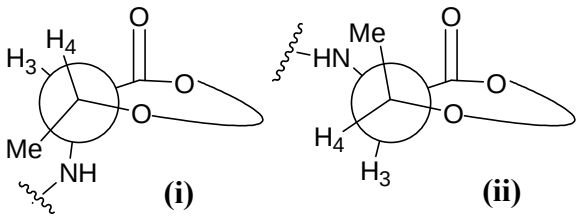

Figure III.2i: Orientations of L (i) and D (ii) threonine as would be seen with *cis*-relative configurations within the dilactone ring.

Since only splenocin J (**10**) was a feasible candidate for Mosher's analysis, we used a series of Circular Dichroism (CD) comparison experiments to confirm the absolute configurations of splenocins A-I (**1-9)**. Circular Dichroism is a spectroscopic method that relies on the effects of chiral molecules on circularly polarized light. In a CD experiment, both left and right circularly polarized light are radiated through a solution of a chiral molecule in a pathway of a given length.[16] Since both the light and the molecule are chiral, each of the chiral light pathways will interact with the molecular solution differently (one absorbs more than the other).[16] Measurement of these differences over many different wavelengths results in a CD spectrum.[16] When a molecule contains two or more chromophores that are nearby in space, and constitute a chiral system, the energy level of their excited states split.[16] This split can be observed in the CD spectrum and is referred to as a Cotton effect.[16] Comparisons of the splenocin CD spectra allowed us to group the splenocins into two different CD spectral categories (Figure III.2j). Splenocins A-C (**1-3**) and J (**10**) contain only one major chromophore, the N-formyl salicylamide group and consequently display only a weak positive signal λ 220 nm. Splenocins D-I (**4-9**) have 2 major chromophores, the N-formyl salicylamide group and also the benzoate group at C-8. Compounds **4-9** all possess a negative cotton effect at 240 nm and corresponding positive Cotton effect at 225 nm (Figure III.2j). Due to the close similarities between their CD spectra, it can be assumed that splenocins D-I (**4-9**) all have the same absolute configurations.

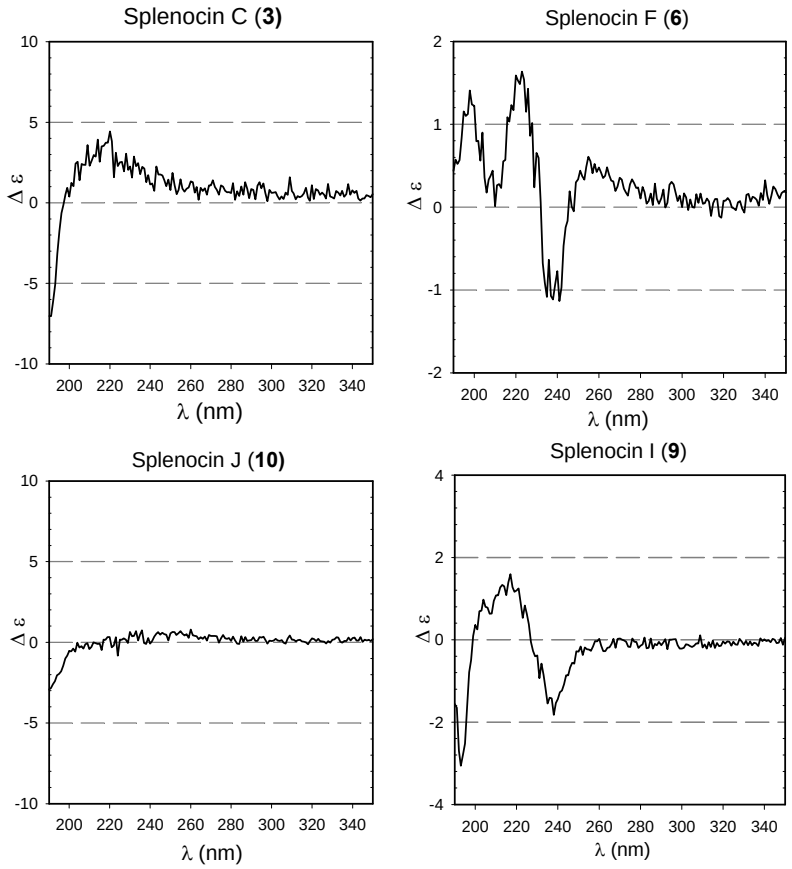

Figure III.2j: Representative CD spectra of splenocin structural groups indicating configurational similarity.

As the negative Cotton effect seen in **4**-**9** is only observable in compounds containing the C-8 benzoyl functionality, it is likely that this Cotton effect is due to Exciton Coupling of the 8-*O*-benzoyl group with the 3-*N*-formyl salicylamide moiety (Figure III.2k.i). In following the rules for Exciton Coupling of two chromophores, we analyzed a three dimensional representation of splenocins D-I (**4**-**9**) to estimate angular orientations of the electronic transition dipole moment vectors for both the 8-

O-benzoate and the 3-*N*-formyl salicylamide (Figure III.2k.ii).[16] The resulting vectors fit the observed CD spectral data supporting our absolute configurational assignment.

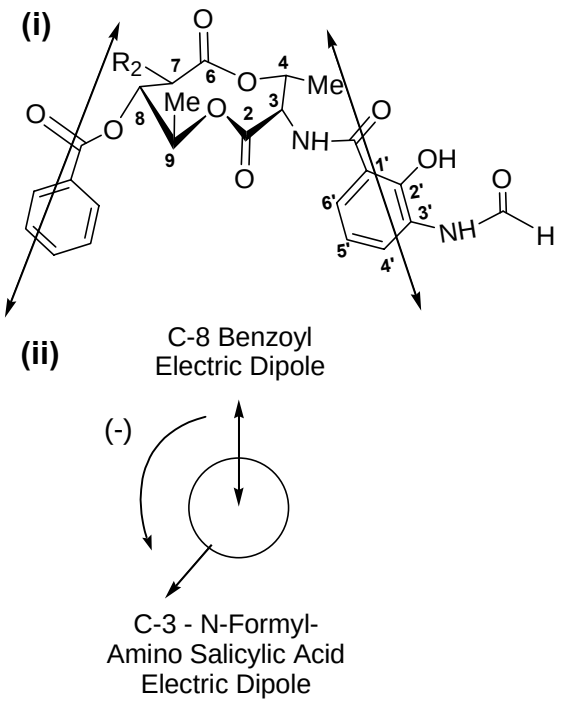

Figure III.2k: **Conformational structure (i) and vector diagram (ii) for splenocins D-I (4-9), and 10g, illustrating the observed CD Cotton effect.**

To further confirm the absolute configurations of splenocins D-I (**4-9**), we performed benzoylation reactions on splenocin I (**9**) as well as on splenocin J (**10**) whose absolute configuration had already been established chemically. These reactions created identical tri-benzoylated products (**9b** and **10g**, Figure III.2l). The CD spectra for these two compounds proved to be identical, displaying a negative cotton effect at 235 nm and a corresponding positive signal at 213 nm. Since the absolute configuration of splenocin J (**10**) had already been determined through

Mosher's and Marfey's analyses, it can now be unambiguously assumed that splenocin I (**9**) also shares this configuration. Further, as the initial set of CD experiments showed that splenocins D-I (**4-9**) all have nearly identical Cotton effects, it is reasonable to assume that they all have the same absolute configuration as splenocin J (**10**).

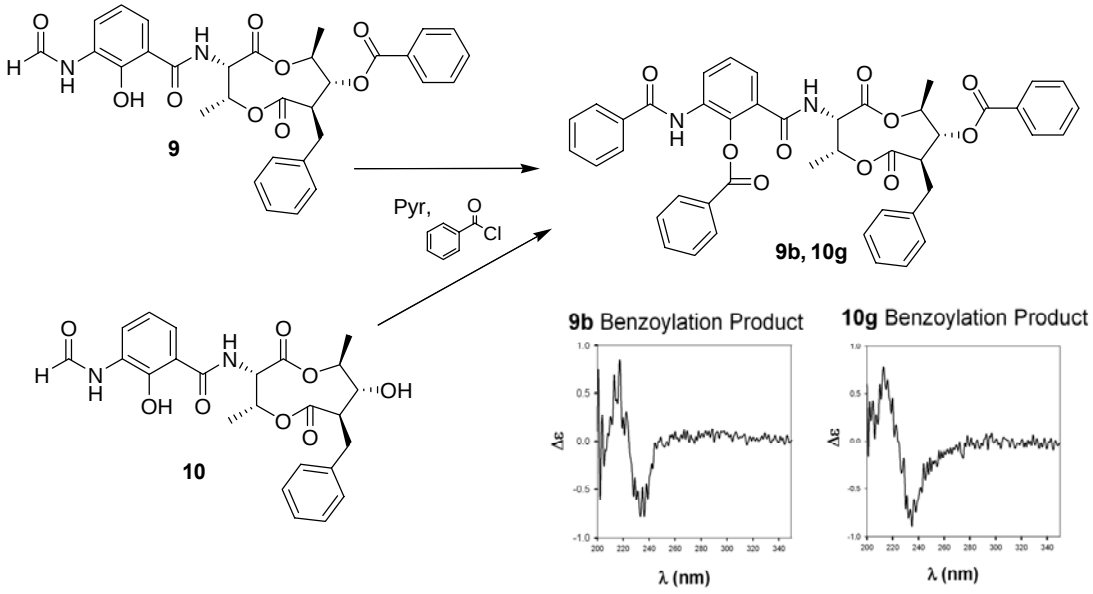

Figure III.2l: Reaction scheme for the benzoylation of splenocins I (9) and J (10) into identical tri-benzoylated products (9b, 10g) and corresponding CD spectra.

A similar set of benzoylation reactions was also performed with the benzyl-substituted splenocins A-C (**1-3**) in an attempt to create Exciton Coupling between the increased chromophore of the di-benzoylated salicylic acid and the C-7 benzyl group. However, these products yielded no observable change in the Cotton effect of their CD spectra and so a different technique was needed. Due to their close structural

similarity to splenocin J (**10**), we measured the optical rotation values in order to determine if they share identical absolute configurations. Splenocin B (**2**) had a sodium D line optical rotation value of +68.0 while splenocin J (**10**) had an optical rotation value of +69.6. These data, combined with the similarities of the CD spectra provide strong evidence that splenocins A-C have the same absolute configuration as splenocins D-J. These series of experiments confirm that splenocins A-J (**1**-**10**) all share the same absolute configuration, 3*S*, 4*R*, 7*R*, 8*R*, and 9*S,* which is identical with that of the stereocenters reported for the dilactone ring of the antimycins.[17]

III.3

Activity of Splenocins A-J in the Mouse Splenocyte Assay

III.3. Activity of Splenocins A-J in the Splenocyte Assay

The splenocins show potent biological activities in an *in vitro* mouse model of allergen induced Th2 splenocyte cytokine production characteristic of allergic asthma. As mentioned above, the parent bacterial strain CNQ-431 was selected due to the low μg/ml non-cytotoxic inhibition of OVA stimulated splenocyte cytokine interleukin 5 (IL-5) production seen in the crude extract. Upon isolation, splenocins A-I (**1-9**) showed low nanomolar suppression of IL-5 production, while splenomycin J (**10**) showed inhibition in low micromolar concentrations (Table III.3a). The inhibitory activities of splenocins A-I are comparable to the corticosteroid drug dexamethasone at similar nanomolar concentrations (Figure III.3a). Currently, corticosteriods are the most potent suppressors of cytokine production in asthma. Both dexamethasone and splenocin B inhibit antigen induced IL-5 production by greater than 80% which is comparable to production levels measured in unstimulated splenocytes.

Table III.3a: Splenocin A-J (1-10) and dexamethasone IC-80 values for Th2 Cytokines IL-5 and IL-13.

	IL-5 IC-80 (nM)	IL-13 IC-80 (nM)	Cytotoxicity LD-50 (nM)
Dexamethasone	5	5	>7100
Splenocin A (1)	8	not available	>1800
Splenocin B (2)	2	2	>1700
Splenocin C (3)	7	21	>560
Splenocin D (4)	66	66	>5500
Splenocin E (5)	7	22	>570
Splenocin F (6)	7	7	>560
Splenocin G (7)	2	7	>550
Splenocin H (8)	7	21	>1600
Splenocin I (9)	59	21	>540
Splenocin J (10)	3200	660	>6000

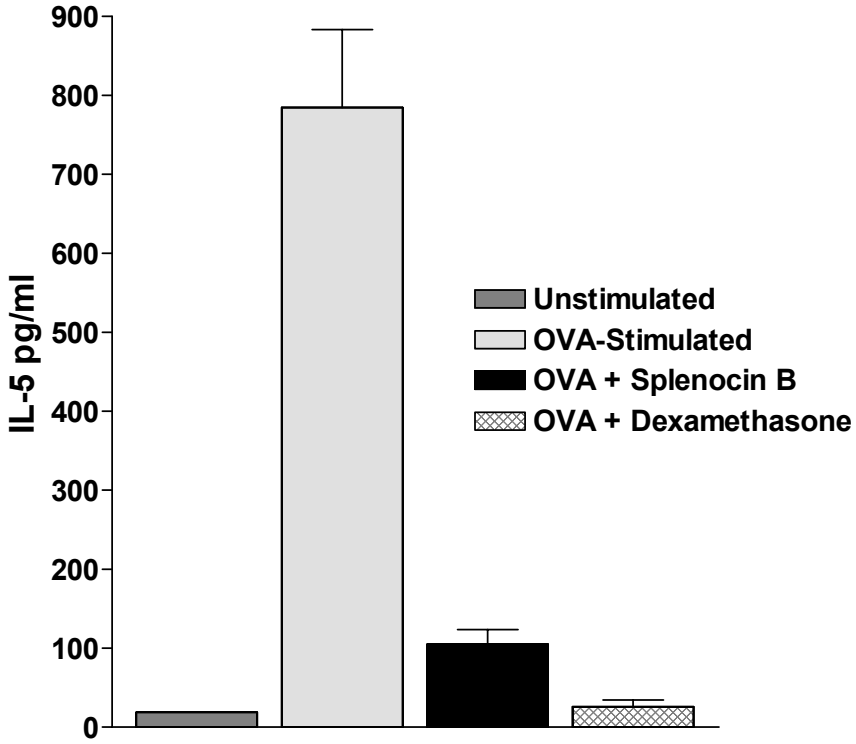

Figure III.3a: Interleukin 5 (IL-5) levels of cultured splenocytes. (A) unstimulated control. (B) OVA-stimulated control. (C) OVA-stimulated + Splenocin B (2) (5 nM). (D) OVA-stimulated + dexamethasone (5 nM).

In order to determine whether the splenocins inhibited other Th2 cytokines in addition to IL-5, levels of the Th2 cytokine IL-13 were also analyzed in the splenocyte cultures (Table III.3a, Figure III.3b). These data indicate that splenocins A-J inhibit multiple Th2 cytokines including IL-5 and IL-13 at low ng/ml concentrations *in vitro*.

Since the splenocyte cell culture population is a heterogeneous mixture of cell types, we were interested in determining whether splenocins were acting solely on Th2 cells or if they also inhibited the cytokine production capabilities of APC's. To investigate this, we quantified cytokine levels of the APC derived cytokines IL-1β and TNF-α. These studies demonstrate that splenocins are capable of inhibiting both Th2 and APC derived cytokines (Figure III.3b). Splenocins B and G (**2** and **7**) inhibited IL-1 by approximately 85 % and TNF-α by approximately 75%. Splenocins B (**2**) and G (**7**) are as effective as dexamethasone in inhibiting Th2 cytokine production and are only slightly less effective than dexamethasone in suppressing APC cytokine production of IL-1 and TNF-α (Figure III.3b).

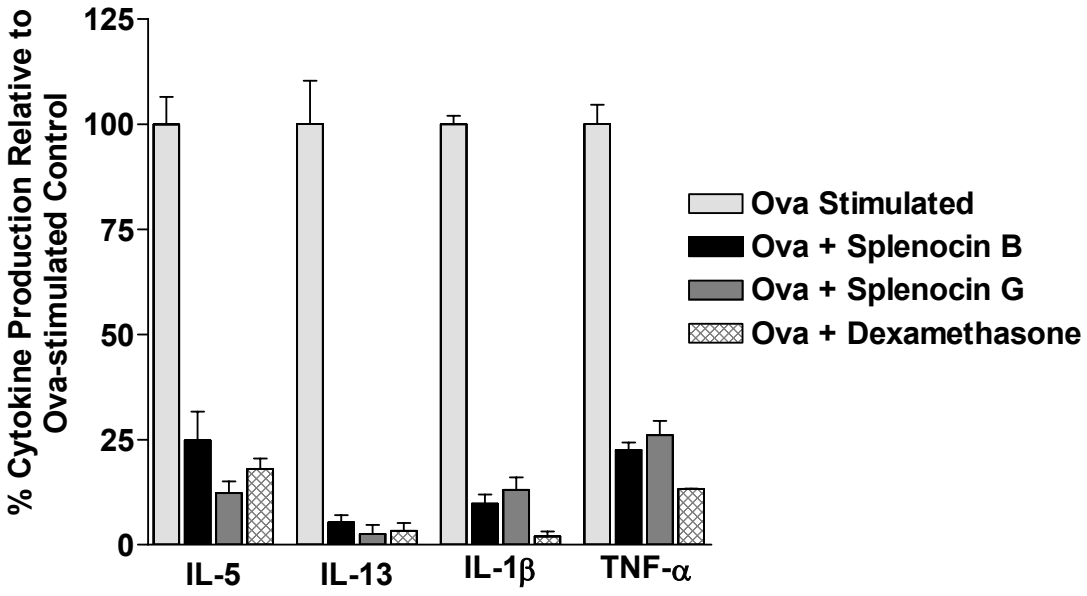

Figure III.3b: Splenocyte cytokine inhibition: Levels of Th2 (IL-5, IL-13) and APC related (IL-1β, TNF-α) cytokines of Ova-stimulated splenocytes incubated with either splenocins B or G (2 or 7) at 10nM, or dexamethasone at 10nM.

Due to their structural similarity of the splenocins to the known antimycins, antimycin A_2 (Sigma) was also tested in this assay. Antimycin A_2, which has a hexyl alkyl chain at C-7and a propyl acyl chain at C-8, displayed a similar activity profile to that seen from the splenocins. Recent studies have shown that antimycins induce cellular apoptosis in hepatocytes by binding to the hydrophobic groove of Bcl-2/Bcl-x_L proteins on the surface of mitochondria.[18] However, these studies report cell death in the micromolar ranges and similar experiments with lymphocytes or splenocytes have not been reported. Recently reported studies with antimycins have also shown that at concentrations lower than the cytotoxic threshold, immunosuppressive anti-cancer activities are observed. Specifically, *in vivo* cancer models explored by Nose

and co-workers have shown non-toxic inhibition of angiogenesis and HIF-1α inhibition by antimycins at concentrations similar to those used in our investigations.[19] Another recent *in vivo* study investigated the non-toxic cardio-protective effects of antimycin in combating ischemia, while *in vitro* studies have examined the non-toxic effects of antimycins in mouse hepatocytes.[20] However, to our knowledge, the present study reflects the first investigations of the novel splenocins and the structurally related antimycins in a model of allergic inflammation.

The splenocyte assay we have utilized provides a novel assay to screen natural extract libraries for compounds with the ability to inhibit pro-inflammatory cytokines produced by the antigen-presenting cell T-cell interaction. By using corticosteroids as our control therapy, we are able to compare the anti-inflammatory potency of novel compounds to the most potent anti-inflammatory molecules in clinical use today. Interestingly, in this study, we have identified a series of compounds (splenocins A-I) that display potency levels equal to those of the corticosteriods. As corticosteriods are the current most effective therapy in asthma, identifying compounds that have as potent anti-inflammatory actions, but do not have the same negative side effects associated with corticosteroid therapy, would be an important therapeutic advance.

While further immunological experiments are in preparation to investigate this activity further within the mouse allergic asthma model *in vivo*, our initial data suggests a potential for therapeutic development of splenocins in inflammatory diseases such as asthma, as well as their potential uses as anti-inflammatory agents in other diseases in which suppression of cytokines by APCs and T-cells may be beneficial.

III.4

Experimental

III.4. Experimental

General Experimental Procedures. ^{1}H, ^{13}C, and 2D NMR spectral data were obtained on Varian Inova 300 MHz and 500 MHz NMR spectrometers. UV spectra were recorded on a Varian Cary 50 Conc UV Visible spectrophotometer with a path length of 1 cm. IR spectra were recorded in a Nicolet IR100 FT-IR spectrometer. Optical rotations were measured using a Rudolph Research Autopol III Automatic polarimeter with a 10 cm cell. High resolution MALDI-FTMS data were collected on an IonSpec Ultima mass spectrometer at the Scripps Research Institute, La Jolla. Low resolution LC/MS data were obtained on a Hewlett-Packard series 1100 LC/MS system with a reversed phase C18 column (Agilent, 4.6 mm X 100 mm, 5 μm) with a 0.7 mL/min flow rate. CD Spectra were obtained on a Jasco 810 spectropolarimeter with a 1 cm path length. OD measurements of ELISA experiments were recoded at 450 nm on a Biorad Model 680 microplate reader.

Isolation of CNQ-431 Strain, Identification, Cultivation, and Extraction. Marine-derived *Streptomyces* strain CNQ-431 was isolated on growth medium A1+C (10 g of starch, 4 g of peptone, 2 g of yeast extract, 1 g of calcium carbonate, 18 g of agar, and 1 L of sea water) from a marine sediment collected from a depth of 30 m 1 mile Northwest of the Scripps Institution of Oceanography (La Jolla, CA). Strain CNQ-431 was classified as a *Streptomyces* sp. based on 16S rDNA analysis which showed 100% sequence identity between strain CNQ-431 and 5 strains including *Streptomyces fungicidus*, AY636155; two strains of an unidentified *Streptomyces*, AF429400 and AM21770.1; and two strains of bacteria in the order Actinomycetales, AY944261 and AY944255. The strain was cultured in 60 x 1 L volumes of media

A1 while shaking at 230 rpm for 3 days. After 72 hours, 20 g/L of XAD-7 adsorbent resin was added to each flask and the flasks were allowed to shake for an additional 24 hours. At this time, an additional 20 g/L of XAD-7 adsorbent resin was added. The cultures were allowed to shake for an additional 24 hours, at which time the resin was collected by filtration through cheesecloth, washed with deionized water and eluted twice with acetone. Evaporation of the extraction solvent *in vacuo* left a wet residue that was partitioned with EtOAc, providing approximately 130 mg of dry organic extract per 1 L of culture after solvent removal.

Isolation and Purification of Splenocins A-J (1-10). The EtOAc extracts of a 60 x 1 L fermentations (7.0 g) was subjected to silica gel column chromatography purification eluting with solvent mixtures of *n*-hexanes-EtOAc (10:1), *n*-hexanes-EtOAc (5:1), *n*-hexanes-EtOAc (2.5:1), *n*-hexanes-EtOAc (1:1), EtOAc, EtOAc – MeOH (10:1), and 100% MeOH, successively. The EtOAc – MeOH (2.5:1) and EtOAc – MeOH (1:1) eluting fractions (Q431-3 and 4) showed the most potent IL-5 inhibition levels in the mouse splenocyte assay and by LCMS, contained splenocins A-I (**1-9**) as well as several antimycins. The 100% EtOAc (CNQ431-5) fraction contained splenocin J (**10**) as well as the 8-hydroxy-antimycins. Fractions CNQ-431-3,4, and 5 were re-fractionated by C-18 reversed-phase HPLC with an MeCN-H_2O step gradient from 40% MeCN to 100% MeCN over 110 min. to obtain nearly pure splenocins (A-J). Final purification was performed with C-8 and C-18 semi-preparative reversed phase HPLC using isocratic solvent systems ranging between 50:50 and 90:10 MeCN:H_2O.

Splenocin A (1) White amorphous powder, CD (MeCN) $\Delta\varepsilon_{220}$ +2.5, $\Delta\varepsilon_{190}$ –4.8; UV (EtOH): 230 (ϵ = 23,000), 360 (ϵ =5,750) nm. IR (film) ν_{max} 3381, 1748, 1527, 1368, and 736 cm^{-1}. HR ESI-TOF MS: Obsd. *m/z* 535.1683 $[M+Na]^+$ ($C_{26}H_{28}N_2O_9Na$ requires 535.1687). See Table III.2a for NMR data.

Splenocin B (2) White amorphous powder, $[\alpha]_D$ = +68 (0.1, CH_3OH) CD (MeCN) $\Delta\varepsilon_{213}$ +4.2, $\Delta\varepsilon_{190}$ –10.8; UV (EtOH): 230 (ϵ = 18,000), 320 (ϵ = 4,300) nm. IR (film) ν_{max} 3361, 1746, 1527, 1369, and 737 cm^{-1}. HR ESI-TOF MS: Obsd. *m/z* 541.2167 $[M+H]^+$ ($C_{28}H_{32}N_2O_9$ requires 541.2180). See Table III.2a for NMR data.

Splenocin C (3) White amorphous powder, CD (MeCN) $\Delta\varepsilon_{220}$ +4.4, $\Delta\varepsilon_{190}$ –7.0; UV (EtOH): 230 (ϵ = 19,400), 320 (ϵ = 4,400) nm. IR (film) ν_{max} 3381, 1747, 1527, 1355, and 744 cm^{-1}. HR ESI-TOF MS: Obsd. *m/z* 555.2322 $[M+H]^+$ ($C_{29}H_{35}N_2O_9$) requires 555.2337). See Table III.2a for NMR data.

Splenocin D (4) White amorphous powder, CD (MeCN) $\Delta\varepsilon_{238}$ –2.2, $\Delta\varepsilon_{220}$ +2.3; UV (EtOH): 230 (ϵ = 16,400), 320 (ϵ = 3,000) nm. IR (film) ν_{max} 3361, 1740, 1537, 1350, and 702 cm^{-1}. HR ESI-TOF MS: Obsd. *m/z* 511.1716 $[M-H]^-$ ($C_{26}H_{27}N_2O_9$ requires 511.1722). See Table III.2b for NMR data.

Splenocin E (5) White amorphous powder, CD (MeCN) $\Delta\varepsilon_{237}$ –2.9, $\Delta\varepsilon_{221}$ +4.0; UV (EtOH): 230 (ϵ = 18,400), 320 (ϵ = 3,300) nm. IR (film) ν_{max} 3381, 1753, 1534, 1345, and 737 cm^{-1}. HR ESI-TOF MS: Obsd. *m/z* 541.2168 $[M+H]^+$ ($C_{28}H_{33}N_2O_9$ requires 541.2180). See Table III.2b for NMR data.

Splenocin F (6) White amorphous powder, CD (MeCN) $\Delta\varepsilon_{241}$ –2.2, $\Delta\varepsilon_{220}$ +4.5; UV (EtOH): 230(ϵ = 21,100), 320 (ϵ = 4,400) nm. IR (film) ν_{max} 3347, 1760, 1540,

1369, and 744 cm^{-1}. HR ESI-TOF MS: Obsd. *m/z* 555.2326 $[M+H]^+$, ($C_{29}H_{35}N_2O_9$ requires 555.2337). See Table III.2b for NMR data.

Splenocin G (7) White amorphous powder, CD (MeCN) $\Delta\varepsilon_{239}$ –2.1, $\Delta\varepsilon_{221}$ +2.8; UV (EtOH): 230 (ϵ = 22,700), 320 (ϵ = 5,700) nm. IR (film) ν_{max} 3347, 1740, and 764 cm^{-1}. HR ESI-TOF MS: Obsd. *m/z* 569.2481 $[M+H]^+$ ($C_{30}H_{37}N_2O_9$ requires 569.2493). See Table III.2b for NMR data.

Splenocin H (8) White amorphous powder, CD (MeCN) $\Delta\varepsilon_{240}$ –10.3, $\Delta\varepsilon_{221}$ +14.9; UV (EtOH): 230(ϵ =23,000), 320 (ϵ = 6,000) nm. IR (film) ν_{max} 3315, 1725, 1534, 1275, 785 cm^{-1}. HR ESI-TOF MS: Obsd. *m/z* 583.2664 $[M+H]^+$ ($C_{31}H_{39}N_2O_9$ requires 583.2577). See Table III.2b for NMR data.

Splenocin I (9) White amorphous powder, CD (MeCN) $\Delta\varepsilon_{238}$ –4.5, $\Delta\varepsilon_{217}$ +3.9; UV (EtOH): 230 (ϵ = 23,000), 350 (ϵ = 5,750) nm. IR (film) ν_{max} 3374, 1744, 1535, 1370, and 734 cm^{-1}. HR ESI-TOF MS: Obsd. *m/z* 575.2000 $[M+H]^+$ ($C_{21}H_{31}N_2O_9$ requires 575.2024). See table III.2c for NMR data.

Splenocin J (10) White amorphous powder, $[\alpha]_D$ = +70 (0.18, CH_3OH). UV (EtOH): 230 (ϵ = 29,600), 337 (ϵ = 5,600) nm. IR (film) ν_{max} 3375, 1740, 1540, 1360, and 730 cm^{-1}. HR ESI-TOF MS: Obsd. *m/z* 493.1573 $[M+Na]^+$ ($C_{24}H_{26}N_2O_8Na$ requires 493.1581). See Table III.2c for NMR data.

Mosher MTPA esters 10a/10b, 10c/10d, 10e/10f. Splenocin J (**10**) (1.0 mg) was divided into two equal portions and each was dissolved in 500 μL of pyridine in separate reaction vials. To each, 5mg of DMAP and either 10 μL of (R)-MTPA-Cl or 10 μL of (S)-MTPA-Cl was added. After 5 hours, equal amounts of di- and tri-Mosher ester products were formed. The reaction was terminated and reaction

products separated by C-18 reversed phase HPLC. The ^{1}H NMR spectra for the (R)-MTPA-Cl and (S)-MTPA-Cl di- and tri-Mosher esters were recorded.

Benzoylation of Splenocins I (9) and J (10) to yield 9b and 10g. 0.5 mg of splenocins I (**9**) and J(**10**) were each dissolved in separate 1.0 mL volumes of pyridine. To each sample, DMAP (5 mg) and benzoyl chloride (1 mg) were added and the reaction was allowed to proceed for 12 hours. The reaction mixture was filtered and concentrated under reduced pressure. The resulting benzoylated products **9b** and **10g** were purified by C-18 HPLC and analyzed by LC-MS. LRMS (ESI) **9b, 10b**, *m/z* 777.24 [M+Na], *m/z* 777.24 [M+Na].

Marfey's Analysis of the Splenocin H (6) and J (10) derived Threonine. Approximately 0.2 mg each of splenocin H (6) and splenocin J (10) were separately hydrolyzed with 6N HCl (0.8 mL) overnight in a hot oil bath at 105˚C. The hydrolysates were then evaporated to dryness and re-suspended in 0.2 mL H_2O. To each aqueous hydrolysate, 0.5 mg of 1-fluoro-2,4-dinitrophenyl-5-L-leucinamide (L-FDLA) suspended in 0.1 mL of acetone and 20 µL of 1N $NaHCO_3$ were added and the mixtures heated at 40˚C for 5 minutes. The mixtures were then cooled to room temperature, neutralized with 2N HCl and evaporated to dryness. The residues were then re-suspended in 500 µL of MeCN and subjected to LCMS analysis by comparison to standard D-threonine and L-threonine L-FDLA derivatives that had been prepared in the same fashion. The derivatized threonine molecules, derived from splenocins H (6) and J (10), were found to elute at the same time as the L-threonine derivatized standard (L-threonine = 19.7 min; D-threonine = 22.7min).

References

1. Barrow, C. J.; Oleynek, J. J.; Marinelli, V.; Sun, H. H., ;; Kaplita, P.; Sedlock, D. M.; Gillum, A. M.; Chadwisk, C. C.; Cooper, R., Antimycins, Inhibitors of ATP-Citrate Lyase, from a *Streptomyces* sp. *The Journal of Antibiotics* **1997,** 50, (9), 729-733.

2. Hosotani, N.; Kumagai, K.; Nakagawa, H.; Shimatani, T.; Saji, I., Antimycins A_{10}~A_{16}, Seven New Antimycin Antibiotics Produced by *Streptomyces* spp. SPA10191 and SPA-8893. *Journal of Antibiotics* **2005,** 58, (7), 460-467.

3. Shiomi, K.; Hatae, K.; Hatano, H.; Matsomoto, A.; Takahashi, Y.; Jiang, C.-L.; Tomoda, H.; Kobayashi, S.; Tanaka, H.; Omura, S., A New Antibiotic, Antimycin A_9, Produced by *Streptomyces* sp. K01-0031. *Journal of Antibiotics* **2005,** 58, (1), 74-78.

4. Fondja Yao, C. B.; Schiebel, M.; Helmke, E.; Anke, H.; Laatsch, H., Prefluostatin and New Urauchimycin Derivatives Produced by *Streptomycete* Isolates. *Z. Naturforsch.* **2006,** 61b, 320-325.

5. Ishiyama, T.; Endo, T.; Otake, N.; Yonehara, H., Deisovalerylblastmycin Produced by *Streptomyces* sp. *The Journal of Antibiotics* **1976,** 29, (8), 804-808.

6. Imamura, N.; Nishijima, M.; Adachi, K.; Sano, H., Novel Antimycin Antibiotics, Urauchimycins A and B, Produced by a Marine Actinomycete. *The Journal of Antibiotics* **1992,** 46, (2), 241-246.

7. Hayashi, K.-I.; Nozaki, H., Kitamycins, New Antimycin Antibiotics Produced by *Streptomyces* sp. *The Journal of Antibiotics* **1999,** 52, (3), 325-328.

8. Gunther, H., *NMR Spectroscopy - Basic Principles, Concepts, and Applications in Chemistry*. 2nd ed.; John Wiley and Sons: New York, 2001.

9. Crews, P.; Rodriguez, J.; Jaspers, M., *Organic Structure Analysis*. Oxford University Press.

10. Ohtani, I.; Kusumi, T.; Kashman, Y.; Kakisawa, H., High-Field FT NMR Application of Mosher's Method. THe Absolute Configurations of Marine Terpenoids. *The Journal of the American Chemical Society* **1991,** 113, 4092-4096.

11. Ohkawa, S.; Fukatsu, K.; Miki, S.; Hashimoto, T.; Sakamoto, J.; Doi, T.; Nagai, Y.; Aono, T., 5-Aminocoumarans: Dual Inhibitors of Lipid Peroxidation and Dopamine Release with Protective Effects against Central Nervous System Trauma and Ischemia. *Journal of Medicinal Chemistry* **1997,** 40, (4), 559-573.

12. Kikuchi, H.; Saito, Y.; Sekiya, J.; Okano, Y.; Saito, M.; Nakahata, N.; Kubohara, Y.; Oshima, Y., Isolation and Synthesis of a New Aromatic Compound, Brefelamide, from Dictyostelium Cellular Slime Molds and Its Inhibitory Effect on the Proliferation of Astrocytoma Cells. *Journal of Organic Chemistry* **2005,** 70, (22), 8854-8858.

13. Campbell, T. W.; McCoy, V. E.; Kauer, J. C.; Foldi, V. S., Preparation of Some 9,10-Difunctional Derivatives of 9,10-Dihydro-9,10-ethanoanthracene. *Journal of Organic Chemistry* **1961,** 26, (5), 1422-1426.

14. Fujii, K.; Ikai, Y.; Mayumi, T.; Oka, H.; Suzuki, M.; Harada, K., A Nonempirical Method Using LC/MS for Determination of the Absolute Configuration of Constituent Amino Acids in a Peptide: Elucidation of Limitations of Marfey's Method and of Its Seperation Mechanism. *Analytical Chemistry* **1997,** 69.

15. Fujii, K.; Ikai, Y.; Oka, H.; Suzuki, M.; Harada, K., A Nonempirical Method Using LC/MS for Determination of the Absolute Configuration of Constituent Amino Acids in a Peptide: Combination of Marfey's Method and WIth Mass Spectrometry and Its Practical Application. *Analytical Chemistry* **1997,** 69, 5146-5151.

16. Berova, N.; Nakanishi, K.; Woody, R. W., *Circular Dichroism Principles and Practice*. 2nd ed.; Wiley-VCH, Inc.: New York, 2000.

17. Kinoshita, M.; Aburaki, S.; Umezawa, S., Absolute Configurations of Antimycin Lactones and Antimycin A. *The Journal of Antibiotics* **1972,** 15, (6), 373-376.

18. Tzung, S.-P.; Kim, K. M.; Basanez, G.; Giedt, C. D.; Simon, J.; Zimmerberg, J.; Zhang, K. Y. J.; Hockenbery, D. M., Antimycin A Mimics a Cell-Death-Inducing Bcl-2 Homolgy Domain 3. *Nature Cell Biology* **2001,** 3, 183-191.

19. Maeda, M.; Hasebe, Y.; Egawa, K.; Shibanuma, M.; Nose, K., Inhibition of Angiogenesis and HIF-1α Activity by Antimycin A1. *Biol. Pharm. Bull.* **2006,** 29, (7), 1344-1348.

20. Kabir, A. M. N.; Cao, X.; Gorog, D. A.; Bassi, R.; Bellahcene, M.; Quinlan, R. A.; Davis, R. J.; Flavell, R. A.; Shattock, M. J.; Marber, M. S., Antimycin A Induced Cardioprotection is Dependant on Pre-ischemic p38 MAPK activation but independant of MKK3. *Journal of Molecular and Cellular Cardiology* **2005,** 39, 709-717.

IV

Anti-Inflammatory Nor-Diterpenes from a Marine Bacterium: Marinenes A and B

IV.1

Bacterial Terpene Production

IV.1. Bacterial Terpene Production

Terpenoids include a wide variety of structurally diverse natural products, all arising from a basic 5 carbon isoprene unit.[1] They are the largest class of natural products with over 24,000 different structures described to date.[2] The biosynthesis of these compounds begins via one of two pathways, the mevalonate pathway or the mevalonate-independent (or deoxyxylulose) pathway.[1, 3] Terpenoids include both the pure terpenes, whose carbon backbones are derived purely from isoprene units, and the meroterpenoids in which a portion is derived from another biosynthetic pathway (*e.g.* polyketide synthase, or amino acid biosynthesis pathway).[1] Terpenoids are classified by number of isoprene units. C_{10} compounds are classified as monoterpenes, C_{15} as sesquiterpenes, C_{20} as diterpenes, C_{25} as sesterterpenes, C_{30} as triterpenes and C_{40} as tetraterpenes.[1] Mono and sesquiterpenes are usually volatile and have many ecological roles in communication, as attractants, and in defense against other organisms.[4] Metabolites such as chlorophyll, vitamin K, as well as the potent anti-cancer drug Taxol, all contain diterpenes in their structures.[1] The triterpenes include important molecules such as cholesterol, and the sugar-containing saponins, and are the precursors for the anti-inflammatory corticosteroids.[1] Tetraterpenoids are also called the carotenoids and include β-carotene, lycopene, and vitamin A_1 (retinol).[1] Nor-terpenes are terpenes that have undergone an enzymatic cleavage to remove one carbon atom.

All living organisms produce terpenoids as part of primary metabolism and phyla such as plants, fungi, cyanobacteria, porifera, and insects are all well documented as prolific producers of terpenoids as secondary metabolites.[1, 5]

However, there are few documented examples of terpenoid secondary metabolites from bacteria.[3] The majority of these are meroterpenoids (*e.g.* the napyradiomycins,[6] furaquinocins[7], and napthterpin[8]). While reports of bacterial meroterpenoids are rare, reported production of pure terpenes by bacteria is even more elusive. Recently, several mono- and sesquiterpenes have been isolated from bacteria, the most famous of these being geosmin, a tri-nor sesquiterpenoid which gives soil its earthy scent.[9] However, these compounds comprise only a few dozen out of the tens of thousands of reported bacterial secondary metabolites. A literature search produced only ten references describing pure terpenes produced by bacteria (Figure IV.1.a).[2-4, 10-16] Two of these were produced by gram negative gliding bacteria[10, 11] and the rest by gram positive actinobacteria[4, 12-16].

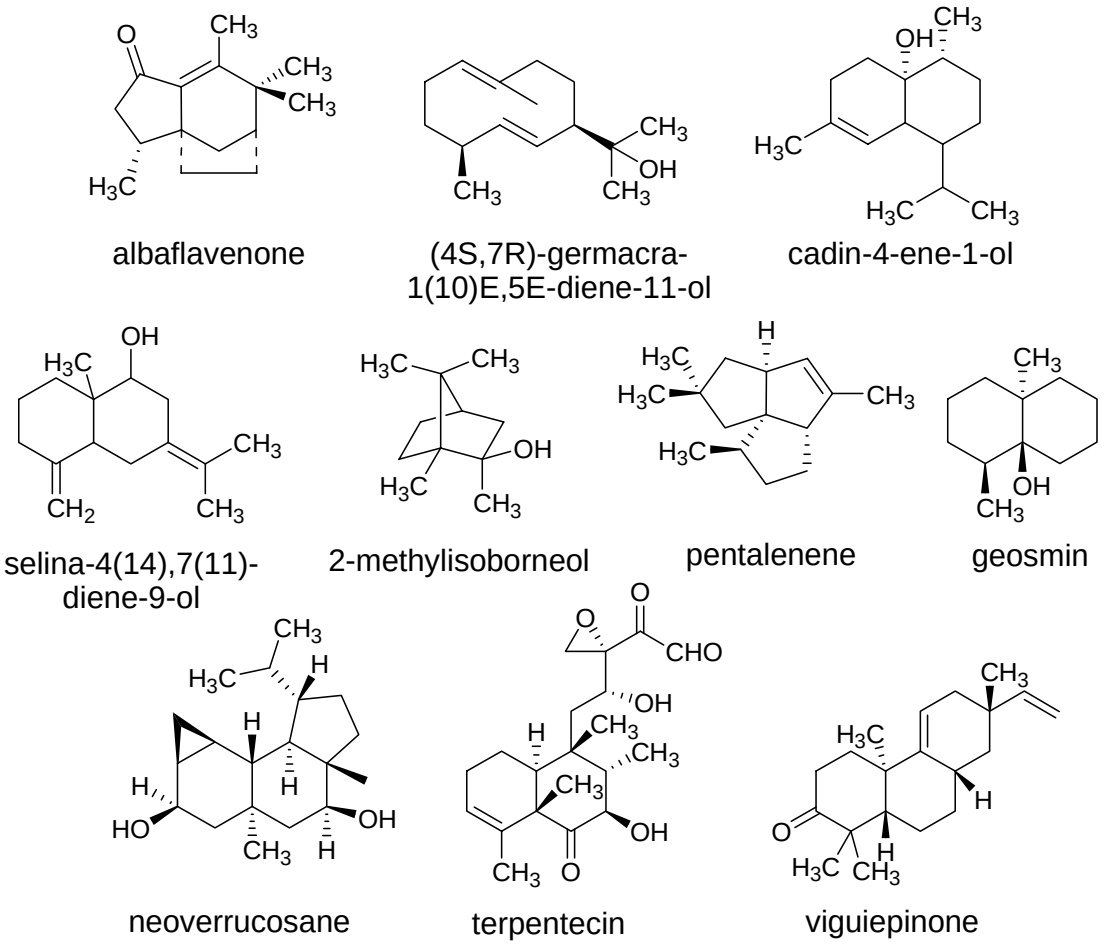

Figure IV.1a: Some known pure terpenes produced by bacteria

It is unclear whether the dearth of reported examples of bacterial terpene production is due to an actual lack of production by bacteria, or whether bacterial terpenes have been overlooked by natural product chemists, although the former is more likely. Another possibility is that some terpenes discovered in macroorganisms may actually be produced by associated bacteria. In this chapter, we describe the isolation, structure elucidation, and biological activity of the marinenes, two new C19 nor-diterpenes from a marine derived bacterial strain of the genus *Micromonospora* (Figure IV.1b). To our knowledge, this is the first report of a nor-diterpene isolated

from a bacterium and only the fourth report of a pure diterpene isolated from a gram-positive bacterium. Marinenes A and B display low micromolar activity in the mouse splenocyte assay.

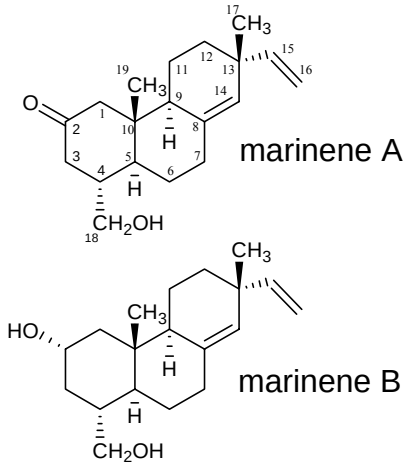

Figure IV.1b: Structures of marinenes A and B.

IV.2

Culturing, Isolation and Structure Elucidation of Marinenes A and B

IV.2. Cultivation, Isolation, and Structure Elucidation of Marinenes A and B.

The organic extract of bacterial strain CNR291 displayed potent activity in the mouse splenocyte assay ($IC_{75} < 42\mu g/ml$). In order to obtain enough material for further chemical and biological investigations, a 40L large-scale fermentation of strain CNR291 was extracted with XAD resin, the resin was extracted with acetone and concentrated to dryness by rotary evaporation prior to partitioning between water and ethyl acetate. The EtOAc fraction was fractionated by C-18 preparative HPLC using a step gradient of acetonitrile and water to give 26 fractions. Fraction 22 showed low micromolar suppression of IL-5 production in the splenocyte assay and was selected for further chemical investigation.

The proton NMR spectrum of fraction 22 obtained in deuterated acetone revealed the presence of a nearly pure compound (Figure IV.2a). Subsequent LCMS analysis showed a single major UV active peak. The compound was further purified by semi-preparative C_{18} reversed-phase HPLC under isocratic conditions (69% $MeCN/H_2O$) and was observed to elute at 17 minutes. Marinene A was isolated as an optically active white solid that gave an indistinct UV chromophore with a maximum absorbtion at 210 nm. High resolution ESI-TOF mass spectrometry gave an $[M+H]^+$ ion of 289.2170 which corresponds to a molecular formula of $C_{19}H_{29}O_2$. A strong, broad IR band at 3420 cm^{-1} indicated the presence of a hydroxyl functionality while a strong, sharp band at 1690 cm^{-1} indicated the presence of a ketone group (Figure IV.2h).

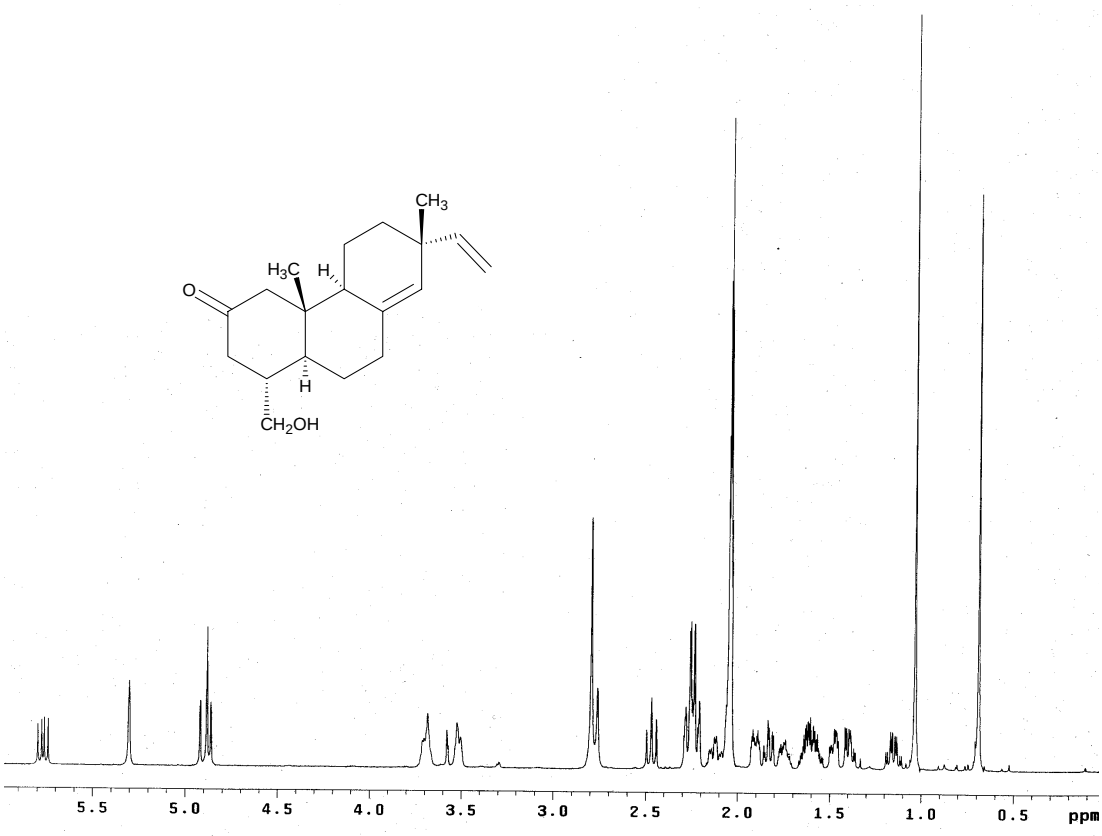

Figure IV.2a. Proton NMR spectrum of Marinene A in acetone-d_6 (500MHz).

Analyses of ^{1}H, COSY and TOCSY (Total Correlation Spectroscopy) NMR experiments revealed several spin systems (Table IV.2a and Figure IV.2b). Like the COSY experiment, the TOCSY NMR experiment detects protons in the same spin system.[17] However, the TOCSY experiment extends spin systems by showing ^{1}H-^{1}H connectivities up to seven bonds away and is therefore quite useful in compounds where proton resonances are very close together.[17] The first spin system in marinene A was assembled starting with a methine proton at H-9 (δ_H 2.05), which showed ^{1}H-^{1}H COSY correlations to H-11a and H-11b (δ_{Ha} 1.58, δ_{Hb} 1.63). Protons H-11a and H-11b correlated to H-12a and H-12b (δ_{Ha} 1.47, δ_{Hb} 1.40). A second spin system

started with methine proton H-4 (δ_H 1.75) which showed ^{1}H-^{1}H COSY correlations to two pairs of methylene protons H-3a and H-3b (δ_{Ha} 2.47, δ_{Hb} 2.22), and H-18a and H-18b (δ_{Ha} 3.69, δ_{Hb} 3.51) as well as a methine proton H-5 (δ_H 1.83). Protons H-18a and H-18b both showed ^{1}H-^{1}H TOCSY correlations to a hydroxyl proton (δ_H 2.79). This spin system was further extended from methine proton H-5 (δ_H 1.83), which showed additional COSY correlations with methylene proton H-6b (δ_{Hb} 1.15). This methylene correlated to the protons of a second methylene H-7a and H-7b (δ_{Ha} 2.27, δ_{Hb} 2.12). A third and final spin system linked proton H-15 (δ_H 5.74) with exomethylene protons H-16a and H-16b (δ_{Ha} 4.908, δ_{Hb} 4.88).

Table IV.2a. 1D and 2D NMR data for marinene A in acetone-d_6.

#	δ_C[a]	δ_H[b] (*J* in Hz)	COSY	NOESY	HMBC
1	53.7	2.26 br d[c] (13.0)		19	2, 19, 10, 9, 5
		2.22 br d[c] (13.0)	19		
2	211.0				
3	44.9	2.47ddd (13.0, 13.0, 2.5)	4, 3b		18, 4, 2, 1
		2.22 m[c]	4, 3a	18b, 5, 4,	4, 2, 1
4	42.0	1.75m	18a[e], 18b, 5, 3	19, 18b, 3b	5, 10[e]
5	45.7	1.83 ddd (12.0, 12.0, 3.0)	6b, 4	7b, 3b,	19, 10, 7[e], 6, 4
6	25.6	1.90 br dddd (12.0, 5.5, 3.0, 2.5)	7a[e], 7b, 6b, 5	18a, 18b, 7a, 7b,	10, 8, 7[e], 5,
		1.15 dddd (12.0. 12.0, 12.0, 4.5)	7, 6a, 5	19, 7a	10, 7, 5, 4,
7	35.5	2.27 m[c]	7b, 6	14, 6a, 6b	14, 8, 6
		2.12 br ddd (12.0, 12.0, 5.5)	7a, 6	6a, 5	14, 8, 6, 5
8	137.0				
9	48.5	2.05 m[d]	11, 14[e]	12a, 12b, 11a, 5	19, 14, 11, 10, 8, 5, 1
10	43.2				
11	19.7	1.63 br dddd (13.0, 6.0, 6.0, 4.0)	12, 9	12	13, 12, 10, 9, 8
		1.58 br dddd (13.0, 11.0, 6.0, 3.5)	12, 9	19, 17, 9	13, 12, 9
12	35.0	1.47 br ddd (13.0, 6.0, 3.5)	12b, 11	19, 17, 11b, 9	15, 14, 13, 11, 9, 6
		1.40 ddd (13.0, 11.0, 4.0)	12a, 11	11b, 9	15, 13, 11, 9, 6
13	38.0				
14	129.9	5.30 br s.	9[e]	17, 7a	17[e], 15, 13, 12, 9, 7
15	149.3	5.74 dd (17.5, 11.0)	16	17[e]	17, 14, 13
16	111.0	4.90 dd (17.5, 1.5)	15	17	15, 13
		4.88 dd (11.0, 1.5)	15		
17	26.5	1.03 s		16a, 15[e], 14, 12a,11a	16, 15, 14, 12, 13
18	63.7	3.69 br m[c]	4	6a	
		3.51 br d (11.0)	4	6a, 4, 3b,	5
18-OH		3.69 br s[c]			
19	14.5	0.69 s	1b	12a, 1la, 6b, 4, 1a	10, 9, 5, 1

[a] Assignment by 1-D ^{13}C methods at 125 MHz.
[b] Assignment by ^{1}H, gHSQC, and gHMBC NMR methods at 500MHz.
[c] Overlapping signals
[d] Overlapping signal with a solvent peak
[e] Weak signals
[f] Correlation peak in ^{1}H-^{1}H TOCSY spectrum

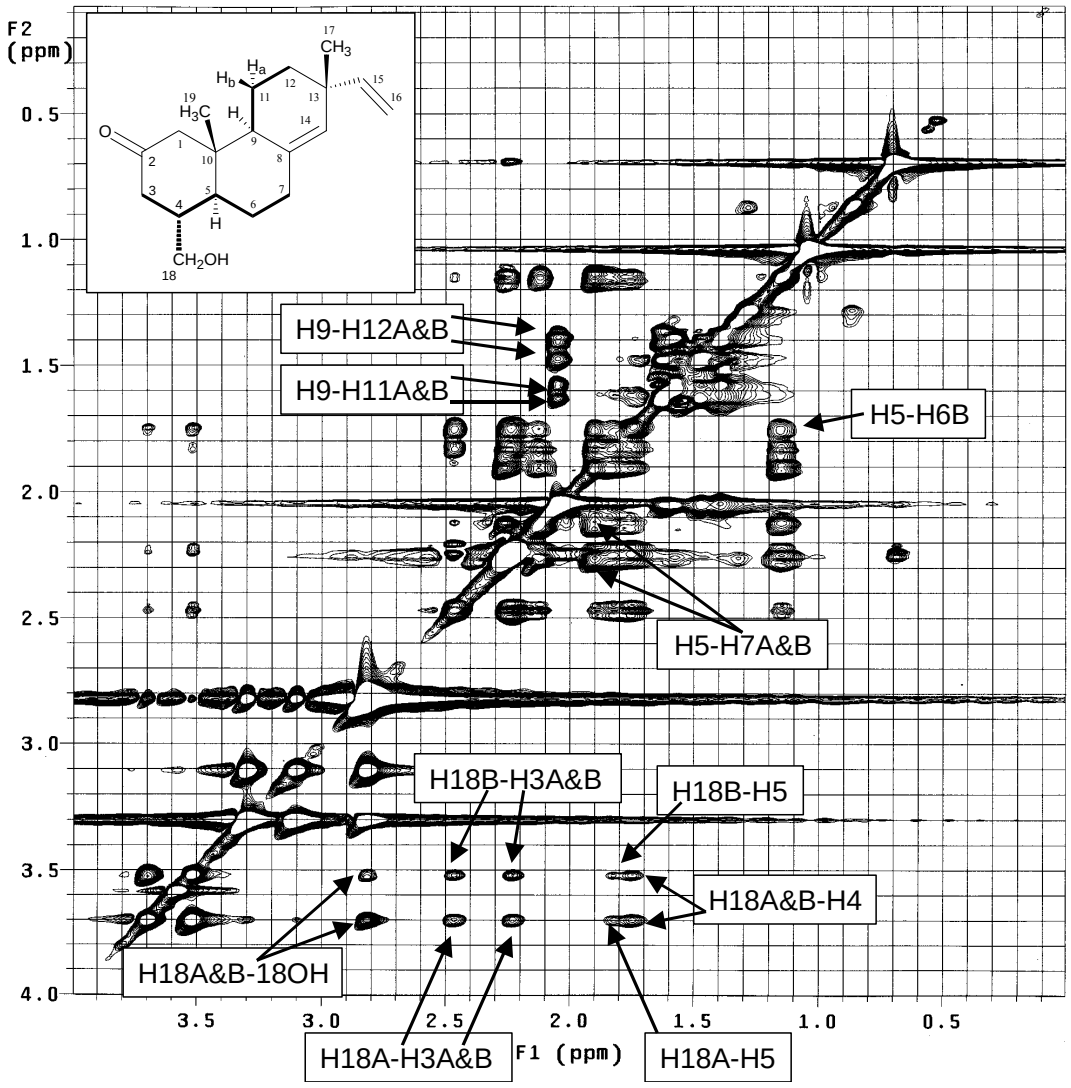

Figure IV.2b. Expansion of the TOCSY NMR spectrum for marinene A (500MHz, acetone-d_6). Key ^{1}H-^{1}H correlations are noted. Spin systems are indicated by bold lines in the structure inset.

The connectivity of the substructures was assigned by analysis of an HMBC NMR experiment (Figures IV.2c and IV.2d). Methylenes protons H-3a, H-3b and H-1a, H1-b (δ_{Ha} 2.26, δ_{Hb} 2.22) showed C-H long-range correlations to a carbonyl carbon

at δ_C 211.0. H-1a and H-1b also showed HMBC correlations to quaternary carbon C-10 (δ_C 43.2). Protons from the C-19 methyl (δ_H 0.69), H-5 and H-9 also showed HMBC correlations to the same quaternary carbon C-10, allowing us to assemble the first ring. Proton H-9 showed a further long range correlation to the quaternary carbon C-8 (δ_C 137.0). The methylene protons H-7a and H-7b, as well as vinyl proton H-14 (δ_H 5.30) also correlate to C-8 closing the second ring. H-14 also correlates to a final quaternary carbon C-13 (δ_C 38.0). Methylene protons H-12a and H-12b, vinyl proton H-15, and methyl protons H-17 (δ_H 1.03), also correlate to this quaternary carbon permitting closure of the third ring and placement of the vinyl functionality.

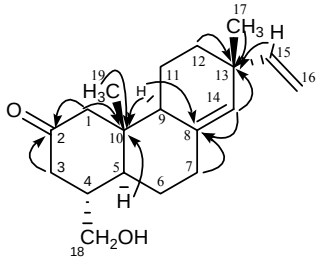

Figure IV.2 c: Key HMBC correlations for establishing the planar structure of marinene A.

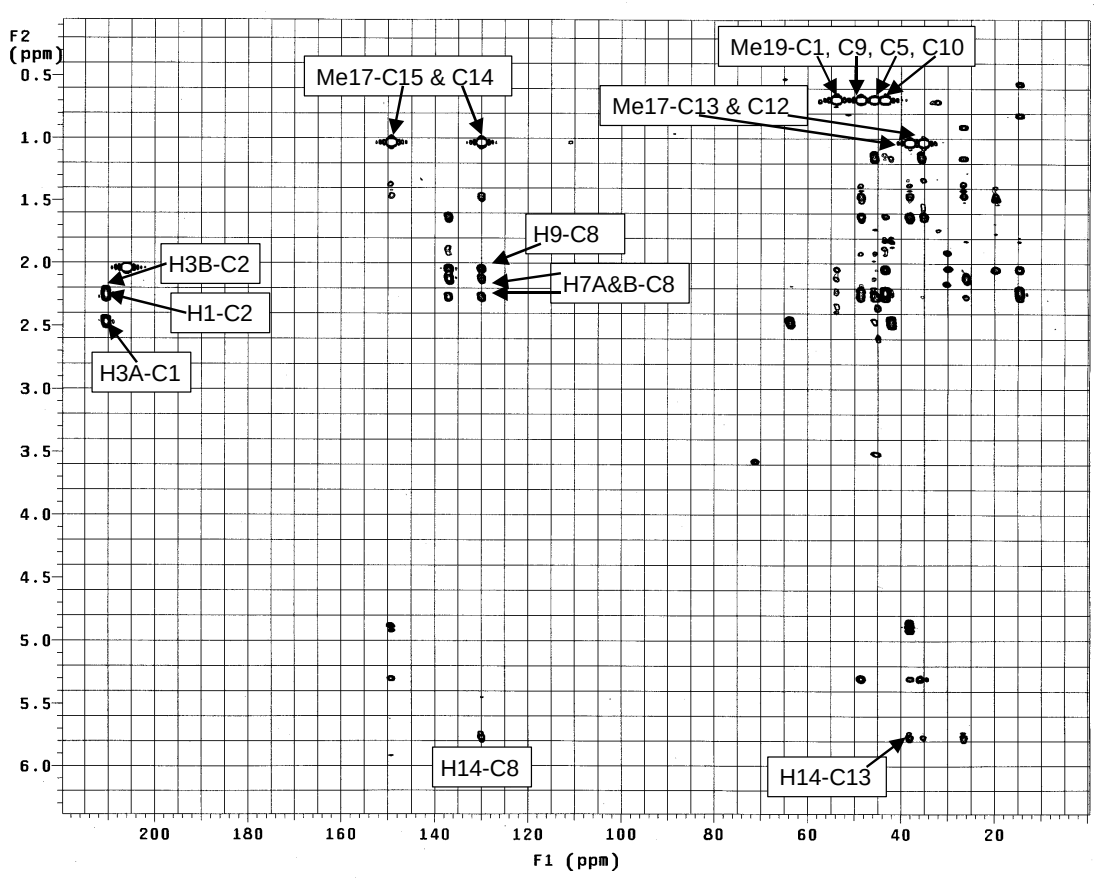

Figure IV.2d: gHMBC NMR spectrum of marinene A (500MHz, acetone-d_6). Key correlations are noted.

The structures of the marinenes closely resemble the trifoliones, a family of diterpenes isolated from the tuber of an aquatic plant *Sagittaria trifolia* (Figure IV.2e)[18, 19]. Both the trifoliones and marinenes have three 6-membered rings and vinyl substituents at C-13. Additionally, both sets of compounds have methyl groups at C-10 and C-17, a double bond between C-14 and C-15, and oxygenated functionalities at C-2. Marinenes A and B, however, are nor-diterpenes which lack the C-19 methyl group.

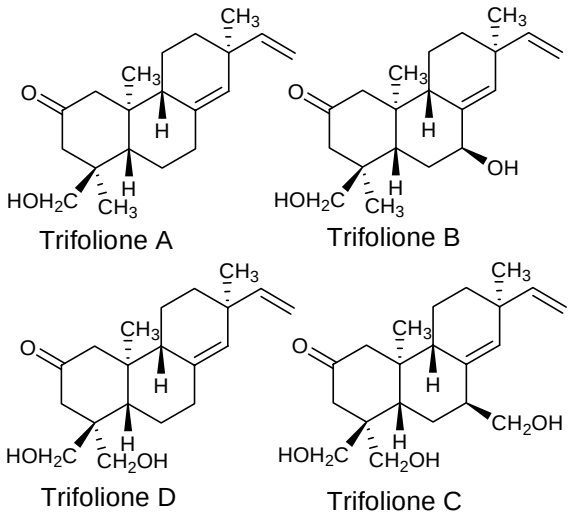

Figure IV.2e: Structures of Trifoliones

The relative configuration of marinene A was determined by analysis of NOESY correlations (Figure IV.2f and IV.2g). Important NOESY correlations between proton H-4 and the protons of the methyl at C-19, from the C-19 methyl to the axial proton H-11b, and then from H-11b to the protons of the C-17 methyl revealed the relative configuration of the bottom half of the molecule (Figure IV.2f). On the opposite half of the molecule, key NOESY correlations include a resonance between axial proton s H-5 and H-9, and one from H-9 to equatorial proton H-11a. These data support an identical relative configuration to that of the trifoliones.[19]

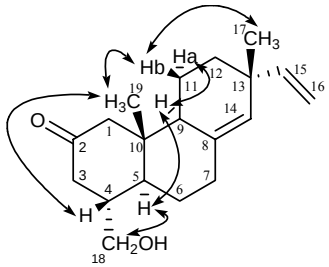

Figure IV.2f: Relative configuration of marinene A. Arrows indicate key NOESY correlations

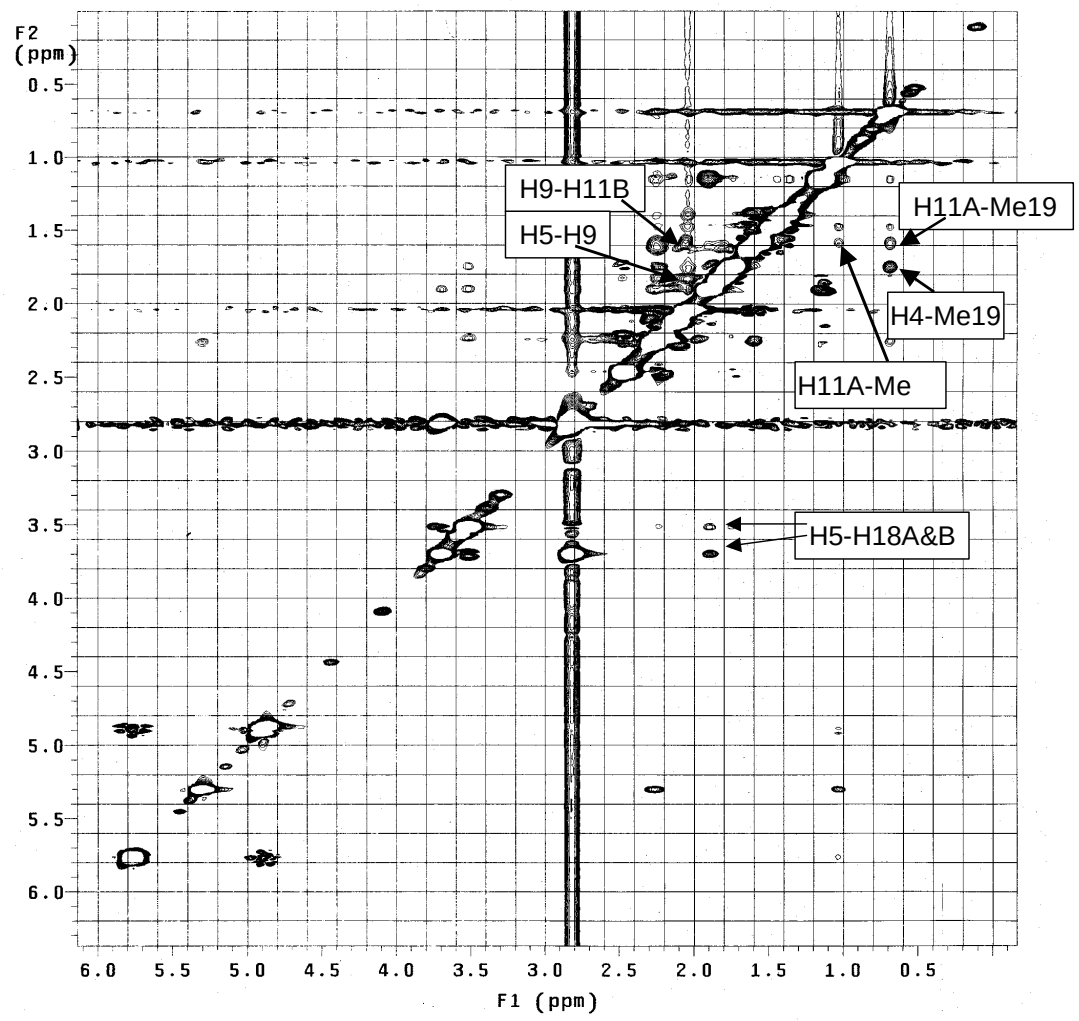

Figure IV.2g: NOESY spectrum for marinene A (500MHz, acetone-d_6). Key ^{1}H-^{1}H NOESY correlations are noted.

The absolute configuration of marinene A was determined using Circular Dichroism (CD) spectroscopy. Comparison of the CD spectrum with those of the trifoliones suggested that they have opposite absolute configurations. The CD spectrum of marinene A showed a positive maximum at 290 nm due to the n-π* transition and a negative minimum at 210nm which is opposite that of the trifolione diterpenes (negative min at 290 nm and positive max at 210 nm).[19] The optical

rotation of marinene A $[\alpha]_D^{20}$ +821 (c = 0.18, acetone), also possesses the opposite sign of that of the trifoliones [19].

The presence of at least one structural analog of marinene A was detected by LCMS analysis of the extract of CNR291 (Table IV.2b). Marinene B was isolated from the organic extract of CNR291 by preparative reversed phase HPLC with an acetonitrile: water gradient. If was further purified using semi-preparative reversed phase HPLC with isocratic acetonitrile: water conditions. The structure was determined by a combination of IR and 1D and 2D NMR. In marinene B, the ketone at C-2 has been reduced to a hydroxyl group (Figure IV.1h). The relative configuration of the new stereocenter at the C-2 hydroxyl was determined through analysis of NOESY correlations (Figure IV.2h). The reduction of the ketone at C-2 in marinene B can also be observed in the IR spectrum where the strong sharp ketone band at 1690 cm^{-1} in marinene A is no longer present and instead, there are not two strong, broad bands in the hydroxyl region at 3350 cm^{-1} and 3250 cm^{-1} (Figure IV.2i). The optical rotation of marinene B ($[\alpha]_D^{20}$ +811 (c = 0.18, acetone)) revealed that marinene B has the same absolute configuration as that of marinene A.

Table IV.2.b: ^{1}H and ^{13}C NMR data for marinenes A and B in acetone-d_6.

	Compound A		Compound B	
#	δ_C [a]	δ_H [b] (*J* in Hz)	δ_C [b]	δ_H [b] (*J* in Hz)
1	53.7	2.26 br d [c] (13.0) 2.22 br d [c] (13.0)	48.4	2.00 m [d] 0.95 dd (12.0, 12.0)
2	211.0		66.5	3.68 m
3	44.9	2.47ddd (13.0, 13.0, 2.5) 2.22 m [c]	41.2	2.02 m [d] 1.17 m
4	42.0	1.75m	39.2	1.42 m
5	45.7	1.83 ddd (12.0, 12.0, 3.0)	48.4	2.02 m [d]
6	25.6	1.90 br dddd (12.0, 5.5, 3.0, 2.5) 1.15 dddd (12.0. 12.0, 12.0, 4.5)	25.2	1.76 br dddd (12.0, 5.5, 3.0, 2.5) 1.05 dddd (12.0, 12.0, 12.0, 4.5)
7	35.5	2.27 m [c] 2.12 br ddd (12.0, 12.0, 5.5)	35.8	2.20 br ddd (14.0, 2.5, 1.5) 2.02 m [d]
8	137.0		137.5	
9	48.5	2.05 m [d]	49.5	1.81 br t (8.5, 6.5) [e]
10	43.2		40.0	
11	19.7	1.63 br dddd (13.0, 6.0, 6.0, 4.0) 1.58 br dddd (13.0, 11.0, 6.0, 3.5)	19.8	1.68 br dddd (13.0, 6.5, 6.0, 4.0) 1.60 br dddd (13.0, 12.0, 8.5, 3.5)
12	35.0	1.47 br ddd (13.0, 6.0, 3.5) 1.40 ddd (13.0, 11.0, 4.0)	35.1	1.49 br ddd (13.0, 6.0, 3.5) 1.37 ddd (13.0, 12.0, 4.0)
13	38.0		38.0	
14	129.9	5.30 br s.	129.0	5.25 br s.
15	149.3	5.74 dd (17.5, 11.0)	149.9	5.77 dd (17.5, 11.0)
16	111.0	4.90 dd (17.5, 1.5) 4.88 dd (11.0, 1.5)	110.5	4.90 dd (17.5, 1.5) 4.85 dd (11.0, 1.5)
17	26.5	1.03 s	26.0	1.03 s
18	63.7	3.69 br m [c] 3.51 br d (11.0)	64.7	3.55 br d (10.0) 3.51 br m
19	14.5	0.69 s	15.5	0.75 s
2-OH				
18-OH		3.69 br s [c]		3.36 br s

[a] Assignment by 1-D ^{13}C methods at 125 MHz.
[b] Assignment by ^{1}H, gHSQC, and gHMBC NMR methods at 500MHz.
[c] Overlapping signals.
[d] Overlapping signal with a solvent peak.
[e] Broad triplet like signal, coupling constant is obscure.

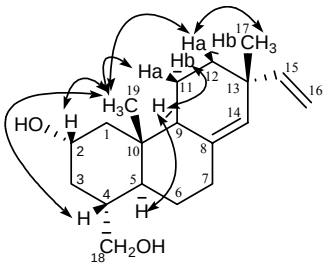

Figure IV.2 h: Structure and relative configuration of marinene B. Arrows indicate key NOESY correlations.

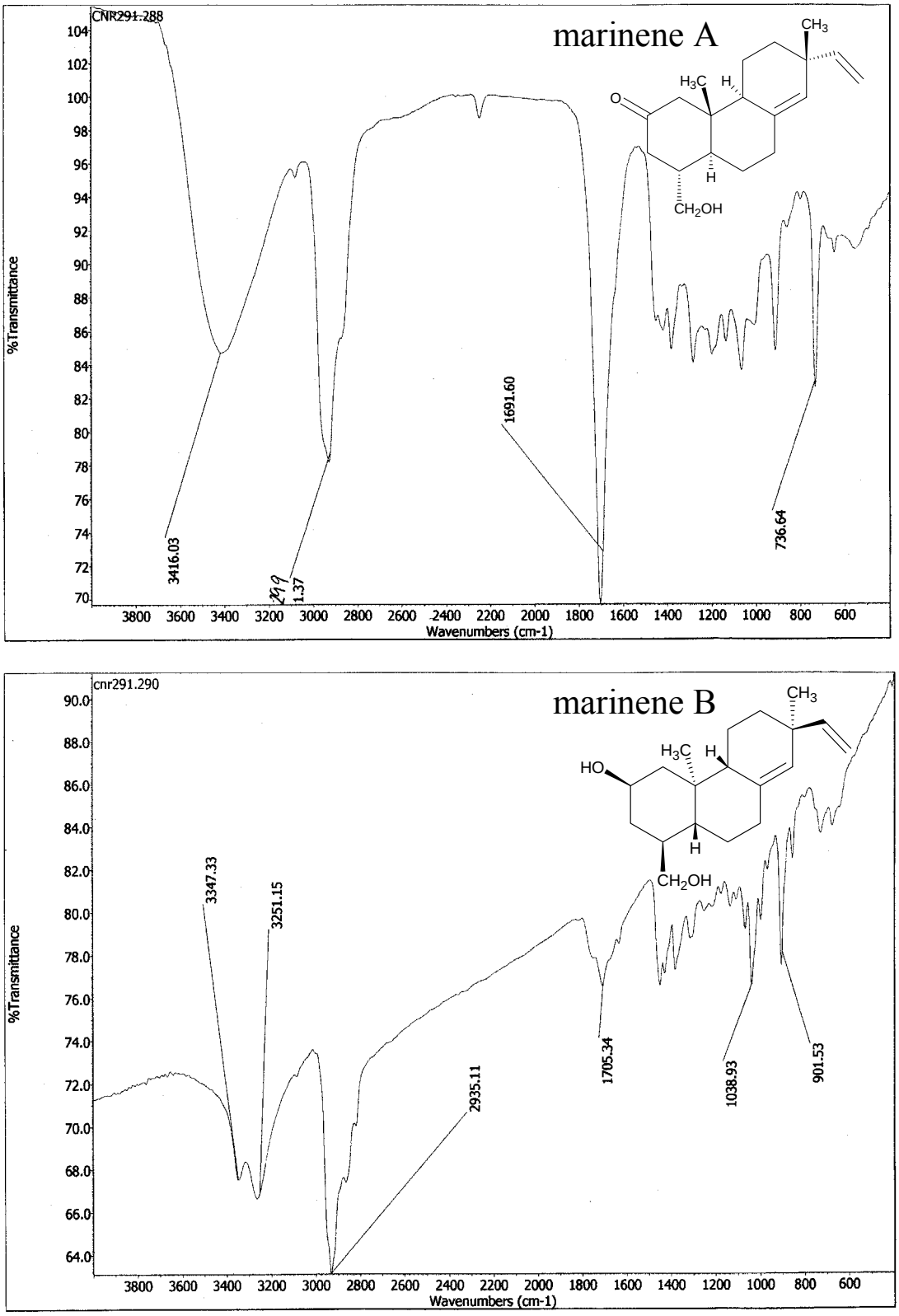

Figure IV.2i: IR spectra of marinenes A and B.

Since diterpene production by gram-positive bacteria is exceedingly rare while fungi are prolific producers of terpenes, we at first suspected that the marinenes might have been produced by a fungal contaminant in the bacterial culture. However, a confirmed pure culture of CNR291 was revealed by ^{1}H NMR to produce the marinenes. Interpretation of 16S ribosomal DNA gene sequence data revealed the terpene-producing bacterium to be 98% similar to *Micromonospora echinaurantiaca*, which was originally isolated from soil in China.[20]

IV.3

In Vitro Cytokine Inhibition Studies

IV.3. *In Vitro* Cytokine Inhibition Studies

Microbial strain CNR291 displayed potent activity in the mouse splenocyte assay. Each fraction of the 40L culture extract was tested in duplicate at each of three different dilution concentrations with final concentrations of 25, 8, and 3 μg/mL culture medium. Although fraction 22 (1.1mg) exhibited 100% cytotoxicity at 25 μg/mL at the next dilution step of 8 μg/mL the fraction was no longer cytotoxic despite inhibiting IL-5 production levels to only 35% of the stimulated control. From this fraction, marinenes A and B were purified.

Several phthalate esters were also purified from the active fraction, but these are likely artifacts of the isolation procedure. A purified phthalate ester was tested in the splenocyte assay. The purified phthalate ester displayed potent cytotoxicity towards splenocytes, showing 100 percent cell death at 0.1 μg/ml. However it did not display non-cytotoxic cytokine suppressive activity.

As with the partially purified fractions, marinenes A and B both displayed 100% splenocyte toxicity at 25 μg/ml while exhibiting non-cytotoxic inhibition of IL-5 production at 8 μg/ml (Figure IV.3a). Marinene A is slightly more potent than marinene B, inhibiting IL-5 production by 65% while marinene B inhibited IL-5 production by 42% at 8 μg/ml. At 3 μg/ml, marinenes A and B continued to show inhibition of IL-5 production by 34% and 19% respectively.

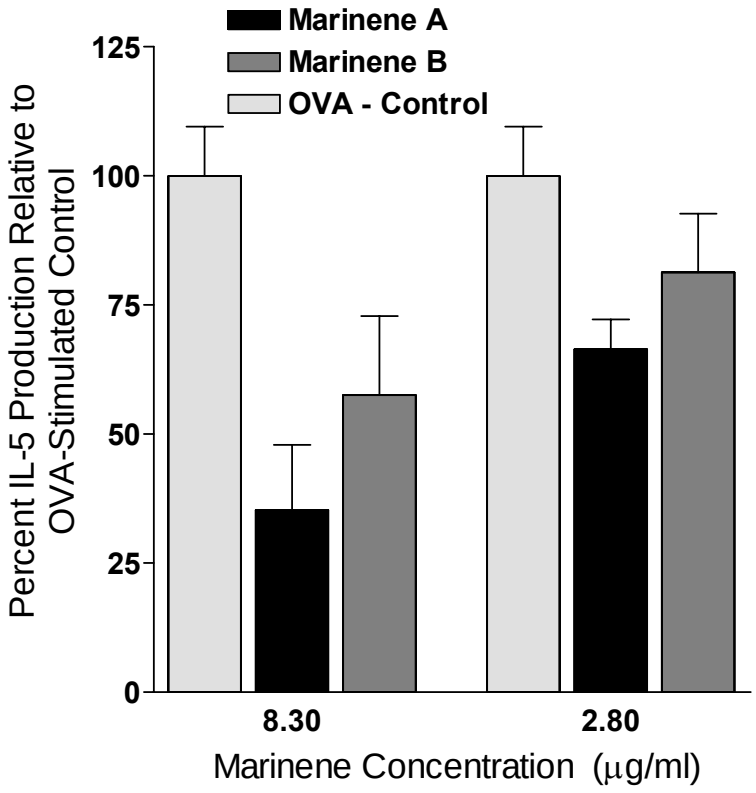

Figure IV.3a: Non-cytotoxic inhibition of IL-5 production in OVA stimulated splenocytes by Marinenes A and B.

In addition to inhibiting IL-5, marinenes A and B also show inhibition of cytokines IL-1 and IL-13 indicating a more general anti-inflammatory mechanism of action (Figure IV.3b). In all cases, marinene A displayed greater inhibition of cytokine production relative to marinene B. This is most pronounced in the inhibition of IL-1, a cytokine produced by the dendritic cellular component of the heterogeneous splenocyte population.

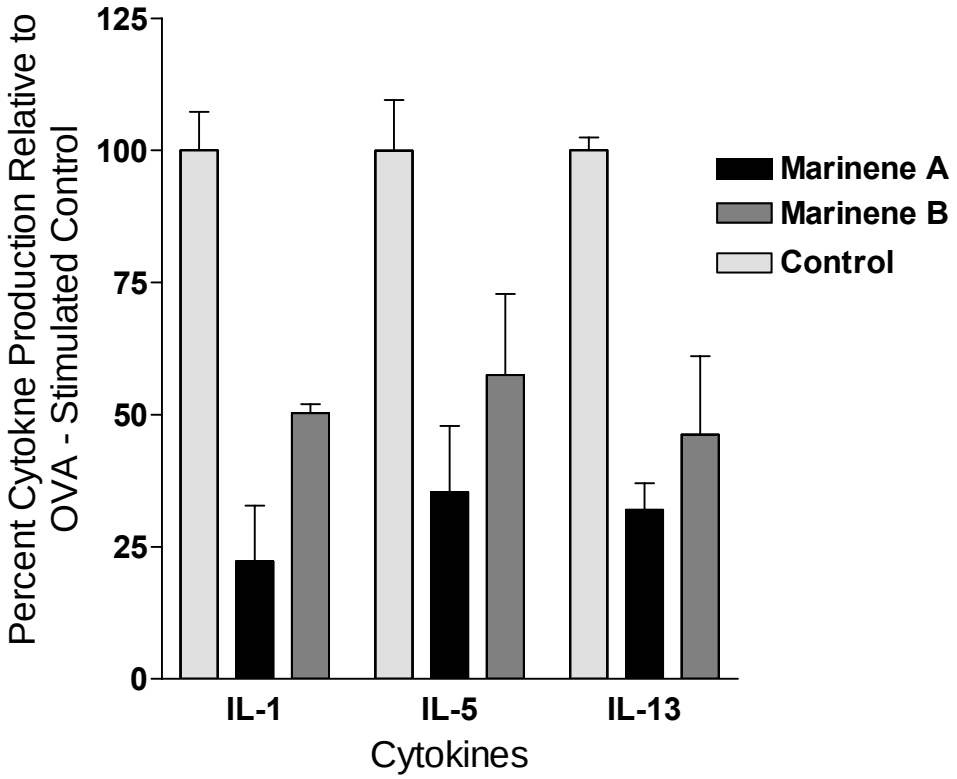

Figure IV.3b: Inhibition of OVA-stimulated splenocyte APC (IL-1) and Th2 (IL-5 and IL-13) cytokine production by marinenes A and B at 8 μg/ml.

Several sesquiterpenes, diterpenes and at least two nor-diterpenes with anti-inflammatory properties have previously been isolated from fungi, sponges and other macroorganisms.[21] These molecules are believed to be acting by inhibiting nuclear factor kappa-B (NFκB), a transcription factor that plays a central role in immune response by virtue of its ability to initiate the transcription of a variety of pro-inflammatory cytokines.[22-25] Acanthoic acid is a pimaradiene terpene originally isolated from the root bark of the Korean medicinal plant, *Acanthopanax koreanum* which closely resembles the marinenes (Figure IV.3c).[23] Other related molecules

include viguiepinone (Figure IV.1a) and the recently described oxaloterpins, both isolated from bacteria.[2] These compounds possess the both the tri-cyclic backbone and vinyl functionality at C-13 as the marinenes. These molecules differ from the marinenes in the position of the double bond, the absence of oxygen at C-2, the retention of the terminal methyl, and the relative configuration.

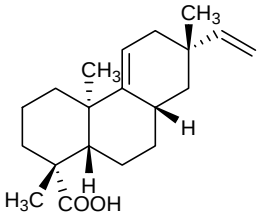

Figure IV.3c: Structure of acanthoic acid.

Studies have shown that acanthoic and its structural analogs inhibit production of IL-1 and TNF-α at 10 μg/ml *in vitro*.[25] Acanthoic acid has also been shown to be orally active, and non-cytotoxic in a rat model of neutrophil induced inflammation.[24] Recent work has shown that these molecules inhibit TNF-α production in lipopolysaccharide mononucleocytes at 10 μg/ml, likely by inhibiting NFκB-mediated cytokine synthesis.[24] It is possible that a similar mechanism is responsible for the inhibition of cytokine production by the marinenes seen in the mouse splenocyte assay although further studies are needed to elucidate the mechanism of action of the marinenes.

IV.4

Experimental

IV.4. Experimental.

General Experimental Procedures. ^{1}H, ^{13}C, and 2D NMR spectral data were obtained on Varian Inova 300 MHz and 500 MHz NMR spectrometers in acetone-d_6 solvent. UV spectra were recorded on a Beckman Coulter DU 800 UV vis spectrophotometer with a path length of 1 cm. IR spectra were recorded in a Nicolet IR100 FT-IR spectrometer. Optical rotations were measured using a Jasco P-2000 polarimeter with a 10 cm cell. High-resolution HR ESI-TOF MS data were collected on an IonSpec Ultima mass spectrometer at the Scripps Research Institute, La Jolla. Low resolution LC/MS data were obtained on a Hewlett-Packard series 1100 LC/MS system with a reversed phase C18 column (Agilent, 4.6 mm X 100 mm, 5 μm) with a 0.7 mL/min flow rate. CD spectra were obtained on a Jasco 810 spectropolarimeter with a 1 cm path length. OD measurements of ELISA experiments were recoded at 450 nm on a Biorad Model 680 microplate reader.

Isolation of CNQ-431 Strain, Identification, Cultivation, and Extraction. Marine-derived *Micromonospora* strain CNR-291 was isolated on growth medium A1bFe+C (10 g of starch, 2 g of peptone, 4 g of yeast extract, 5 ml of KBr, 5 ml of $FeSO_4$, 1 g of calcium carbonate, and 1 L of sea water) from a marine sediment collected from a depth of 30 m 1 mile off the coast of Guam. 16S rDNA analysis gene sequence analysis allowed us to determine that strain CNR-291 was 98% similar to *Micromonospora echinaurantiaca*. The strain was cultured in 40 x 1 L volumes of A1bFe+C while shaking at 230 rpm for 7 days. After 7 days, 20 g/L of XAD-7 adsorbent resin was added to each flask and the flasks were allowed to shake for an additional 24 hours. At this time, an additional 20 g/L of XAD-7 adsorbent resin was

added. The cultures were allowed to shake for an additional 24 hours, at which time the resin was collected by filtration through cheesecloth, washed with deionized water and eluted twice with acetone. Evaporation of the extraction solvent *in vacuo* left a wet residue that was partitioned with EtOAc, providing approximately 600 mg of dry organic extract per 1 L of culture after solvent removal.

Isolation and Purification of Marinenes A and B (1 and 2). The 600 mg organic extract was fractionated by C-18 preparative reversed-phase HPLC with an MeCN-H_2O step gradient from 20% MeCN to 100% MeCN over 70 min. to obtain nearly pure marinenes A and B (**1** and **2**). Final purification was performed with semi-preparative C-18 reversed-phase HPLC with isocratic solvent systems of 67:33 MeCN:H_2O.

Marinene A (1) White amorphous powder, CD (MeCN) $\Delta\varepsilon_{215}$ –50.4, $\Delta\varepsilon_{290}$ +7.8; $[\alpha]_D^{20}$ +821 (c = 0.18, acetone), UV (MeCN): 210 nm (ϵ = 14, 450). IR (film) ν_{max} 3416, 2991, 1691, and 736 cm^{-1}. HR ESI-TOF MS: Obsd. *m/z* 289.2170 $[M+H]^+$ ($C_{19}H_{29}O_2$ requires 289.2167) See Tables IV.2a and IV.2b for NMR data.

Marinene B (2) White amorphous powder, $[\alpha]_D^{20}$ +811 (c = 0.18, acetone), UV (MeCN): 220 nm (ϵ = 4,400). IR (film) ν_{max} 3347, 3251, 2935, 1038, 901 cm^{-1}. ($C_{19}H_{31}O_2$ requires 291.2324). See Table IV.2b for NMR data.

References:

1. Dewick, P. M., *Medicinal Natural Products, A Biosynthetic Approact*. 2nd ed.; John Wiley and Sons Ltd.: Hoboken, 2001.

2. Motohashi, K.; Ueno, R.; Sue, M.; Furihata, K.; Matsumoto, T.; Dairi, T.; Omura, S.; Seto, H., Studies on Terpenoids Produced by Actinomycetes: Oxaloterpins A, B, C, D, and E, Diterpenes from Streptomyces sp. KO-3988. *Journal of Natural Products* **2007**, (ASAP).

3. Kuzuyama, T.; Seto, H., Diversity of the Biosynthesis of the Isoprene Units. *Natural Products Reports* **2003,** 20, 171-183.

4. Schulz, S.; Dickschat, J. S., Bacterial Volatiles: the Smell of Small Organisms. *Natural Products Reports* **2007,** 24, 814-842.

5. Gross, H.; Konig, G. M., Terpenoids from Marine Organisms: Unique Structures and their Pharmacological Potential *Phytochemistry Reviews* **2006,** 5, (1), 115-141.

6. Shiomi, K.; Iimura, H.; Naganawa, H.; Isshiki, K.; Takeuchi, T.; Umezawa, H., *Journal of Antibiotics* **1987,** 40, 1740.

7. Funayuma, S.; Eda, S.; Komiyama, K.; Omura, S.; Tokunaga, T., Biosynthesis of furaquinocins A and B. *Journal of Organic Chemistry* **19990,** 55, 1132-1133.

8. Shin-ya, K.; Imai, S.; Furihata, K.; Hayakawa, Y.; Kato, Y.; VanDuyne, G. D.; Clardy, J.; Seto, H., *Journal of Antibiotics* **1990,** 43, 444.

9. Gerber, N. N.; Lechevalier, H. A., Geosmin, an Earthy-Smelling Substance Isolated from Actinomycetes. *Applied and Environmental Microbiology* **1965,** 13, (6), 935-938.

10. Pierson, B. K.; Castenholz, R. W., *Archives of Microbiology* **1974,** 100, 5-24.

11. Spyere, A.; Rowley, D. C.; Jensen, P. R.; Fenical, W., New Neoverrucosane Diterpenoids Produced by the Marine Gliding Bacterium *Saprospira grandis*. *Journal of Natural Products* **2003,** 66, 818-822.

12. Takeuchi, S.; Ogawa, Y.; Yonehara, H., The Structure of Pentalenolactone (PA-132). *Tetrahedron Letters* **1969,** 10, 2737-2740.

13. Nakanishi, S.; Osawa, K.; Saito, Y.; Kawamoto, I.; Kuroda, K.; Kase, H., *Journal of Antibiotics* **1992,** 45, 341.

14. Gurtler, H.; Pedersen, R.; Anthoni, U.; Christophersen, C.; Nierlson, P. H.; Wellington, E. M. H.; Pedersen, C.; Bock, K., Albaflavenone, a Sesquiterpene

Ketone with a Zizaene Skeleton Produced by a Streptomycete with a New Morphology. *Journal of Antibiotics* **1994,** 47, 434-439.

15. Gansser, D.; Pollak, F. C.; Berger, R. G., *Journal of Natural Products* **1995,** 58, 1790.

16. Tamamura, T.; Sawa, T.; Isshiki, K.; Masuda, T.; Homma, Y.; Inuma, H.; Naganawa, H.; Hamada, M.; Takeuchi, T.; Umezawa, H., Isolation and Characterization of Terpentecin, a New Antitumor Antibiotic. *Journal of Antibiotics* **1985,** 38, (12), 1664-1669.

17. Crews, P.; Rodriguez, J.; Jaspers, M., *Organic Structure Analysis*. Oxford University Press.

18. Yoshikawa, M.; Yoshizumi, S.; Murakami, S.; Matsuda, H.; Yamahara, J.; Murakami, N., Medicinal Foodstuffs. II.[1)] On the Bioactive COnstituents of the Tuber of *Sagittaria trifolia* L. (Kuwai, Alismataceae): Absolute Stereostructures of Trifoliones A, B, C, and D, Sagittariosides a and b, and Arabinothalictoside. *Chem. Pharm. Bull.* **1996,** 44, (3), 492-499.

19. Yoshikawa, M.; Yamaguchi, S.; Murakami, T.; Matsuda, H.; Yamahara, J.; Murakami, N., Absolute Stereostructures of Trifoliones A, B, A, and D, New Biologically Active Diterpenes from the Tuber of *Sagittaria trifolia* L. *Chem. Pharm. Bull.* **1993,** 41, (9), 1677-1679.

20. Kroppenstedt, R. M.; Mayilraj, S.; Wink, J. M.; Kallow, W.; Schumann, P.; Secondini, C.; Stackebrandt, E., Eight new species of the genus *Micromonospora, Micromonospora citrea* sp. nov., *Micromonospora echinaurantiaca* sp. nov., *Micromonospora echinofusca* sp. nov. *Micromonospora fulviviridis* sp. nov., *Micromonospora inyonensis* sp. nov., *Micromonospora peucetia* sp. nov., *Micromonospora sagamiensis* sp. nov., and *Micromonospora viridifaciens* sp. nov. *Systematic and Applied Microbiology* **2005,** 28, (4), 328-339.

21. Keyzers, R. A.; Davies-Coleman, M. T., Anti-Inflammatory Metabolites from Marine Sponges. *Chemical Society Reviews* **2005,** 34, (4), 355-365.

22. Barilea; Fattorussob, E.; Ialentic, A.; Ianaroc, A.; Lanzotti, V., Paraliane and Pepluane Diterpenes as Anti-Inflammatory Agents: First Insights in Structure–Activity Relationships. *Bioorganic and Medicinal Chemistry Letters* **2007,** 17, 4197-4200.

23. Kim, Y. h.; Chung, B. S.; Sankawa, U., Pimaradiene Diterpenes from *Acanthopanax koreanum*. *Journal of Natural Products* **1988,** 51, (6), 1080-1083.

24. Chao, T. H.; Lam, T.; Vong, B. G.; P.G.;, T.; Hortelano, S.; Chowdhury, C.; Bahjat, F. R.; Lloyd, G. K.; Moldawer, L. L.; Boscá, L.; Palladino, M. A.; Theodorakis, E. A., A New Family of Synthetic Diterpenes that Regulates Cytokine Synthesis by Inhibiting IkappaBalpha Phosphorylation. *Chembiochem* **2005,** 6, (1), 133-144.

25. Kang, H. S.; Kim, Y. H.; Lee, C. S.; Lee, J. J.; Choi, I.; Pyun, K. H., Suppression of Interleukin-1 and Tumor Necrosis Factor-alpha Production by Acanthoic Acid, (-)-Pimara-9(11),15-dien-19-oic Acid, and Its Antifibrotic Effects I*n Vivo*. *Cellular Immunology* **1996,** 170, (2), 212-221.

V

Conclusion

V. Conclusion:

The goal of this thesis was to investigate the biological capabilities of compounds from a marine microbial extract library for their abilities to inhibit allergic inflammation. To this end, we developed an assay system using allergen sensitized mouse splenocytes to screen the marine microbial extracts for their ability to inhibit the stimulated cells' production of pro-inflammatory cytokines. This is the first time that we are aware of that marine natural products have been investigated in this type of model. Because asthma is a complex, multi-faceted disease, using a splenocyte heterogeneous cell population taken directly from allergen sensitized mice allowed me to more fully probe the cellular interactions involved in allergic inflammation. Additionally, this *in vitro* assay system allowed me to more easily transition the active molecules into an *in vivo* mouse model because the splenocytes are derived from the whole animal model.

In the splenocyte cellular assay, I screened over 2,500 marine microbial extracts, focusing further on only those extracts with potent inhibition of the Th2 cytokine IL-5. I discovered that roughly 2% of these extracts potently inhibited IL-5 production at low μg/ml concentrations. Active extracts were then examined chemically to determine the structures of the active components.

Several new groups of molecules were discovered through these investigations. Marine derived bacterial strain CNQ431 produced the splenocins, a new group of highly unusual molecules, containing a rare N-formyl-salicylamide group, a rare 9-membered dilactone ring core, as well as benzyl and benzoyl groups. The splenocins are by far the most potent cytokine inhibitors to be isolated through the screening

process. I have shown that the splenocins exhibit low nanomolar inhibition of a range of both Th2 and APC cytokines at levels far below the cytotoxic threshold. Additionally, the splenocins posed several interesting chemical challenges regarding the determination of their relative and absolute configurations, which were resolved using several spectroscopic and chemical techniques.

I also discovered two new tricyclic nor-diterpenes, marinenes A and B, which were isolated from a culture of a marine actinomycete of the genus *Micromonospora*. While terpene production is prolific among many organisms such as plants, fungi, and sponges, bacterial terpene production is quite rare. Marinenes A and B are the first nor-diterpenes shown to be produced by a bacterium. Marinenes A and B also exhibit potent cytokine inhibition in low μg/ml concentrations.

Through collaborative efforts with others in the Fenical Laboratory, I was able to find interesting activities for a number of other new molecules with interesting chemical structures, from phylogenetically unique marine bacterial species. These molecules had proven to be inactive in a host of other biological assays including anti-cancer, anti-fungal and anti-bacterial screens. Two of these chemical groups, the thalassospiramides and the salinipyrones, inhibited the pro-inflammatory cytokine IL-5 at 5-10 μg/ml. Two other sets of compounds, azamerone and actinofuranones A and B were cytotoxic to splenocytes at low μg/ml concentrations, but were not toxic to any of the other cell types (HCT, fungal, bacterial) that they were screened against, suggesting their potential in other forms of disease therapy.

This highly interdisciplinary thesis research would not have been possible without the open and collaborative environment of UCSD, and specifically the unique

spirit of collaboration between the Scripps Institution of Oceanography and the UCSD Medical School campuses. The unique collaboration between the Fenical and Broide laboratories exposed me to top-notch science and scientists in both marine natural products chemistry and molecular and cellular immunology, and allowed the research to be performed in a high level fashion. It is my sincere hope that the results of this thesis will lay the framework for both expanded research in the field of anti-inflammatory natural products research and to further collaborative efforts in the future.